Winter 2014

Effects of Discharge in Residence Time Distributions in a Small Headwaters Wetland in the Ipswich River Watershed

Katherine D. Lawrence
University of New Hampshire, Durham

EFFECTS OF DISCHARGE ON RESIDENCE TIME DISTRIBUTIONS IN A SMALL HEADWATER WETLAND IN THE IPSWICH RIVER WATERSHED

BY

KATHERINE D. LAWRENCE
Master Degree (MS), University of New Hampshire, 2014

THESIS

Submitted to the University of New Hampshire in Partial Fulfillment of the Requirements for the Degree of

Master of Science
In
Hydrology

December, 2014

This thesis has been examined and approved in partial fulfillment of the requirements for the degree of Master of Science in Hydrology by:

Thesis Director, Anne Lightbody, Assistant Professor of Hydrology

J. Matthew Davis, Associate Professor of Hydrology

Wilfred M. Wollheim, Assistant Professor of Aquatic Biogeochemistry

On December 12, 2014

Original approval signatures are on file with the University of New Hampshire Graduate School.

ACKNOWLEDGEMENTS

I would like to thank my thesis advisor, Anne Lightbody, for sharing her wonderful insights and knowledge, for keeping me moving in the right direction, and especially for all of her patience and encouragement. Also, my committee members: Wil Wollheim for his enthusiasm for this project, and Matt Davis for helping me see the bigger picture.

I would also like to thank several others who made this project possible. In particular, Greg Disanto for spending his summer trudging through Chestnut Wetland with me; Nat Morse, for kindly introducing me to Chestnut Wetland; Shan Zuidema for his insights; and Mark Greene for analyzing so many water samples.

This project would not have been possible without funding provided by the Dingman Scholarship, for which I am very grateful.

Lastly, I would like to thank my friends for reminding me it's okay to step back and breathe and my family for their unending support and encouragement.

TABLE OF CONTENTS

LIST OF TABLES

TABLE OF FIGURES

ABSTRACT

EFFECTS OF DISCHARGE ON RESIDENCE TIME DISTRIBUTION IN A SMALL HEADWATERS WETLAND IN THE IPSWICH RIVER WATERSHED

By

Katherine Lawrence

University of New Hampshire, December, 2014

The Ipswich River Watershed, a 401 km^2 watershed located in northeastern Massachusetts, has been observed to be undergoing increasing urbanization with resulting increases in nutrient loading, in particular, nitrogen. Nitrogen uptake occurs in a 1^{st}-order process which is dependent on the concentration of nitrogen as well as the amount of time the water containing nitrogen remains within the wetland, which is described as the residence time distribution (RTD). To better understand how discharge affects the RTD of the wetland, a number of tracer studies were conducted between May 2011 and August 2011. Additionally, fluxes into and out of the wetland were calculated for this same period to estimate groundwater flow into or out of the wetland in order to understand interactions of groundwater with the wetland. The RTDs calculated from four tracer studies suggest that lower discharges result in longer detention times and higher discharges result in shorter detention times, though the results are not conclusive. Estimates of water budget fluxes suggest that the direction and magnitude of groundwater flow may change depending on whether the wetland is at base flow or flood flow.

CHAPTER 1

INTRODUCTION

The transport of nutrients through river networks can have dramatic effects on bodies of water located farther downstream. Though nutrients are necessary for the growth of aquatic plants and beneficial organisms, an overload of them can cause algal blooms, destroy eel grass beds, harm fish and shellfish species, and cause other wide-ranging ecosystem problems (Smil 2001 p.133; Valiela & Bowen 2002). Watershed contaminants often enter a river network far upstream, which provides an opportunity for removal before discharge into the estuary (Valiela & Bowen 2002). However, not much is known about the precise locations of nutrient uptake, which limits our ability to predict the efficiency of future removal (Wollheim et al. 2008). One possible defense against the transport of nutrients downstream of the source is wetlands, either natural or constructed (Kadlec & Knight 1996).

There are several ways in which human activity and land use can affect nitrogen loads to a watershed and its estuary. Local sources of anthropogenic nitrogen loading include fertilizer use on agricultural fields and residential lawns, human sewage and wastewater from septic systems and municipal sewer systems, and animal wastes from pastures and

feed lots (Valiela & Bowen 2002; Boyer et al. 2002). Nitrogen can also be produced both inside the watershed and outside of the watershed and transported into it through atmospheric deposition as a result of higher industrial and automotive emissions (Valiela & Bowen 2002; Boyer et al. 2002). The nitrogen in these emissions are precipitated during rain events (Boyer et al. 2002). Higher rates of storm runoff in urban environments help facilitate the transport of this deposited nitrogen into streams (Pellerin 2004). According to Boyer et al. (2002) watersheds that remain primarily forested tend to have lower nitrogen loading to their estuary. Therefore, urbanization within a watershed may increase the amount of nitrogen that flows into the estuary and contribute to the degradation of the estuary through eutrophication.

Nitrogen exists in several different chemical species and, primarily with the aid of microorganisms and bacteria, each species can be converted to each of the others. Organic nitrogen includes a variety of dissolved organic nitrogen (DON) such as amino acids and urea/uric acids and particulate organic nitrogen (PON) such as tiny suspended fragments of nitrogen containing organic matter (Kadlec & Knight 1996). These forms of organic nitrogen can undergo a process of ammonification which turns it into ammonium NH_4^+ which is an inorganic form of nitrogen. While ammonium is generally preferred by wetland plants as the primary nutrient form, it can be easily reduced to its unionized form, NH_3, which results in significant decrease in dissolved oxygen and which is also toxic to many aquatic organism (Kadlec & Knight 1996). Ammonium itself

can again be assimilated into plant biomass or undergo nitrification in which it is transformed into nitrite, NO_2^-, or nitrate, NO_3^-. The NO_3^- can then be taken up by plants and algae as food and incorporated into chlorophyll. When those plants die and decay the assimilated nitrogen is again broken down by microorganisms into ammonia during ammonification (Kadlec & Knight 1996). For the complete cycle to occur both aerobic and anaerobic situations must occur. Nitrogen cycling in wetlands can progress quickly because both aerobic and anaerobic conditions are present. When the water level is low and the top surface of the wetland platform substrate is exposed areas of aerobic conditions increase. When the water level rises and submerges that upper layer of substrate it becomes an anaerobic environment.

One of the most well known examples of the negative effects of excessive nutrient loads is the seasonal eutrophication in the Gulf of Mexico at the mouth of the Mississippi River. Six independent studies of nutrient loading in the Mississippi River Basin determined that drastic increases in nitrogen loading, largely due to agricultural non-point sources, have resulted in a recurring hypoxic region in the Gulf of Mexico (Scavia & Bricker 2006). The area covered by the eutrophic region, which doubled in size from 8300 km^2 to 16,000 km^2 between 1985 and 2001, is directly related to the nitrogen load entering the Gulf from the Mississippi River (Scavia & Bricker 2006). Scavia and Bricker (2006) suggest that 2.5 million metric tons of the total nitrogen (approximately 8.3 million metric tons) input could be kept out of the Gulf of Mexico by better

agricultural management practices (~1.8 million metric tons) and wetlands/riparian buffers (~0.6 million metric tons).

Another example of an estuary suffering from increased nitrogen loads is Waquoit Bay located in East Falmouth, MA. Aerial photographs of the Waquoit Bay watershed were taken over a period of several decades (1938-1990) to estimate land use cover which in turn was used to estimate the nitrogen input from atmospheric deposition, fertilizer, and wastewater (Valiela & Bowen 2002). Natural vegetative cover decreased from 84% to 68% over the 52 years (Valiela & Bowen 2002). This coincided with an increase of NO_3^- from 0.9 kg N ha^{-1} yr^{-1} in 1925 to 4 kg N ha^{-1} yr^{-1} (Valiela & Bowen 2002). Estuaries that receive nitrogen primarily in the form of NO_3^- tend to experience more eutrophication than estuaries that receive nitrogen primarily as DON (Valiela & Bowen 2002). As NO_3^- loading to Waquoit Bay increased, biomass production in the estuary shifted from primarily seagrasses to algae, which leads to eutrophication when the algae decays. (Valiela & Bowen 2002).

A third well known example of anthropogenic nutrient overloading to an estuary occurs in Chesapeake Bay on the mid-Atlantic coast. It is the largest estuary in the United States and has a population growth rate between 1.7-2.9% per year depending on the region within the watershed (McConnell 1995). Nitrogen inputs into the estuary increased at least 2% between 1985 and 1995 (McConnell 1995). In the Susquehanna River, one of

the more important rivers that export nitrogen to the Chesapeake Bay, NO_3^- concentrations increased three fold between 1945 and 1989 (Hagy et al. 2004). The primary sources of these increasing nitrogen inputs are sewage treatment plants, agricultural runoff, and atmospheric deposition from fossil-fueled power plants and motor vehicles (McConnell 1995). Some of the consequences of this nitrogen input are a 95% decrease in oyster population, a 90% decrease in the area covered by aquatic vegetation which provides fish habitat and a persistent anoxic condition in the deeper waters of the estuary (McConnell 1995). Specifically, the volume of near anoxic water within the estuary increased from zero (modeled) to 3.6×10^9 m^3 (observed) during the time period between 1950 and 2001 (Hagy et al. 2004). Analysis of sediment cores from the Bay indicate that historically significant changes in the health of the estuary coincide with major changes in land-use within the watershed (McConnell 1995). As noted above, wetlands can be a significant nitrogen sink upstream of the estuary. However, the area covered by inland wetlands was reduced by 54.6% from the mid-1950s to the late 1970s (McConnell 1995).

The present study focuses on the Ipswich River watershed, which is a 401 km^2 suburbanizing watershed (Wollheim et al. 2008). In the Ipswich River watershed, increased nitrogen loading has been observed in the more urbanized locations compared to less disturbed areas within the watershed (Wollheim et al. 2005). This is of concern because this watershed basin is becoming increasingly urbanized (Wollheim et al. 2005).

The increase in impervious surfaces that comes with urbanization, as well as increased use of fertilizers on lawns and nitrogen inputs from septic systems, is expected to result in an increase in nitrogen loading into streams and wetlands within the Ipswich River watershed and, ultimately, into Plum Island Sound (Wollheim et al. 2005).

Wetlands are one type of ecosystem where nutrients can be intercepted between the nutrient source and the estuary which may reduce the potential risks posed to the estuary (Kadlec & Knight p3-5). The uptake of nutrients from water in a wetland increases with the amount of time that water spends in the wetland due to increased contact with microbes on submerged plants and sediment. The average time that water remains in a system is defined as its residence time, calculated by dividing volume by discharge (Kadlec & Knight p241). Since there are, in general, many flow paths by which water can move through a wetland including through the main channel, secondary channels, patches of aquatic vegetation and shallow groundwater regions there is a range of residence times for any system. Channelization or other fast flow paths within the wetland can direct flow out of the wetland before the average residence time. This condition is called short-circuiting and can reduce the potential for nutrient removal from that water (Lightbody 2008) The detention time takes into account any "dead zones" of stagnant water and therefore reflects the active volume. For this to be true the tracer being measured must be chemically and biologically conservative (ie – cannot degrade or

be consumed by organisms). Because of this, the detention time of a real system will often be shorter than the theoretical (mean) residence time.

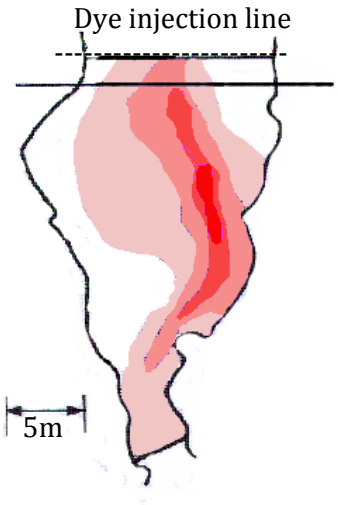

1 (a)

Kadlec and Knight, 1996

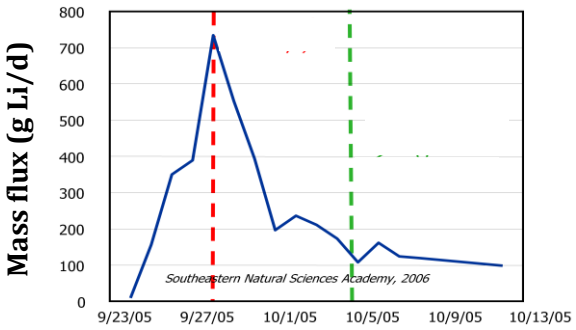

(b)

Southeastern Natural Sciences Academy, 2006

Figure 1– (a) The intensity of the red is proportional to the concentration of bromide dye in the wetland. Tracer study was conducted in a natural wetland in New Zealand. The horizontal line is drawn at the position of the elapsed time as a fraction of the theoretical detention time. Figure adapted from Kadlec and Knight 1996 (pp 239) (b) The graph characterizes the outlet mass flux of lithium tracer in a constructed wetland (a). The vertical red line is the arrival time of the peak mass flux. The vertical green line is the nominal hydraulic residence time.

An example of short-circuiting is shown in Figure 1. A conservative tracer was injected at the dashed line across the width of the wetland shown in Figure 1a. If the wetland were a plug flow system, one would expect to see the tracer concentrated across the wetland at the location of the solid line. However, the dye was observed to have quickly

traveled along one path, indicating that this flow path short-circuits the wetland (Kadlec and Knight 1996).

Short-circuiting can be characterized by the wetlands residence time distribution, which is the probability densitiy function for how long different parcels of water remain in the wetland. The outlet concentration time series shown in Figure 1b is for a different wetland (Southeastern Natural Science Academy 2006). Here, the first observed dye concentration at the wetland outlet represents the fastest flow path, the peak at 4 days (red dashed line) represents the largest flow path, and the two smaller peaks may be smaller, slower flow paths (Southeastern Natural Science Academy 2006). The green dashed line at 12 days is the nominal residence time for the wetland based on volume and discharge. This is the time when the tracer should arrive at the outlet; because it arrives sooner there must be excluded zones not contributing to flow. The long tail of the RTD indicates that some fraction of water stays in the wetland for a very long time, perhaps in a stagnant pool or stored in shallow sediments.

The shape of the RTD can be affected by several physical and hydraulic characteristics within the wetland including geometry, vegetation, and water depth (Lightbody et al. 2008, Holland et al. 2004). Channelization will cause short-circuiting which will decrease the peak arrival time of a tracer (Lightbody et al. 2008). If the floodplain or additional flow paths are accessed at different water depths the RTD will likely change. A Rhodamine WT dye tracer study conducted at a treatment wetland at the Ohio State

University found that the shape of the normalized RTD differed based on water depth (Holland et al.2004). This suggests that a single wetland may have multiple RTDs, with each RTD being relevant within a specific range of water depths (Holland et al. 2004).

In addition to short-circuiting, dilution is also an important wetland mechanism to consider. Dilution occurs when an additional water input containing low concentration of NO_3^-, such as from groundwater, precipitation, or overland flow, causes there to be an increase in discharge and a lower concentration of a constituent at the downstream end of the wetland even though the total mass of the constituent has not changed (Shabaga and Hill 2010). Another mechanism occurs when inflowing surface water and water stored in the wetland have different concentrations of a constituent. When the two mix within the wetland, the outlet concentration will be something between the two. This results in a downstream concentration that is different from the current influent (Buda and DeWalle 2009, Kadlec 2010).

In predicting nitrogen uptake within a wetland it is necessary to understand the kinetic order of the reaction that is affecting nitrate. Uptake is the difference in tracer mass measured at the inlet of the wetland from the tracer mass measured at the outlet. A zeroth-order reaction will be independent of the concentration of the reactant and will, therefore, proceed at a constant rate. A first-order reaction will depend on the concentration of the reactant at any given time and will change accordingly over time. A

higer-order reaction depends on the concentrations of multiple reactants (or is non-linearly related to the concentration of one of the reactants) and will change over time as the concentrations of the reactants change. Nitrate removal reactions are often found to be 1st-order reactions. Over four years, nitrate was removed at the Des Plaines River Wetlands Demonstration Project in Wadsworth, IL in a 1st-order reaction with an average removal of 67% and a range of 17-100% (Kadlec 2010).

Groundwater inputs can affect nutrient uptake in the wetland in addition to diluting nutrient concentrations. Mixing of groundwater discharging to the wetland and the surface water can greatly affect the potential for nutrient uptake. For instance, nutrient-poor groundwater entering the system in the floodplain may mix with more nutrient-rich surface water, decreasing the overall nutrient concentration. If there is limited vertical mixing then the combined groundwater-surface water nutrient concentration will be more similar to the groundwater concentration. Not only can groundwater inputs result in changes in nutrient concentrations, but the additional contribution to surface water discharge may reduce the residence time.

Because nutrient removal is dependent on the amount of time that water remains in the wetland it is important to understand the RTD of the wetland. This is often done by introducing a conservative tracer at the inlet of the wetland and measuring the tracer concentration at the outlet of the wetland. One of the tracers that is often used in these

types of studies is Rhodamine WT (RWT). RWT has been observed to slowly sorb and photodegrade which can confound results in studies longer than approximately one week. A study conducted at the Tres Rios Demonstration Wetland facility in Phoenix, AZ used RWT as a reactive tracer and sodium bromide as a conservative tracer to evaluate conservative transport and first-order reactivity of the tracers (Keefe et al. 2004). Since RWT both photodegrades and sorbs to sediment surfaces, controlled experiments were conducted in a laboratory to study each of the two reactions separately (Keefe et al 2004). Keefe et al. (2004) reported 1^{st}-order sorption rates of 2.92×10^{-7} s^{-1} to 5.89×10^{-6} s^{-1} and 1^{st}-order photolysis rates of 1.01×10^{-8} s^{-1} to 9.93×10^{-8} s^{-1}. While the Keefe et al. (2004) study does show that RWT is non-conservative over long periods of time it also shows that at time-scales of less than a week sorption and photolysis are negligible.

This study seeks to understand the hydrology of a small headwaters wetland in an urbanizing watershed. This was done by, first, describing the water budget and determining what the interaction is with groundwater. For instance, inflowing groundwater can dilute existing nitrate, while losses of surface water to groundwater can draw more nitrate into the hyporheic zone where more it is more likely to undergo transformation or uptake. Second, flow patterns and how long water remains in the wetland where described by determining the residence time distribution of the wetland. Lastly, all of this was used to help predict NO_3^- uptake.

CHAPTER 2

SITE DESCRIPTION

The study site, Chestnut wetland, is a small wetland located in Wilmington, MA, in the headwaters of the Ipswich River watershed (Figure 2). The second-order stream Saw Mill Brook flows through the wetland. Its drainage basin is 4.8 km² and is approximately 72% residential, 14% forested, 5% industrial/commercial, 4% agricultural/open field, and 4% wetland with approximately 25% of the basin covered in impervious surfaces (Wollheim et al. 2005). The wetland drainage basin is primarily composed of glacial till with some sand and gravel and small amounts of alluvial deposits (Figure 3).

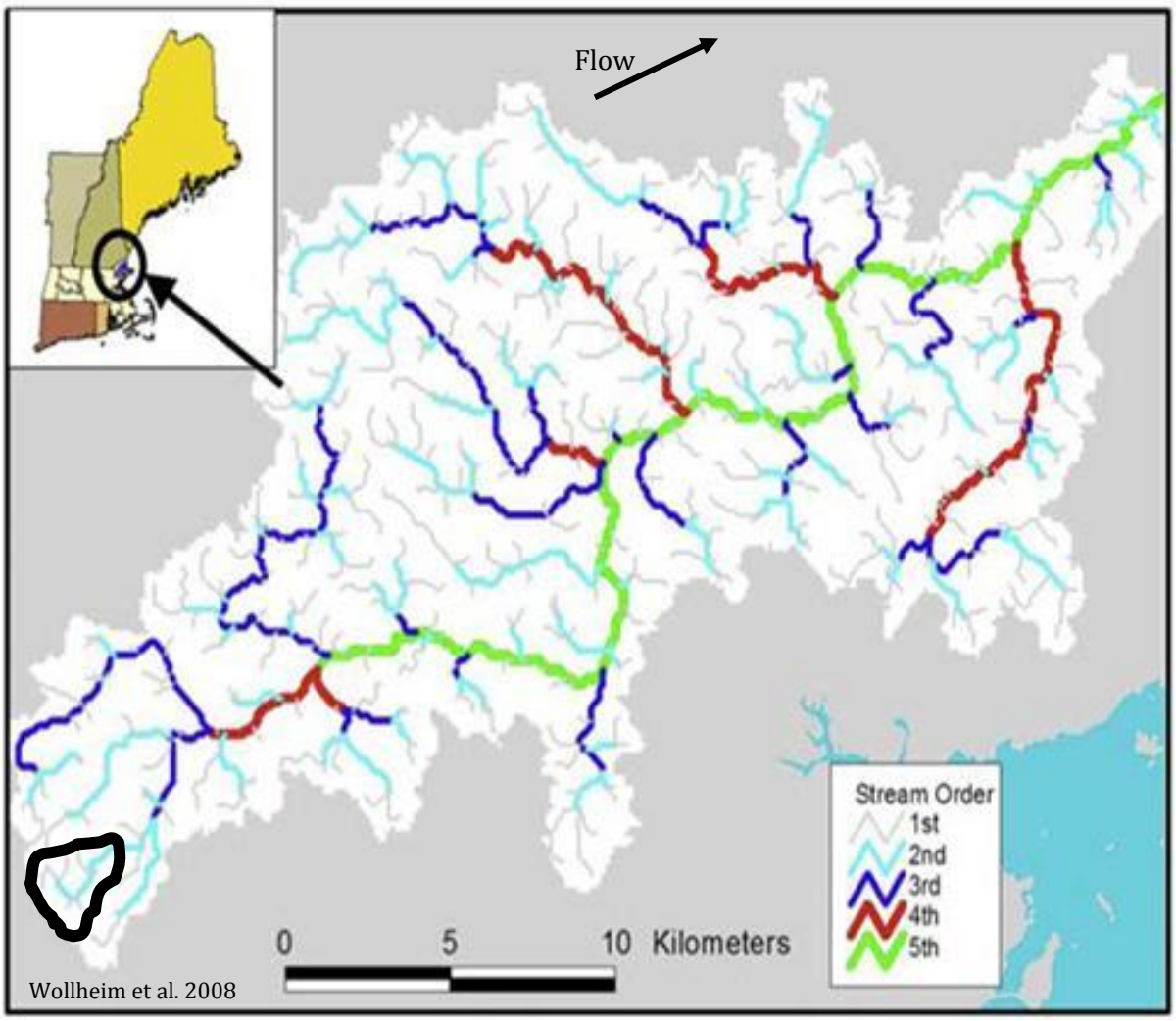

Figure 2– The Ipswich River watershed is located in northeastern Massachusetts and flows east toward Plum Island Sound. The approximate basin of the study site is indicated by the black polygon at the south-western edge of the watershed. Figure modified from Wollheim et al. 2008.

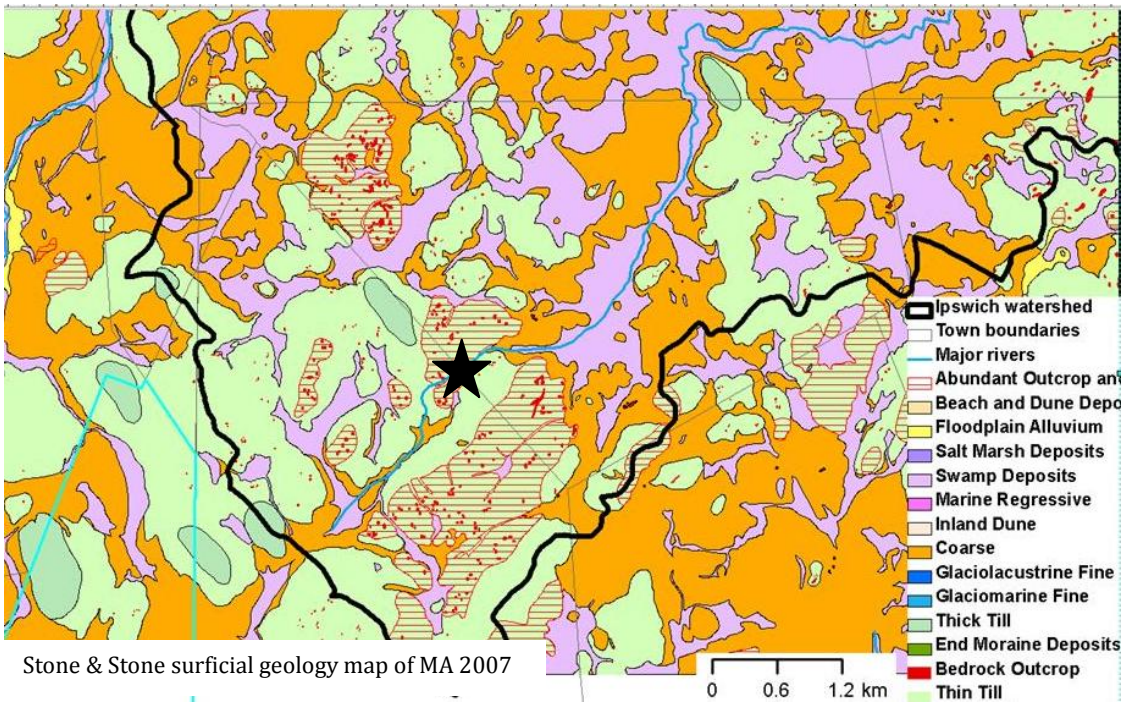

Figure 3 - Surficial geology of the region of the Ipswich River Watershed in which Chestnut Wetland is located.

The site consists of a 450 m reach of Sawmill Brook flows from west to east (Figure 4). The upper 130 m of the reach is a well-defined stream channel, approximately 2-3 m wide and less than 1 m deep,

in a forested area with a closed canopy. The channel bed is primarily cobble and sand with occasional patches of clay. The floodplain on the south edge of the stream is relatively flat with sandy soil, an overstory of deciduous hardwood trees, and minimal understory. The floodplain on the north edge has a steeper slope near the upstream boundary of the site and flattens moving downstream. Soil and vegetation are similar to that along the southern edge. Alterations to the floodplain include several stone walls that parallel the channel and an ATV trail that crosses the channel just below the upstream edge of the study site. Toward the downstream end of this upper section, the vegetation transitions from primarily trees with a clear understory to thick shrubby brush and relatively few mature trees.

(a)

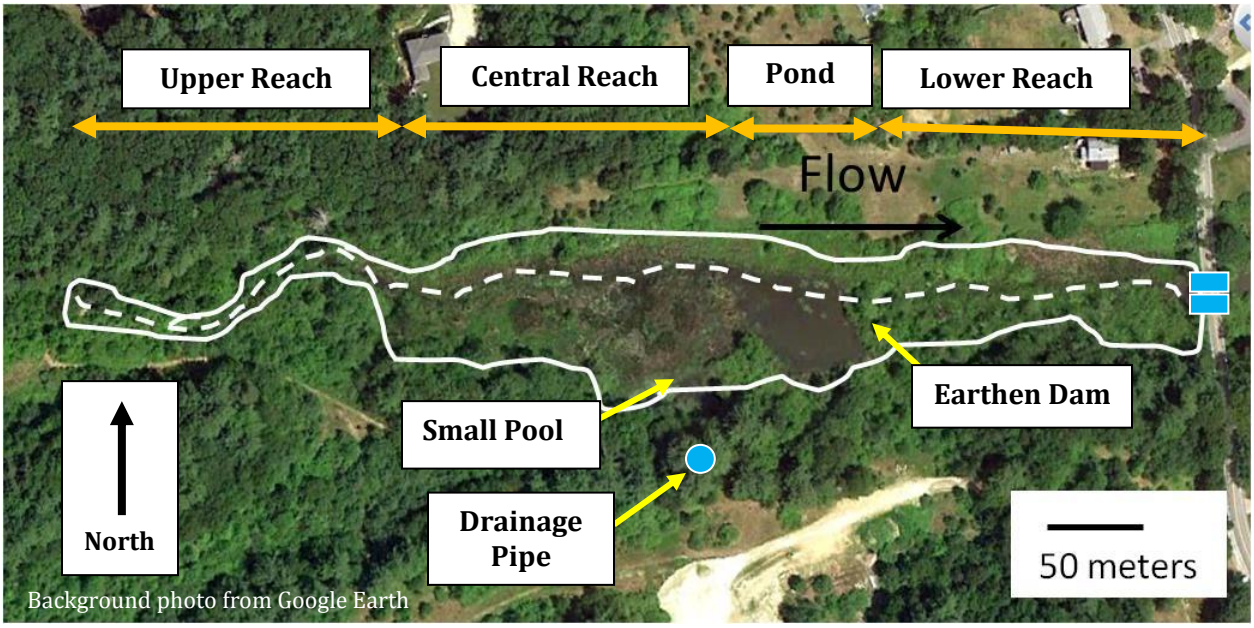

Figure 4– Aerial photograph of Chestnut wetland showing divisions into three smaller reaches. Flow in Sawmill Brook is from left to right. The solid white line indicates the approximate water's edge and the dashed white line indicates the main channel through the wetland. The earthen dam, pond, and small pool are labeled and indicated by yellow arrows. The small drainage pipe is labeled and indicated by a blue dot. The two culverts beneath Chestnut Street are indicated by the two small blue rectangles at the downstream end.

Moving downstream, the well-defined channel then opens up into a wide impoundment with a central deep channel. The channel is approximately 1.5-2 m wide by approximately 0.7-1 m deep. For the first 200 m, the channel is fringed by a marsh platform on either side. The platform on the north edge is narrow, between 4 m and 10 m wide, and contains primarily grasses and cattails. The platform on the south edge is up to 50 m at its widest and contains grasses, cattails, bushes and dead wood trees. There is a small pool (approximately 18 m long by 15 m wide) on the southern edge of the wetland.

An earthen dam constructed from cobbles, earth, and other small debris has created another shallow pond that is approximately 40 m long by 35 m wide by 1 m deep. The upland abutting the northern edge of the central section is primarily lawn with a low slope. The upland abutting the southern edge is steeper and forested with sparse understory. Approximately 80 m into the central section, on the southern edge, there is an outlet from a small concrete drainage pipe approximately 15 m up the slope from the edge of the wetland; the origin of the drainage pipe is unknown but may be from a sandpit or residential development to the south. Drainage pipe discharge is intermittent and only a small amount of moisture is visible near the pipe outlet except immediately after a rain event. Discharge from the pipe at a time of high flow was estimated to be approximately 1.5 L/s, which is much less than surface water discharge through the wetland. No other obvious overland flow into the site was observed.

When water leaves the middle reach, it flows over the dam and continues into the lower portion of the site. This lower portion of the reach is approximately 120 m long and terminates where the stream flows through two culverts beneath Chestnut Street. In the lower reach, the wetland is only about 50 m wide, with a poorly defined channel approximately in the middle. The vegetation in this lower section has fewer grasses and more brush and trees. The northern edge of the lower reach is lawn with a low slope while the southern edge is steep and forested with sparse understory. The wetland substrate in the lower two reaches is composed of organic material, clay, and sand.

A previous study conducted at Sawmill Brook during the 2001-2002 and 2002-2003 water years measured nitrogen loading to and nitrogen export from the wetland. It was found that nitrogen loading to the wetland was 2578 kg km^{-2} yr^{-1} for 2001-2001 and 2581 kg km^{-2} yr^{-1} for 2002-2003 (Wollheim et al. 2005). The total nitrogen export from the wetland was 85 kg km^{-2} yr^{-1} and 78 kg km^{-2} yr^{-1}, respectively (Wollheim et al. 2005). Because the catchment area for the wetland on Sawmill Brook is primarily sewed and therefore has relatively few individual septic systems, it is expected that nitrogen loading from groundwater is less than 15% of the total nitrogen load (Wollheim et al. 2005).

During 2009 and 2010 a study of the Ipswich River watershed was conducted by researchers from the University of New Hampshire and the Plum Island Long-Term Ecological Research Site. One site of this ongoing study is Sawmill Brook at Chestnut Street in Wilmington, MA. Three monitoring stations were established at the site. The upstream location is in the stream channel upstream of the wetland. The downstream monitoring location is at the end of the wetland, just before the culvert under Chestnut Street. At both of these sites discharge and depth were measured in order to create a stage-discharge (rating) curve for each location. The depth of water in the channel was also measured continually using a HOBO stage recorder. Water samples were collected periodically at the upstream and downstream locations and analyzed for dissolved organic nitrogen and a number of conservative ions, including Cl^-. The measured NO_3^- concentrations and Cl^- concentrations were both lower at the downstream location than at

the upstream location. The decrease in Cl^- concentrations is consistent with what would be expected from dilution due to groundwater inputs. The decrease in NO_3^-, however, could be a result of dilution or biogeochemical transformations that occur during the nitrogen cycle. To determine which of these occurred, the ratio of NO_3^- to Cl^- at the upstream location was compared to the ratio at the downstream location over a period of approximately three weeks from June 6, 2010 to July 7, 2010 (Figure 5a). The ratio at the downstream location was consistently smaller than at the upstream location. This indicates that the decrease in NO_3^- concentration at the downstream end is not entirely explained by dilution. It also appears that, in general, the N:Cl^- ratio increases as discharge increases (Figure 5b) which suggests that NO_3^- inputs increase faster than Cl^- during high discharges. Because higher discharges tend to result in shorter detention times, less removal may be occurring at high flow rates.

(a)

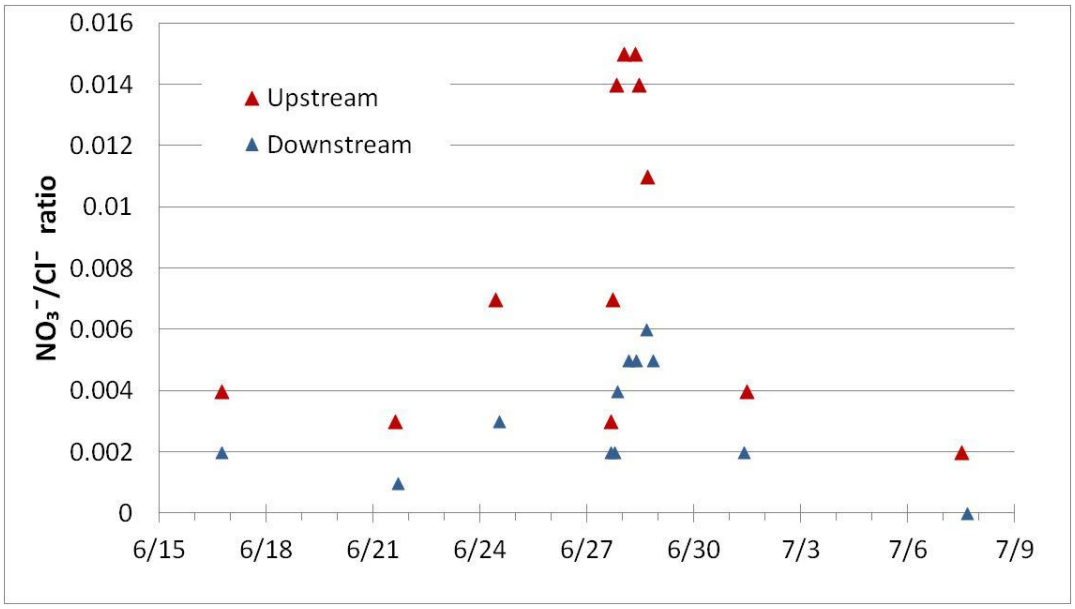

(b)

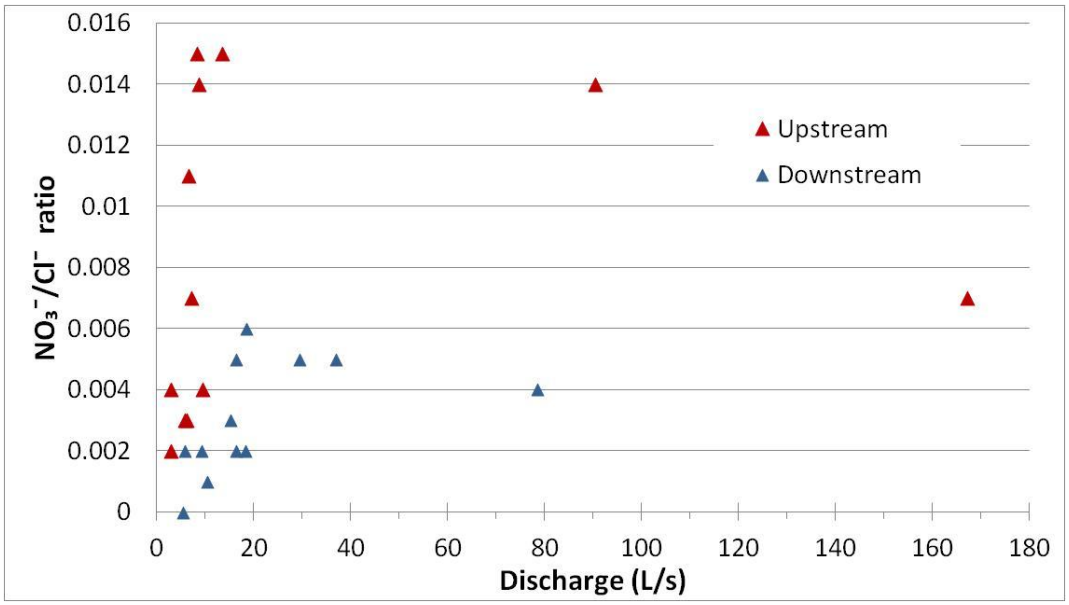

Figure 5– Ratio of NO3- to the Cl+ concentrations (mg/L) (a) over a three week period in the summer of 2010 and (b) the same samples compared to discharge. The ratio is lower at the downstream end indicating the decrease in NO3- from the upstream sampling location to the downstream sampling location is not explained by dilution. The increase in ion ratios in (a) corresponds to a period of higher discharge on June 27 and June 28, 2010.

This study focuses on nitrates rather than other species of inorganic nitrogen, such as ammonia or nitrites, because it is the species that is both readily accessible to plants and algae for the production of biomass as well as the dominant inorganic nitrogen species in the Ipswich River Watershed (Wolhiem 2005). Nitrite is not generally stable enough to occur in high concentrations since it is an intermediate step in the conversion of NH_3 to NO_3^- or vice versa (Kadlec 374). Additionally, NO_3^- is easily dissolved in water and is therefore readily transported in stream channels and groundwater (Smil 67). While ammonium is also easily dissolved in water it tends to bind to some soil minerals, particularly clay, which inhibits downstream transport of nitrogen in this form (Smil 67). This transport of NO_3^- further downstream is what can lead to excessive biomass production in the form of algal blooms and subsequent algal decay resulting in eutrophication in the estuary.

Measurements described here and discussed and analyzed below were conducted at the Chestnut wetland site from June 6 to November 6, 2011. Precipitation in the summer and fall of 2011 was approximately 300 mm/month, which was well above the average monthly precipitation of approximately 80 mm/month (NCDC WBAN station #14739) in Boston, MA.

CHAPTER 3

METHODS

TOPOGRAPHIC SURVEY

A topographic survey was conducted over the course of the summer and fall of 2011 using a Sokkia Total Station (SET5A). The total station was set up at multiple points within the study site. From each station position other fixed control points were surveyed, including other fixed point over which the station had been previously or would later be positioned. In this way, the station was used to leap-frog throughout the reach to obtain continuous topographic data despite thick tree cover through much of the site. Points surveyed from different station positions were rotated and translated into a single reference frame with horizontal origin located on the upstream river-right bank and the vertical origin set at the bottom of the downstream end. Point measurements were then interpolated using Delauney triangulation (MATLAB) to obtain a 0.1 m digital elevation model (DEM).

The total station was used to survey the position of a prism on top of a rod held vertically above the ground to measure the elevation of the ground surface at that position relative to the total station. Where the ground was solid, the target rod was placed so the tip rested on top of the ground. On the wetland platform, where the sediment was primarily

soft mud, the tip of the rod was allowed to sink under its own weight through the softest, upper portion of the muck and then raised so the tip was located approximately in the middle of this soft upper layer. Marsh platform bathymetry therefore accounts for some of the water held within unconsolidated surface sediment. All points where measurements were taken during the tracer studies were surveyed as well as all fixed instruments (e.g. stilling wells and transect points). The total uncertainty associated with survey measurements is 0.68 m in the horizontal plane and 0.05 m in the vertical plane, estimated from repeated measurements of the same fixed points from different station positions.

The thickness of the substrate within the wetland was estimated by inserting a 1.5 m length of rebar to the depth of refusal, possibly representing a solid rock surface. The measured depths, taken at six locations scattered throughout the marsh platform, ranged from less than 0.5 m to over 1.5 m below the platform surface with no obvious pattern (Figure 6).

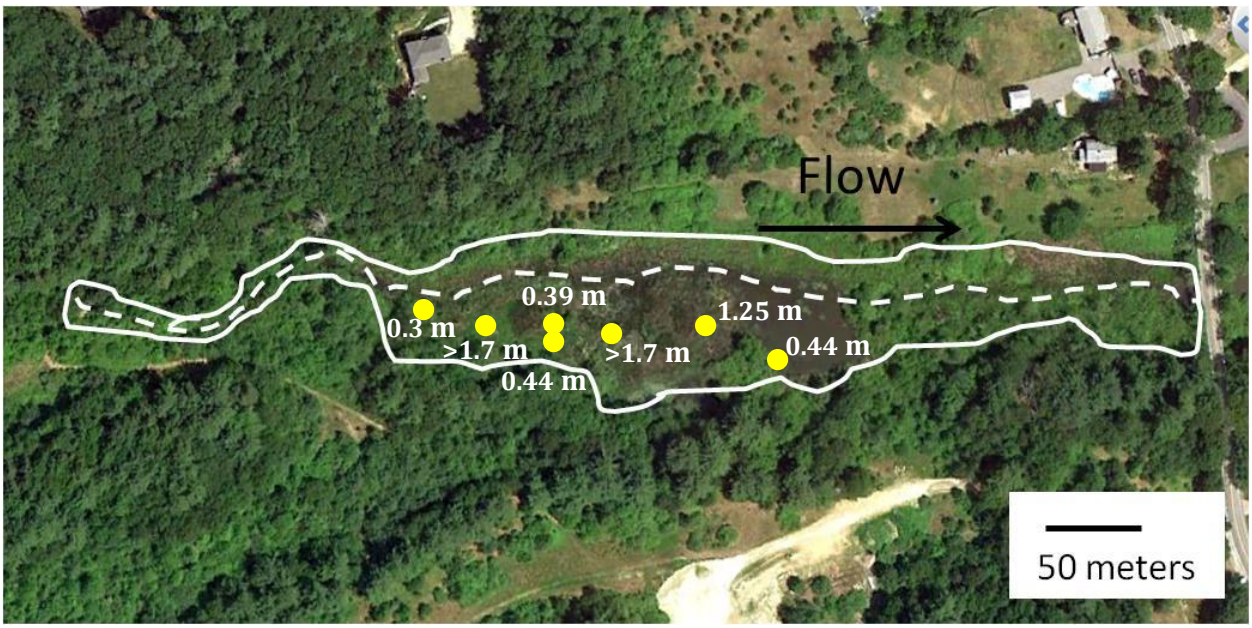

Figure 6– The approximate locations at which substrate thickness was measured are indicated by the yellow dots. Measured substrate depth is shown next to each location.

STAGE

Water level (stage) throughout the wetland was continuously recorded at 15-minute intervals using stage recorders. All pressure loggers were deployed by hanging them in perforated vented PVC stilling wells that were installed vertically in the stream bed and stabilized with rebar. Stage in the middle reach of the wetland was continuously recorded using Solinst stage recorders (Model 3001 Levelogger Junior; ±0.01 m) at three locations: one in the main channel of Sawmill Brook, one in the platform, and the third in the pond. Stage was also recorded at the upstream and downstream ends of the site using

HOBO stage recorders (HOBO U20 automatic water level logger; ±0.005 m) (Figure 7). Pressure recorded by the submerged stage recorders was corrected by subtracting simultaneous air pressure measurements recorded by barometric stage recorders on site (a Solinst barometric stage recorder Model 3001 Barologger Gold, accuracy ±0.05%, placed in the platform at the top of a perforated PVC pipe, and a HOBO stage recorder hanging from a tree on the stream bank at the upstream end) to produce a nearly continuous stage record over the 2011 study period.

Shallow groundwater wells were installed in order analyze samples for stable isotopes of water. The wells were constructed of capped and vented perforated PVC pipe and installed close to the edge of the wetland (refer to map). The shallow groundwater wells produced very little water which resulted in few groundwater samples being collected. Locations of groundwater wells were chosen to avoid bedrock or large cobbles below the surface

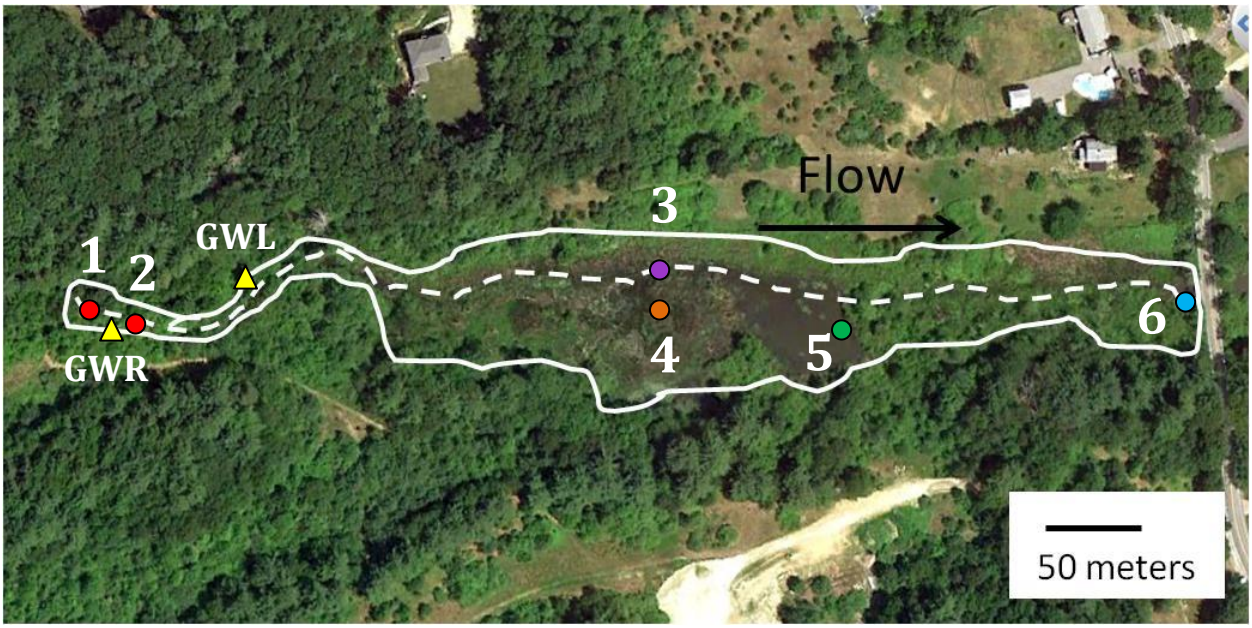

Figure 7– The red dots indicate the locations of the stage recorders throughout the site: #1 – HOBO upstream, #2 – HOBO air pressure, #3 – Solinst channel, #4 Solinst platform & Solinst air pressure, #5 Solinst pond, and #6 HOBO downstream. Yellow triangles near the upstream end indicate locations of the two groundwater wells, GWR and GWL.

Staff gages were installed at both ends of the site. Stages were recorded from these during site visits. The upstream staff gage was positioned with zero on the scale located at the stream bed and the downstream staff gage was positioned with zero on the scale located 0.09 m below the bed. The two staff gages were located approximately 1 m away from the stage recorders. Simultaneous stage measurements from the upstream and downstream loggers and the staff gages were used to develop a consistent relationship between the two (Figure 8). The relationship was linear with a slope of approximately 1, which indicates that a 1 cm change in physical water level is reflected by an equal change in recorded water level. The strong linear relationship between staff gage measurements

and simultaneous stage data recorded by stage recorders allows for the stage data to be reliably converted from logger coordinates to staff gage coordinates and vice versa.

Due to deployment failure, data were not available from the three loggers in the central section of the wetland (loggers #3-5) from 5/24/2011 to 6/7/2011. The mid-channel and pond stage were estimated during this period using a relationship between the downstream stage recorder and the mid-channel stage recorder (Figure 9) and the downstream stage recorder and the wetland platform and pond stage recorders (Figure 10). Due to instrument failure, downstream stage measurements from logger #6 were not available from 7/29/2011 to 8/17/2011. The downstream stage was estimated during this time using a relationship between the stages recorded by the downstream stage recorder and the stage recorder located in the channel in the middle section of the site (Figure 9).

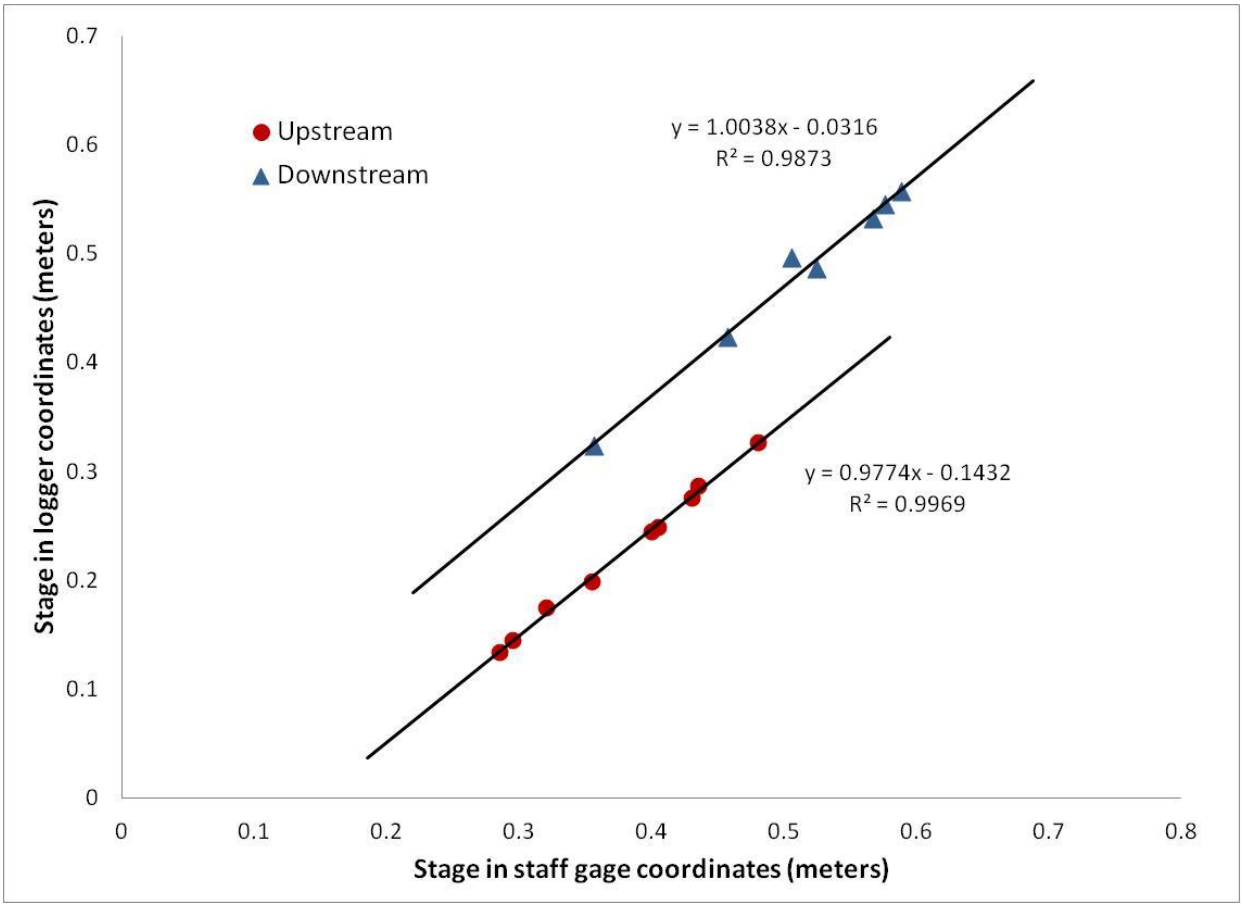

Figure 8–Relationship of simultaneous measurements of stage recorded by a stage recorder hung in a stilling well and the stage manually read off of a nearby staff gage. Data are presented for each of the upstream and downstream ends of the site. Black lines show the best fit linear regression lines for each set of data.

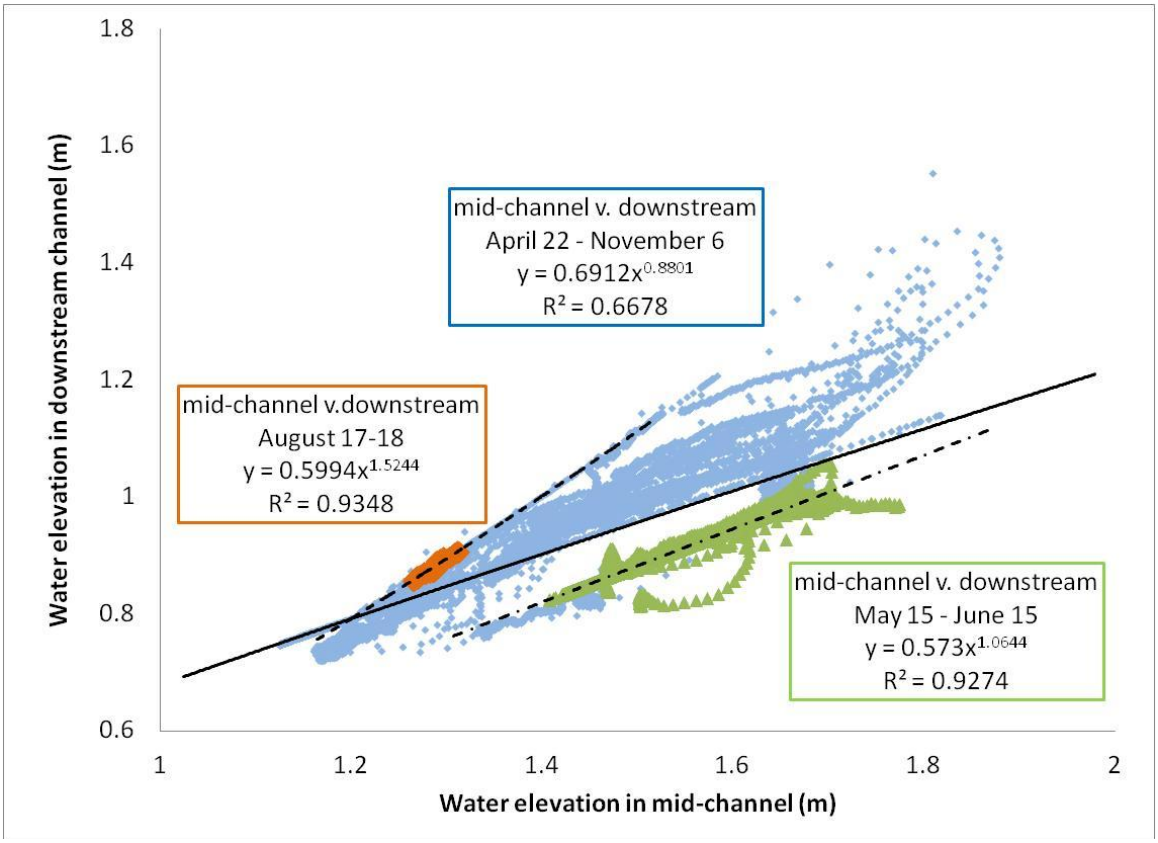

Figure 9– Simultaneous measurements of water elevations at the downstream channel and mid-channel during 2011, along with the best-fit lines. This relationship was used to estimate downstream water elevation between July 28, 2011 and August 17, 2011. The orange points and its associated dashed best-fit line indicate a separate relationship between 1:00 pm August 17, 2011 and 11:45 pm August 18, 2011 which was used to estimate the downstream channel water surface elevation for the previous 18-hour period. The green points and its associated dash/dot best-fit line indicate another relationship from 12:00 am May 15, 2011 to 11:45 pm June 15, 2011 which was used to estimate the mid-channel water surface elevation in the middle of that time period from May 24, 2011 to June 7, 2011.

a) 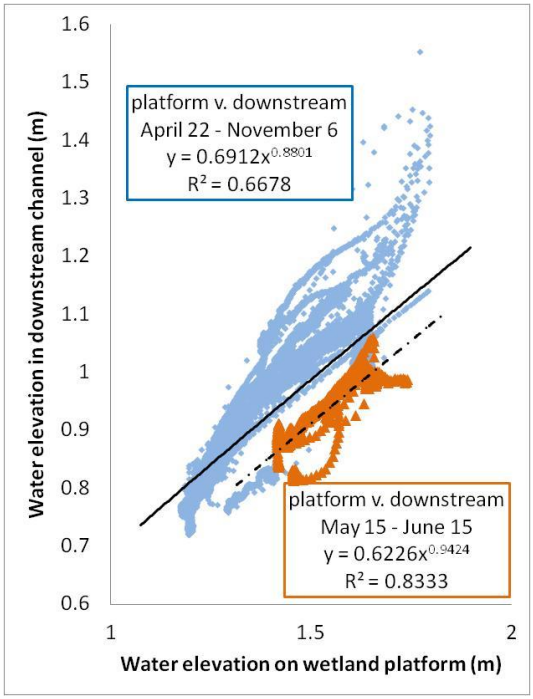

b) 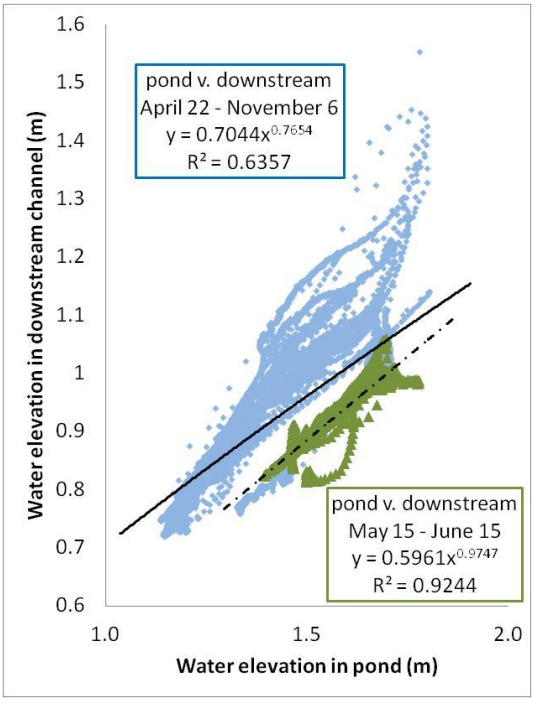

Figure 10 - Simultaneous measurements of water elevations at the downstream channel and a)wetland platform and b) pond during 2011, along with the best-fit lines. The blue points and their associated solid best-fit line indicate all data points available. The a) orange points and b) green points and their associated dashed best-fit line indicate two other relationships from 12:00 am May 15, 2011 to 11:45 pm June 15, 2011 which were used to estimate the platform water surface elevation and the pond water surface elevation, respectively, in the middle of that time period from May 24, 2011 to June 7, 2011.

The distance between the surveyed top of casing (TOC) of the stilling well holding stage recorders and the position of the stage recorder in the casing was measured and used to calculate the elevation of the stage recorders. The data recorded by the stage recorders, converted to depth of water (above the stage recorder) were used in conjunction with the survey data to estimate water surface elevation continuously throughout the wetland

during the study period at the upstream end, middle channel, platform, and downstream end. The water elevation record for the entire wetland was differenced from the DEM of the wetland bathymetry to estimate water depth, wetted wetland area, and submerged wetland volume (storage) on a continuous basis. Uncertainty in the water surface elevation contributed to the uncertainties associated with the water depth, wetted wetland area, and storage. Uncertainty in the DEM was not considered.

DISCHARGE

Stage-discharge relationships at both the upstream and downstream ends of the reach were developed using point field measurements of simulataneous stage and discharge throughout the summer and fall of 2011. Following standard USGS recommendations, monitored cross-sections were located at a straight, narrowing section of the channel, so velocities were higher and the chance of eddies reduced. Point measurements of discharge were obtained using the velocity-area method (Dingman pp 610-611; Figure 11). A measuring tape was strung across the channel at each cross-section and the depth and distance from one bank was recorded at approximately 20 points spaced every 0.2 m plus additional points at each break in bed slope. At each of these points the velocity was measured at six-tenths of the flow depth using a Marsh-McBirney portable flow meter (Model 201D). The area of each segment was calculated via the mid-section method by assigning the depth at each point to half the width between it and the point on each side of it. The velocity measured at each point was multiplied by the area of its respective

segment to calculate that segment's discharge. Segment discharges were summed to calculate the total discharge for that cross-section. Each discharge measurement took approximately 30-45 minutes to complete. Stage was measured on the staff gage at the beginning and end of each discharge measurement; in all cases, stage changed by less than 0.01 ft, confirming steady flow during the interval.

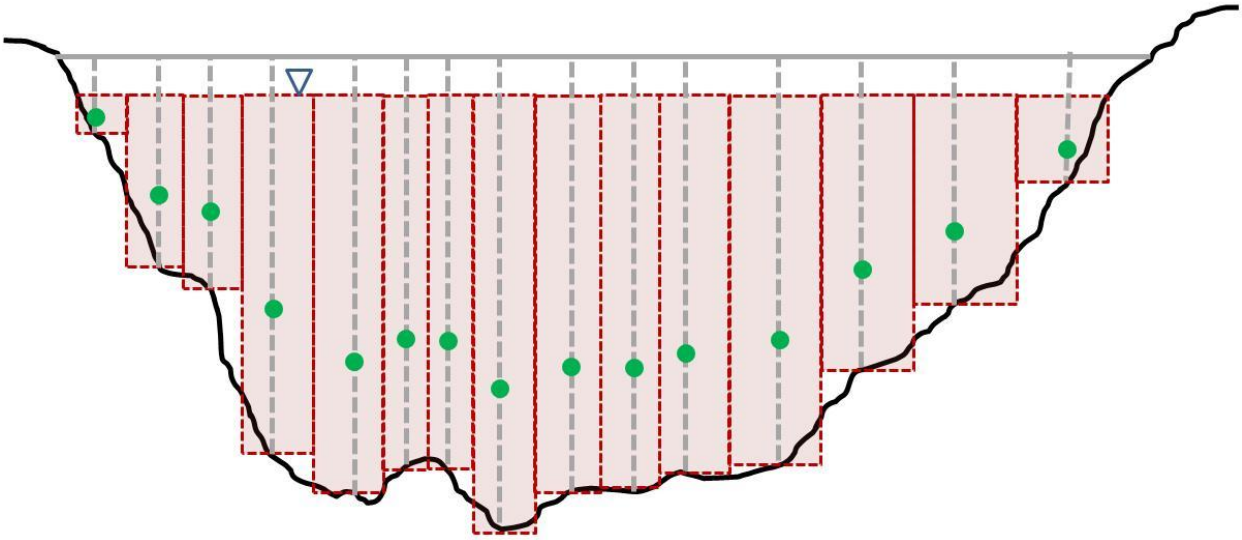

Figure 11– In this illustration of the velocity-area method of discharge measurement, the grey top line is the horizontal tagline, the grey dashed vertical lines are locations where depth was measured, and the green dots are locations where velocity was measured. The red boxes are the segment areas to which each depth/velocity measurement was assigned in order to calculate discharge. The black line indicates the bottom of the channel. The hydrat symbol shows the location of the water surface.

Stream stage during discharge measurements was calculated, when possible, by averaging the measurements from the adjacent stage recorder over the time period during which the discharge was measured. On 5/4/2011 and 5/13/2011, the time of discharge measurements was not recorded, and logger stage was calculated by converting the

observed staff gage reading to logger stage using the relationship shown in Figure 8. On 7/28/2011 no staff gage reading or stage recorder readings were collected at the downstream location. Downstream discharge measurements from this day were not used to determine the rating curve.

The paired point stage and discharge measurements were used to find best-fit power-law rating curves using measured water surface elevation offsets at the upstream and downstream ends of the wetland (Figure 12). The offsets were calculated by finding the difference between the measured depth of water at the stage recorder and comparing it to the water depth recorded by the stage recorder at that time. This allowed the measured water depths to be converted to water surface elevations which were used in the rating curves. The two rating curves were calculated using a log transformation and the associated uncertainties were calculated using the method described by Clarke (1999). Since no measurements were taken in the field at very large discharges there is larger uncertainty in these values, especially when used to extrapolate beyond the highest discharge measurements, which were 180 L/s (0.33 m) at the upstream end and 128 L/s (0.56 m) at the downstream end. Approximately 5% of the measurements recorded by the water pressure recorders required extrapolation from the rating curves.

These rating curves and the stage recorders at the upstream and downstream ends of the wetland were used to calculate a continuous record of discharge into and out of the wetland. Between 9/10/2011 and 10/26/2011, uncharacteristically high stage

measurements recorded by the downstream stage recorder suggest that the stage-discharge relationship at the bottom of the reach had changed, with high stage measurements but relatively low discharge. It is likely that this altered relationship resulted from a blockage in or downstream of the culverts at the lower end of the reach, perhaps due to beaver activity. A second rating curve was estimated for this period. Uncertainty for all rating curves was larger at high discharges. Because the backwater rating curve had only four measurements it had much larger uncertainty than the other two rating curves.

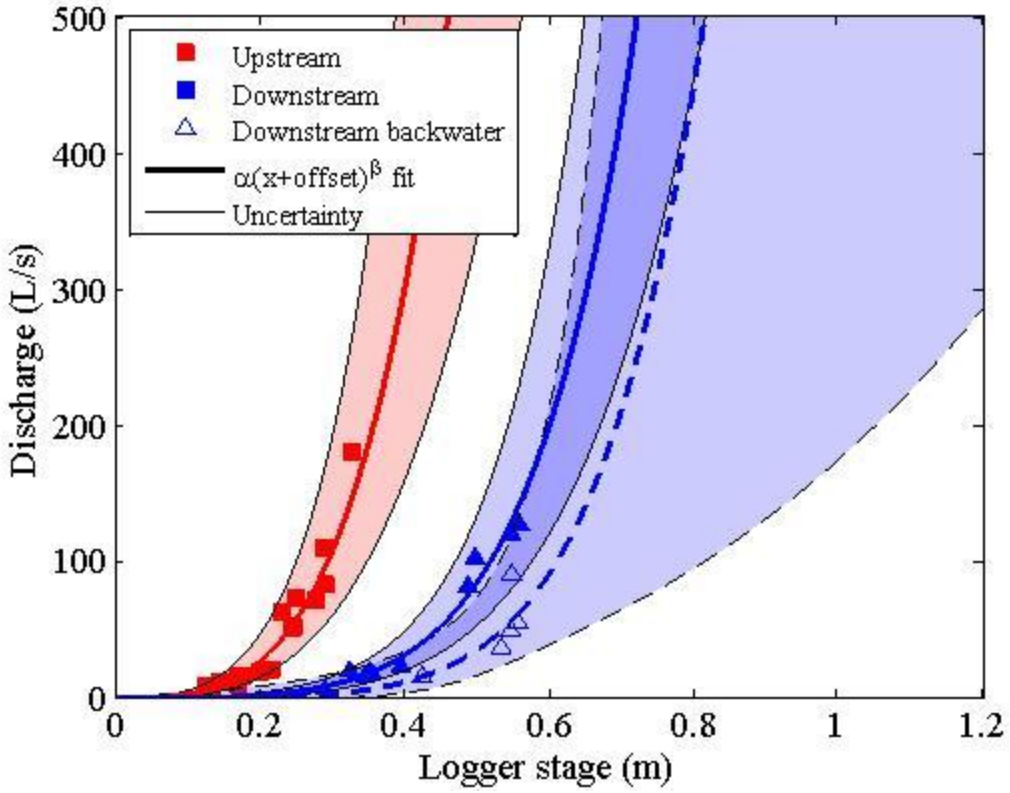

Figure 12– Paired simultaneous stage and discharge measurements at the upstream and downstream ends of the site, along with best-fit rating curves (solid lines). The thick blue and red lines indicate the best-fit lines and the thin lines bracketing these indicate the 95% confidence range. The dashed blue lines indicate the best-fit (heavy line) curve for the period of backwater at the downstream end. The dashed lines and shaded area indicate the 95% confidence range.

The best-fit equations for the rating curves used to calculate discharge are as follows:

Upstream: $Q=7816.7(h+0.043)^{3.9984}$ (1)

Downstream: $Q=534.3(h+0.270)^{7.0131}$ (2)

Backwater: $Q=269.5(h+0.270)^{7.6936}$ (3)

Where Q is discharge in L/s and h is the stage in meters. The uncertainties for the upstream and downstream discharges were calculated using the following equations:

Upstream: $S=-3.4666h^5+10.4127h^4-11.9284^3+6.4451h^2-1.4925h+ 0.2367$ (4)

Downstream: $S=0.2815h^5-0.5173h^4+0.3979h^3+1.4414h^2-0.8656h+0.2527$ (5)

where S is the standard error. For the upstream and downstream discharges, the upper (Q_{high}) and lower (Q_{low}) discharge estimates (with 95% confidence) for each stage measurement were calculated using the following equations:

$$Q_{high}=10^{\log(Q)+2*S} \quad (6)$$

$$Q_{low}=10^{\log(Q)-2*S} \quad (7)$$

where Q is the best-fit discharge. Q_{high} and Q_{low} were used to estimate the largest and smallest discharges expected at each of the entrance and outlet of the wetland.

In the water budget analysis described below the hydrograph was divided into periods of event flow and periods of base flow. Separating these periods was done using hydrograph separation applied to the upstream discharge (Dingman p. 395). The beginning of each event was considered to be the final low discharge immediately before a sharp increase in discharge. A line of slope 0.0936 L/s/hr (converted from slope 0.05 $ft^3/s/mi^2/hr$ given by Dingman and a wetland catchment area of 4.1 km^2) was plotted originating from this point. The point where this line intersects the hydrograph was determined to be the end of the event flow and beginning of base flow.

ATMOSPHERIC DATA AND TEMPERATURE

Water temperature was recorded at 15-minute intervals by all stage recorders at the Chestnut wetland (Figure 7). Air temperature and air pressure data recorded by the HOBO air stage recorder located under a tree canopy near the upstream end of the site were used in calculations of evapotranspiration and evaporation. However, on 8/16 air pressure data were only collected on the wetland platform using a Solinst Baro Logger. During this time period the data from the Solinst Baro Logger were converted from units of meters of water to kPa based on the relationship between the Solinst pressure logger and HOBO pressure logger (Figure 13). Hourly solar radiation data were recorded every 60 minutes by National Climate Data Center (NCDC) WBAN station (#54794) at Thompson Farm in Durham, NH, 70 km NNE of the site. The hourly data were averaged for each day for use in further calculations.

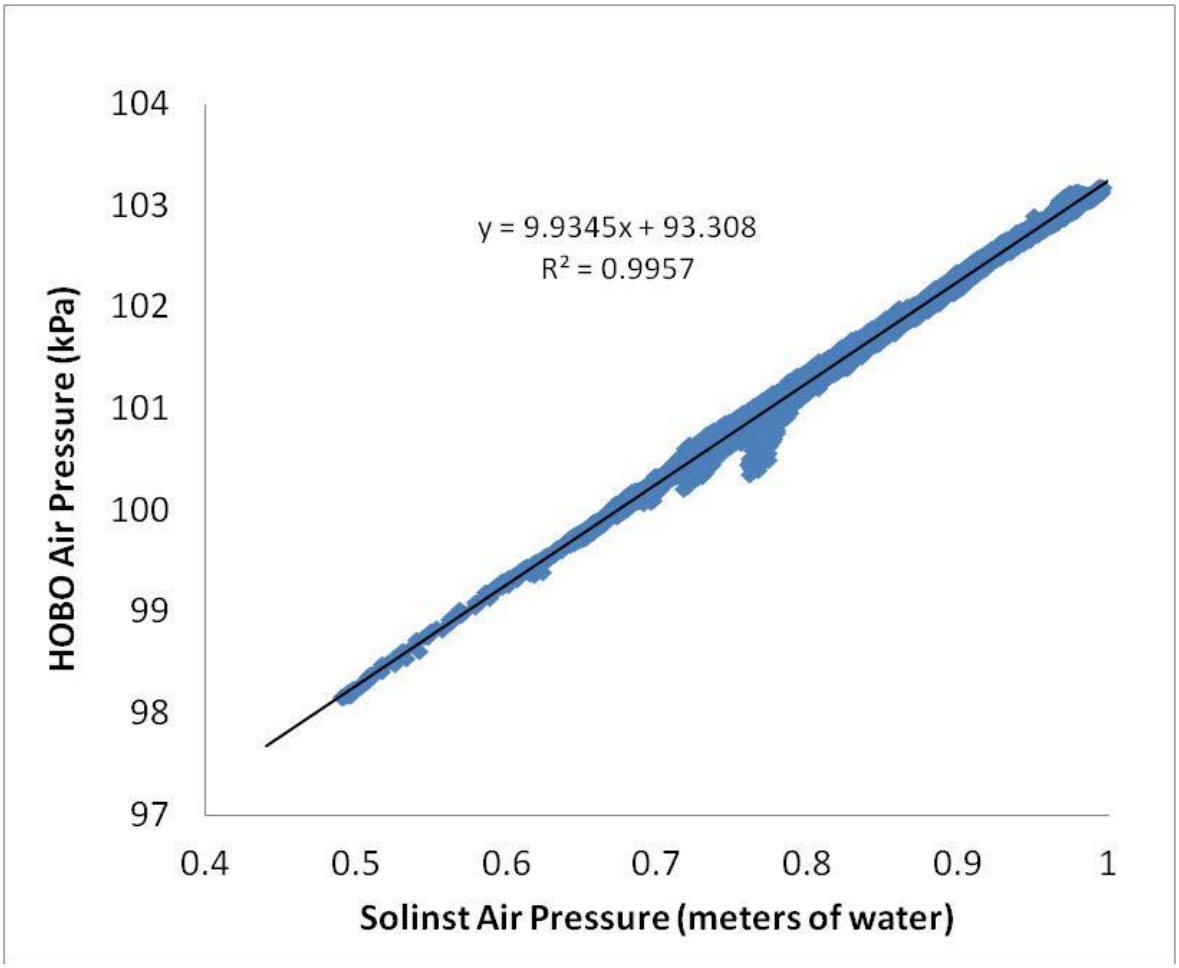

Figure 13– Simultaneous recording of air pressure by a HOBO stage recorder located on the stream bank in the upper section of the site and the Solinst Baro Logger located on the wetland platform. The equation for the linear trend line describes the relationship between the air pressure recorded by the HOBO stage recorder (in kPa) and the Solinst Baro logger (in meters of water).

Wind speed data were recorded every day by NCDC WBAN station (#14739) at Logan International Airport, Boston, MA, located 17 km SE of the site and every day at NCDC WBAN station (#14702) at Hanscom Airfield in Bedford, MA located 12 km SW of the

site. Relative humidity was recorded every day at the Boston station and the Hanscom Airfield station. Dew point was recorded every day at the Boston station. Actual vapor pressure was recorded at the Hanscom Airfield station. Precipitation was recorded at both the Boston station and the Hanscom Airfield station. These data were reported as daily averages from the Boston station and recorded at intervals ranging from 15 minutes to 1 hour at the Hanscom Airfield station. Because of the variability in the timing of data collection, all atmospheric data were converted to daily equivalents before use in subsequent calculations. Further analysis involving precipitation uses the data from the NCDC Boston location. Data from Hanscom Airfield were considered alone and an average of Hanscom Airfield data and Boston data was considered. Neither the averaged precipitation nor the Hanscom Airfield precipitation alone correlated as well with increases in discharge at the Chestnut street site. Due to the distance between the sampling station at Logan International Airport and the study site it is important to note that timing of rain events and amount of precipitation during any event is unlikely to be exactly the same at both locations.

EVAPORATION/EVAPOTRANSPIRATION

Atmospheric data were used to calculate open-water evaporation and evapotranspiration rates using the Penman and Penman-Monteith equations respectively (Dingman 286 & Dingman 299). Variables used in these equations are described in Table 1.

Table 1– Definition and source of variables used in Penman and Penman-Monteith equations.

Variable symbol	Variable	Constant/Equation	Source
Δ	Slope of saturation curve	$\Delta=(e.s-e.a)/(Ts-Ta)$	Calculated
e.s	Saturation vapor pressure at surface	$e.s=0.611*\exp[(17.3*Ts)/(Ts+237.3)]$	Calculated from Ts
e.a	Saturation vapor pressure of air	$e.a=0.611*\exp[(17.3*Ta)/(Ta+237.3)]$	Calculated from Ta
Ts	Surface temperature of water (°C)	--	Water stage recorder on wetland platform at Chestnut site (upstream logger used 5/25-6/7)
Ta	Air temperature (°C)	--	Barometric stage recorder at Chestnut wetland (upstream shaded logger)
ρa	Dry air density	1.22500 kg/m^3	Assumed constant
Ca	Specific heat capacity of air	0.001 MJ/kg*K	Assumed constant
C,at	Atmospheric conductance	$C,at=U/(6.25*(\ln((z_m-z_d)/z_o))^2)$	Calculated
U	Wind speed	Measured	Averaged NCDC data from Hanscom and Boston; wind speed assumed to be measured at height of 10 m (standard NCDC protocol)
Zm	Heigt of wind speed measurements	1.5 m	NCDC documentation
Zd	--	$Zd=0.7*z_{veg}$	Calculated
Zo	--	$Zo=0.1*z_{veg}$	Calculated
Zveg	Average height of vegetation	1.4 m	Estimated by eye at Chestnut site for vegetation within the wetland
Wa	relative humidity	P/e.a	Calculated for NCDC Boston data; given for NCDC Hanscom data
P	Air pressure (kPa)	--	HOBO stage recorder and Solinst Barologger at Chestnut site
Pw	water density	1000.0 kg/m^3	Assumed constant
λv	latent heat of vaporization	$\lambda v=2.495-(2.36*10^{-3})*Ts$	Calculated

γ	psychrometric constant	$\gamma = (Ca*P)/(0.622*\lambda v)$	Calculated
C,can	canopy conductance	$C,can = C_{leaf}*fs*LAI$	Calculated
C_{leaf}	--	$C_{leaf} = C^*_{leaf}*f(\Delta\theta)*f(K_{in})*f(Ta)*f(\Delta\rho_v)$	Calculated
fs	shade factor	0.8	Estimated (cf. Dingman pp. 297-298 and Table 7-5)
LAI	leaf area index	4.0	
C^*_{leaf}	--	6.6 mm/s	
f(Δθ)	soil saturation deficit	0.025 cm	Estimated to be very small due to wetland substrate being primarily saturated
Rn	Net radiation at water surface	--	NCDC Durham data
$f(K_{in})$	function of incoming radiation	$f(K_{in}) = (12.78*Rn)/(11.57*Rn+104.4)$	Calculated
f(Ta)	function of air temperature	$f(Ta) = (Ta*(40-Ta)^{1.18})/691$	Calculated
Δρv	humidity deficit	Δρv=saturation vapor pressure – actual vapor pressure	Calculated
f(Δρv)	function of humidity deficit	$f(\Delta\rho v) = 1-66.6*\Delta\rho_v$	Calculated using dew point at Boston & actual vapor pressure at Hanscom

The Penman equation for evaporation is:

$$E = \frac{\Delta Rn\gamma Ke\rho w\lambda vU(e.a)(1-Wa)}{\rho w\lambda v(\Delta+\gamma)} \quad (8)$$

The Penman-Monteith equation for evapotranspiration is:

$$ET = \frac{\Delta Rn+\rho aCa(C,at)(e.a)(1-Wa)}{\rho w\lambda v\left(\Delta+\gamma\left(1+\frac{C,at}{C,can}\right)\right)} \quad (9)$$

The standard error associated with both the Penman and Penman-Monteith method is approximately 1.48 mm/d (Jacobs 2005). Evaporation and evapotranspiration were calculated on a daily basis. Hanscom data and Boston Logan measurements of wind speed and relative humidity were averaged before calculating evaporation and evapotranspiration.

WATER BUDGET

A water budget was constructed for the Chestnut wetland on a daily basis in order to compare known fluxes and estimate unknown fluxes into and out of the wetland. The water budget equation for the Chestnut wetland is:

$$\Delta V/\Delta t = Q_{in} - Q_{out} + PA - ETA + R \quad (10)$$

where $\Delta V/\Delta t$ is the rate of change in the volume of water stored in the wetland, Q_{in} is stream discharge into the wetland, Q_{out} is stream discharge out of the wetland, P is precipitation on the wetland surface itself, ET is evapotranspiration from the wetland surface, and R is a residual which is assumed to be equal to any other fluxes not accounted for, such as groundwater flowing into or out of the wetland. Stream discharge and wetland storage were measured at 15-minute intervals and integrated over each day. The daily precipitation and evapotranspiration rate were multiplied by the daily average surface area, *A*, of the wetland to estimate the volume of water leaving the wetland by

evapotranspiration and entering as precipitation each day. Rearranging equation 3, the residual is given by the following:

$$R = Q_{out} - Q_{in} - P + ET + \frac{\Delta V}{\Delta t} \quad (11)$$

The residual includes unknown shallow and deep groundwater fluxes into and out of the wetland. When the residual is positive net groundwater flux is directed into the wetland. When the residual is negative net groundwater flux is directed out of the wetland.

A simplified version of the water budget equation excludes evapotranspiration and precipitation, which were both found to be negligible portions of the water budget. The resulting simplified residual equation is shown below.

$$R = Q_{out} - Q_{in} + \frac{\Delta V}{\Delta t} \quad (12)$$

A water budget could not be calculated between 7/29/2011 and 8/28/2011 because of instrument failure at the downstream end of the wetland, or between 9/9/2011 and 10/30/2011 because of backwater conditions at the downstream end of the wetland. Uncertainties for Residual are based on the high and low estimates for $\Delta V/\Delta t$ and Q_{out} - Q_{in}, and are calculated using the equations below.

High Residual: $$R_{high} = Q_{out,high} - Q_{in,low} + \frac{\Delta V}{\Delta t}_{high} \quad (13)$$

Low Residual: $$R_{low} = Q_{out,low} - Q_{in,high} + \frac{\Delta V}{\Delta t}_{low} \quad (14)$$

ISOTOPES

Water samples to be analyzed for stable isotopes of water, ^{18}O and ^{2}H (deuterium), were collected eleven times at the downstream and upstream ends of the site. Less frequent samples were taken from the shallow groundwater wells. Samples were collected using a clean syringe, triple-rinsed with sample water, filtered through a 2.0 µm ashed filter, and injected into an acid-washed vial. The vial was also triple-rinsed with the filtered water and filled so there was no head space in the vial. Analysis of these samples was conducted by Mark Green at Plymouth State University where the samples were filtered and analyzed using a Los Gatos liquid water analyzer (uncertainty ±0.8‰ for δD and ±0.1‰ for $\delta^{18}O$). Isotopic composition is reported as per mille using delta notation with references to the isotopic composition of Standard Mean Ocean Water (SMOW):

$$\delta^{18}O = \frac{\left(\frac{[O^{18}]}{[O^{16}]}\right)_{sample} - \left(\frac{[O^{18}]}{[O^{16}]}\right)_{standard}}{\left(\frac{[O^{18}]}{[O^{16}]}\right)_{standard}} \quad (15)$$

$$\delta D = \frac{\left(\frac{[H^{2}]}{[H^{1}]}\right)_{sample} - \left(\frac{[H^{2}]}{[H^{1}]}\right)_{standard}}{\left(\frac{[H^{2}]}{[H^{1}]}\right)_{standard}} \quad (16)$$

where [*species*] is the abundance (relative number of atoms) of each isotope and *D* is deuterium.

The meteoric water line is the linear equation that describes the average relationship between oxygen and hydrogen isotopes in precipitation and when describing the relationship for a smaller region it is called the local meteoric water line (Harmon 1961). The isotopic composition of a precipitation event at a single location will fall somewhere on the LMWL. The isotopic composition of groundwater is the average annual precipitation isotope signal. An evaporative signal represents deviation from precipitation (e.g., meteoric water line), due to different fractionation processes during precipitation and evaporation. Isotope data from the Chestnut Street wetland site were compared to a Local Meteoric Water Line (LMWL) developed for the headwaters of the Lamprey River watershed (Frades 2007). Evaporation can create δD and $\delta^{18}O$ values that deviate from the LMWL in the direction of greater enrichment of heavy isotopes (Frades 2007). Assuming no recent precipitation, the change in isotopic composition between a water sample taken at an upstream location and a sample taken at a downstream location, will be due to some combination of evaporation and groundwater inflow (Frades 2007). \

CONDUCTIVITY

Measurements of electrical conductivity were obtained on 8/5/2011 and 8/15/2011 at several points throughout the wetland (Figure 14) using a handheld conductivity probe (Corning CD55). Readings were obtained after the probe had been in the water for several minutes and the reading had stabilized.

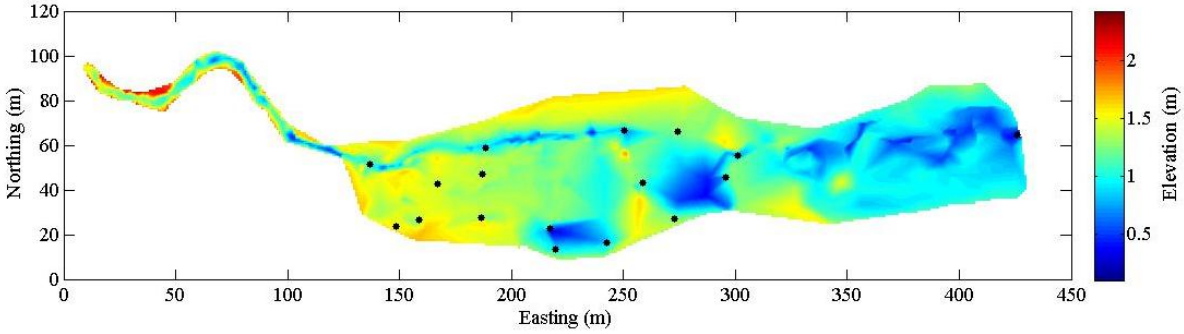

Figure 14- The locations of the conductivity measurements obtained in the wetland are indicated by the black dots.

TRACER STUDIES

Throughout the study period, four tracer studies were conducted using Rhodamine WT (RWT). A submersible fluorometer (Turner Designs C3) was used to measure temperature, relative fluorescence at 570 nm (related to rhodamine WT concentration), relative fluorescence at wavelengths of 685 nm (related to chlorophyll a concentration), and relative fluorescence at 850 nm (related to turbidity). To reduce interference from sunlight, during measurements the fluorometer was oriented vertically above its sampling volume, and a shade cap was used on the fluorometer. Four tracer studies lasting three days each were conducted at least a week apart (often several weeks apart), which was far enough apart that RWT fluorescence after one study decreased to background levels by the start of the following study. The first two studies were started with a slug of RWT released at the upstream stage recorder (logger #1) location, approximately 120 m upstream from the entrance to the central reach of the wetland. For the remaining two studies a slug of RWT was released 30 m upstream of the entrance to the central reach of the wetland. During each release a known volume of stock RWT (20.0 mL, 60.0 mL, 60.0 mL, and 100.0 mL for each of the four studies, respectively) was diluted in a 1 L bottle with stream water and poured across the entire width of the channel over approximately 20-60 seconds. The wetland conditions and tracer study details are summarized in Table 2. Wetland storage was calculated separately for the central section, pond, and downstream section at 15-minute intervals. The average storage of each section for the first 24 hours of each tracer study is reported below.

Table 2 – Summary of wetland conditions for the four tracer studies. Note that the *indicates a value that is estimated. The characteristic discharge of each study is the average discharge of the first 24 hours of the study.

	Tracer Study 1	Tracer Study 2	Tracer Study 3	Tracer Study 4
Date	5/25-27/2011	6/7-9/2011	8/3-5/2011	8/16-18/2011
Tracer release time	10:57 am	12:40 pm	10:57 am	10:48 am
Average downstream Q (L/s)	113	35	17	47*
Mid-channel water depth (m)	1.039*	0.85*	0.57	0.75
Downstream water depth (m)	0.62	0.50	0.43*	0.53*
Tracer volume released (mL)	20	60	60	100
Release location	Upstream end	Upstream end	Wetland entrance	Wetland entrance
Central wetland volume (m^3)	9245*	6059*	2181	4107
Pond storage (m^3)	2337*	1943*	1026	1545
Downstream wetland storage (m^3)	2533	1191	669*	1457*
Average wetland volume (m^3)	14115	9193	3876	7109

Following release, RWT was measured throughout the wetland over a period of three days using a single instrument recording data at 1-2 second intervals. RWT fluorescence were measured in the upstream channel, in the downstream channel, and at eight transects oriented perpendicular to the flow through the wetland (Figure 15). Measurements through the wetland were planned in order to catch the pulse of RWT as it moved through the wetland and to measure the amount of RWT fluorescence exiting the wetland over

time. The RWT was measured as a volume fraction (dilution) and later converted to a concentration using the density of RWT (1.16 g/cm^3).

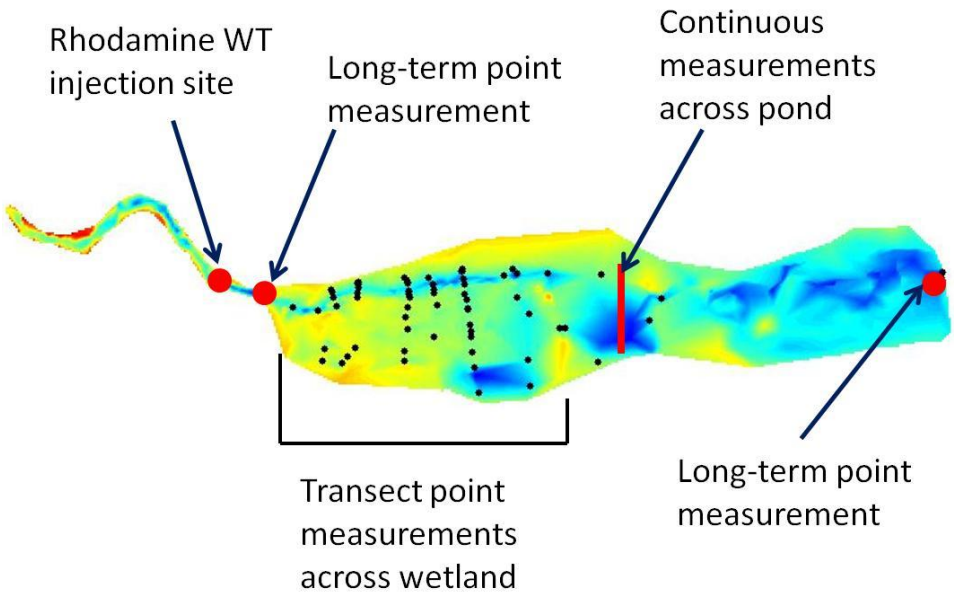

Figure 15– Rhodamine was released 30 m upstream of the entrance to the wetland. Point measurements (small black dots) were located along transects perpendicular to flow. Moving measurements (red line) were taken across the pond. Long-term measurements (red dot) were taken at the entrance to the wetland and the downstream end of the wetland.

Immediately following tracer injection, the fluorometer was attached to rebar located in the channel at the entrance to the central reach of the wetland, at a depth of approximately 8 inches, until the front of the RWT plume had passed the fluorometer. It was also attached to a post at the downstream end of the wetland periodically during each study. Measurements were taken for approximately two and a half days after the tracer was released.

In addition, measurements of RWT concentration were obtained on eight transects perpendicular to flow in order to track the flow of RWT through the wetland. For seven of these transects the fluorometer was deployed by hand on the end of a bent rod. Points along each transect were marked with flagged wooden stakes. During the first study RWT concentration was measured nearly continuously through each transect by keeping the fluorometer in the water while walking along the transect and recorded the time at which each marker was reached. Shallow water in some areas prohibited measurements from being taken at those locations. During the final three studies RWT was measured at fixed points only. If there was enough water present, measurements were taken at each stake and at the midpoints between stakes for 1 to 2 minutes, long enough for suspended material to settle. Before the final two studies, to further reduce sediment suspension caused by the sampling, perforated plastic buckets were inserted into the sediment adjacent to each fixed stake, and fluorometer readings were obtained inside the buckets. Portions of the record with turbidity values greater than 1000 relative fluorescence units (RFU) were later excluded and the remaining RFU measurements were averaged to provide a single value for each position at each depth. On the wetland platform, measurements were taken at a depth of approximately 5-10 cm due to shallow water depths.

One transect was located across the large pond to measure RWT as it flowed through the pond. Measurements were taken on this transect by pulling the fluorometer on a float

across the width of the pond using a single continuous loop of rope marked at 1 m intervals (Figure 16). The time that each mark on the rope reached shore was recorded. Measurements were taken at a depth of approximately 8 inches. On some occasions the clear water above the bottom of the pond was not deep enough to pull the fluorometer across. In this case, measurements were taken at five locations around the perimeter of the pond; in the main channel entering the pond, a small secondary channel entering the pond, the left and right edges of the pond, and next to the stage recorder at the downstream edge of the pond.

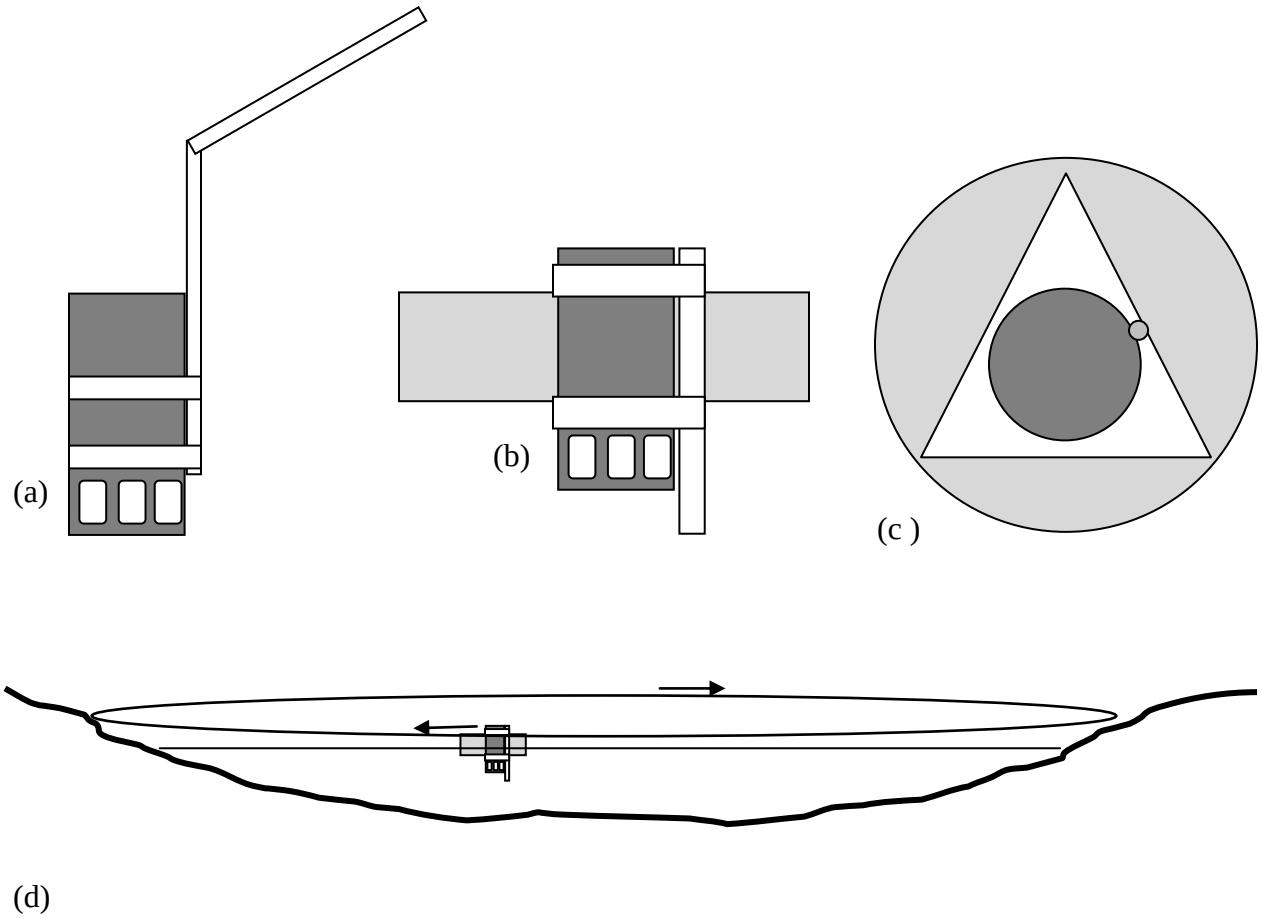

Figure 16– (a) The fluorometer was attached to a hand-held pipe for measurements in the stream channel and in the fringing wetland. Measurements were taken in the water flowing through the shade cap attached to the bottom of the instrument. (b) Side view and (c) top view of the fluorometer and float used in the pond. The light grey circle indicates the foam of which the float was constructed, the white triangle is open space and the small grey circle is the wooden dowel to which the fluorometer was attached. (d) Rope pulley system for pulling the float and fluorometer across the pond (not to scale).

The fluorometer was calibrated in the laboratory by measuring the relative fluorescence units (RFU) of various dilutions of stock RWT in deionized water. A linear relationship between fluorescence and concentration was observed for small concentrations of RWT (r^2=0.996, n=11) (Figure 17). Because the relationship between RFU and RWT concentration changed at approximately 30,000 RFU two separate relationships were developed; one for RFU measurements below 30,000 and one for RFU measurements between 30,000 and 40,000. At values greater than this measurements are not reliable. This is seen in the single point with a known concentration of 10 ppm and an RFU value of approximately 5500. The equation for RFU less than approximately 30,000 is

$$C=(1.034719 \times 10^{-10})F-(5.151253 \times 10^{-9}) \quad (17)$$

and for RFU between 30,000 and 40,000 the equation is

$$C=(2.945506 \times 10^{-5})F-(5.400621 \times 10^{-6}) \quad (18)$$

where C is RWT concentration in parts per million by volume and F is RWT fluorescence in relative fluorescence units.

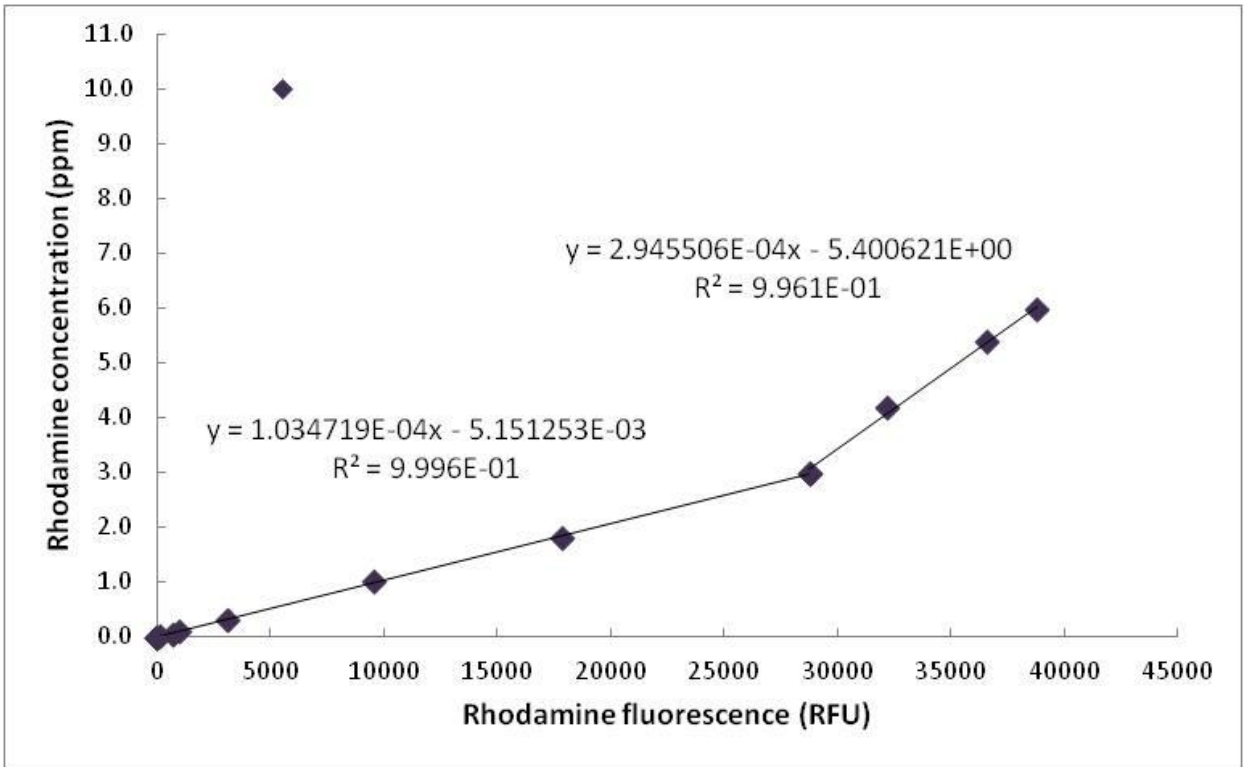

Figure 17– Calibration curve developed in the laboratory that relates measured rhodamine fluorescence (in relative fluorescence units, RFU) to concentration (in parts per million by volume). Two best-fit straight lines are shown for two different fluorescence ranges.

RFU above 40,000 did not exhibit a linear relationship with RWT concentrations. The highest measurements taken in the field were measured at the start of the study at the inlet of the wetland as the pulse of RWT passed the fluorometer and were slightly less than 37,000 RFU. Typical measurements were less than 20,000 RFU. Very high concentrations (greater than 6 ppm) could result in fluorescence values similar to much lower RWT concentrations. However, the color of dye with concentration greater than approximately 5 ppm was visibly distinguishable from lower concentrations of dye, so it

was possible to develop an unambiguous relationship between concentration and fluorescence.

There is a potential for interference with RWT fluorescence by the fluorescence from turbidity, chlorophyll A, and variability due to temperature. Separate investigations of the effects of temperature on RWT fluorescence were conducted in the lab. This calibration indicates that temperature is inversely related to fluorescence. Lab observations showed that temperature changes of about 2°C introduced a change of up to 5% RWT fluorescence. Because the uncertainty in most RWT measurements, due to fluctuations between recorded RFU values, was generally higher than this, typically 10-20% and sometimes as high as 50%, the influence of temperature was not further considered. An analysis of RWT fluorescence and turbidity in the field did not show any clear correlation between turbidity and RWT fluorescence. However, very high turbidity levels were often associated with highly variable RWT fluorescence measurements. Rhodamine measurements obtained simultaneously with turbidity values above 1000 RFU were excluded from data analysis unless the RWT fluorescence measurements were steady and comparable to measurements taken before and after at adjacent locations. For each measurement, the first fifteen and last five data points were excluded from analysis to remove uncertainty introduced while moving the fluorometer into or out of the water. Additionally, any points that were more than three standard deviations from the mean were excluded.

Average background concentrations of RWT were found by averaging RWT fluorescence at the entrance to the central reach of the wetland prior to the arrival of the front of the rhodamine cloud. For each tracer release, the background concentration of RWT was subtracted from the measured RWT concentration values to determine the excess RWT concentration. At the end of the study fluorescence values were within uncertainty of the background, which indicates that the fluorescence had returned to background levels.

RESIDENCE TIME DISTRIBUTIONS

Four tracer studies were conducted to characterize the flow of water through the wetland during different discharges. Tracer study data collected at the wetland outlet were used to calculate the tracer recovery, M_{rec}, in order to compare it with the amount of tracer released.

$$M_{rec} = \sum_{i=1}^{n}(C_{out,i}Q_{out,i}\Delta t_i) \quad (19)$$

where $Q_{out,i}$ is the discharge exiting the wetland at each time i, $C_{out,i}$ is the background-corrected exit concentration, and Δt_i is the time step corresponding to the concentration measurement, calculated using the equation below.

$$\Delta t_i = 0.5(t_i - t_{i-1}) + 0.5(t_{i+1} - t_i) \quad (20)$$

where t_i is the time at which the measurement was taken, t_{i-1} is the time at which the previous measurement was taken, and t_{i+1} is the time at which the following measurement was taken.

RWT concentrations collected at the wetland outlet during the tracer studies were also used to determine residence time distributions (RTD) for water traveling through the wetland during various discharges. The RTD, which is the probability density function for the time it takes different parcels of water to travel through the wetland, was calculated as the flow-weighted RWT concentration observed at the outlet of the wetland following a slug release of RWT at the wetland inlet.

$$RTD_i = \frac{Q_{out,i}C_{out,i}}{\sum_{i=1}^{n}(C_{out,i}Q_{out,i}\Delta t_i)} \quad (21)$$

where $Q_{out,i}$ is the out-flowing discharge during each fluorescence measurement, $C_{out,i}$ is the concentration of RWT measured at the outlet of the wetland minus the background fluorescence, and Δt_i is the time interval for which $Q_{out,i}$ and $C_{out,i}$ are relevant. Equation 21 shows that the RTD was normalized so the area under the curve was equal to 1 which allows easy comparison between studies during which a different tracer mass was released.

Tracer study data were also used to calculate the detention time of the wetland during each study. The detention time, T_d, is the median time that the water actually remains within the wetland and is the first moment of the RTD.

$$T_d = \frac{\sum_{i=1}^{n}(tQ_iC_{out,i}\Delta t_i)}{\sum_{i=1}^{n}(Q_iC_{out,i}\Delta t_i)} \quad (22)$$

SINGLE FLOW PATH MODEL

To determine if the observed RTDs could be predicted using a simple model the RTDs from each of the four tracer studies were compared to model predictions from a tanks-in-series (TIS) equation (Equation 23) for transport of a substance in a single flow path (Kadlec and Knight, p249). A TIS model assumes a number of equally sized continuously stirred tanks in which a fluid travels from one tank to the next in a single direction (i.e. – once the fluid has left a tank it cannot travel backwards to re-enter the tank). The use of a TIS approach allows for longitudinal dispersion in the flow path. The single flow path model assumes a constant discharge between the inlet and outlet. The equation for the outlet concentration of a TIS model given by Kadlec and Knight (p249) was normalized by the measured mean residence time of each tracer study in order to

produce a simulated RTD. Thus, the RTD simulated by the TIS single flow path approach was calculated using the following equation:

$$RTD_i = \frac{\frac{N}{(N-1)!}\left(N\frac{t_i}{T_R}\right)^{N-1}\exp\left(-N\frac{t_i}{T_R}\right)}{T_R} \quad (23)$$

where N is the number of identical tanks in series, t_i is the time since the tracer entered the wetland, and T_R is measured mean residence time for each tracer study. The number of tanks was adjusted manually for each tracer study to produce the minimum deviation between the observed and fit RTDs.

INTERNAL RTD & DECONVOLUTION

Tracer study measurements collected within the wetland interior were used to develop residence time distributions for three subsections of the wetland assuming steady discharge, and taking advantage of the natural segmentation of the site. For the first subsection (upper wetland), RWT concentrations measured at a single point near the end of the central channel were used to construct a RTD for the central channel, and concentration measurements taken along a single transect on the central platform were spatially averaged and used to construct a RTD for the platform. The RTD of the upper portion of the wetland was constructed by weighting these two measured RTDs by the fraction of flow that each conveyed. The fraction of flow entering the wetland that

remained in the channel was estimated to be approximately 70%, though sensitivity to this parameter was assessed and is described below.

For the second subsection (pond), the RTD measured at the exit of the pond represents the convolution of the RTD from the upper wetland with the RTD for the pond. The convolution equation under steady flow conditions is:

$$C_{out,i} = \int_0^T RTD(\tau) C_{in}(t_i - \tau) dt \quad (24)$$

where $C_{out,i}$ is the outlet concentration following a slug release, C_{in} is the inlet concentration, T is the maximum duration of the RTD, t_i is the time since the slug release, and τ is a variable that integrates over the RTD (Cirpka et. al. 2007).

To determine the pond RTD a Monte Carlo analysis was used in MATLAB to produce 100,000 candidate pond RTDs, which were each convoluted with the measured upstream RTD to produce a candidate signal at the pond outlet, which was compared to the concentration measured at the pond outlet. The pond RTD was estimated as the median of the 2500 candidate RTDs with the smallest sum of square error between the synthetic and measured pond outlet RTD.

Similarly, for the third subsection (lower wetland), the RTD measured at the exit of the wetland represents the convolution of the RTD from the two previous sections with the RTD for the lower wetland. To deconvolute these signals, a Monte Carlo analysis was used to produce 100,000 candidate lower wetland RTDs, which were each convoluted with the measured pond RTD to produce a candidate signal at the wetland outlet, which was compared to the concentration measured at the wetland outlet. The lower wetland RTD was estimated as the median of the 2500 candidate RTDs with the smallest sum of square error between the synthetic and measured outlet RTDs.

Sensitivity of nutrient removal to the fraction of flow in the channel was assessed by repeating all calculations assuming 50%, 60%, 70%, 80%, and 90% of flow was transported in the channel with the remaining flow transported over the platform. Sensitivity of nutrient removal to fractionation in the upper section was the highest, ranging from 14%-43% difference in nutrient removal between all fractionation calculations. Sensitivity to fractionation in the pond was moderate with a high of 22% difference in nutrient removal. The lower section had a sensitivity of less than 10% difference in nutrient removal in all three tracer studies.

PREDICTING REMOVAL

Because removal of a non-conservative substance is directly related to the amount of time that the substance remains in the wetland, the RTD can be used to estimate the removal of that substance over time by calculating its concentration at the outlet of the wetland. Assuming a first-order removal process, continuous input of the reactive substance, and steady flow conditions with inlet discharge being equal to the outlet discharge, the outlet concentration, C_{out}, can be calculated using the following equation.

$$C_{out} = \sum_{i=1}^{n} (C_{in,i} \exp(-kt_i)\, RTD) \qquad (25)$$

where C_{in} is the concentration entering the wetland, and k is a spatially uniform and temporally constant volumetric removal rate. For most simulations, a volumetric removal rate, k, of 0.13 d^{-1} was chosen, based on the average uptake velocity, u, 3 cm d^{-1} measured in nearby wetland systems (Wollheim et al. In Review), and an average water depth of the upper platform for each of the tracer studies (Table 3). Sensitivity to the removal rate constant was assessed by also calculating the expected outlet concentration with low and high volumetric removal rate constants of 1 and 10 d^{-1}, also measured in nearby wetlands (Wollheim et al. In Review). The potential nitrate uptake during each tracer study was estimated as a fraction (F_R) of incoming nitrate mass flux using the following equation:

$$F_R = \frac{C_{in}Q_{in} - C_{out}Q_{out}}{C_{in}Q_{in}} \quad (26)$$

where Q is the average discharge during the first 24 hours of the tracer study, and C_{in} is an assumed inlet concentration.

Table 3 - Average platform water depths and range estimated volumetric removal rates for each tracer study.

	Tracer Study 1	Tracer Study 2	Tracer Study 3	Tracer Study 4
Average water depth (m), h	0.25	0.21	0.13	0.23
k (d^{-1}) calculated from u=1 cm d^{-1}	0.04	0.05	0.08	0.04
k (d^{-1}) calculated from u=3 cm d^{-1}	0.12	0.14	0.23	0.13
k (d^{-1}) calculated from u=10 cm d^{-1}	0.4	0.48	0.76	0.44

Similarly, the internal RTDs were used to estimate the amount of time water would remain in each section and the outlet concentration from each section. Cumulative removal was estimated as water traveled through each section and exited the wetland at the outlet. This was done by assuming a constant input concentration to the upper wetland section. The calculated outlet concentration from the upper wetland was assumed to be the inlet concentration to the pond when using equations 25 and 26. In turn, the pond outlet concentration was assumed to be the inlet concentration for the lower wetland. Uptake fractions were calculated assuming a constant volumetric removal

rate constant through the entire wetland as well as spatially variable volumetric removal rates. Analyses with variable volumetric rates assumed a volumetric removal rate of 10 d^{-1} (high of 15 d^{-1} and low of 3 d^{-1}) in one section while keeping the other two the same.

CHAPTER 4

RESULTS

BATHYMETRY

The DEM developed from interpolated survey data is shown in Figure 18. Elevations are relative to an arbitrary zero-elevation at the downstream end of the wetland. The stream channel can be seen in blue along the northern edge of the site and the wetland platform is yellows and green on either side of the channel. The small pool on the southern edge and the pond downstream of that are much deeper. The stream channel in the downstream section is more sinuous and less well defined. There is less difference between the thalweg elevation and wetland platform elevation in the downstream section. The bathymetric survey data were used to estimate the wetland volume and water surface area at any given water surface elevation (Figure 19). Wetland volume (dashed lines) show that volume increases gradually as water surface elevation increases and then increases rapidly when water surface elevation goes over bank. The same in true for the water surface area which changes very little at first and then increases very quick when the water surface elevation tops the bank.

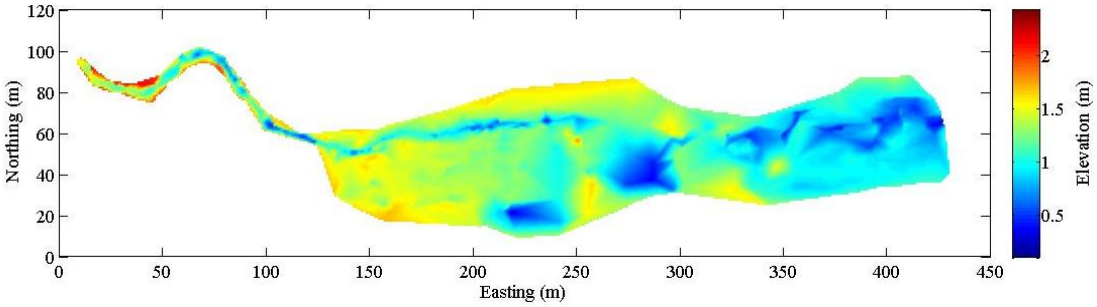

a)

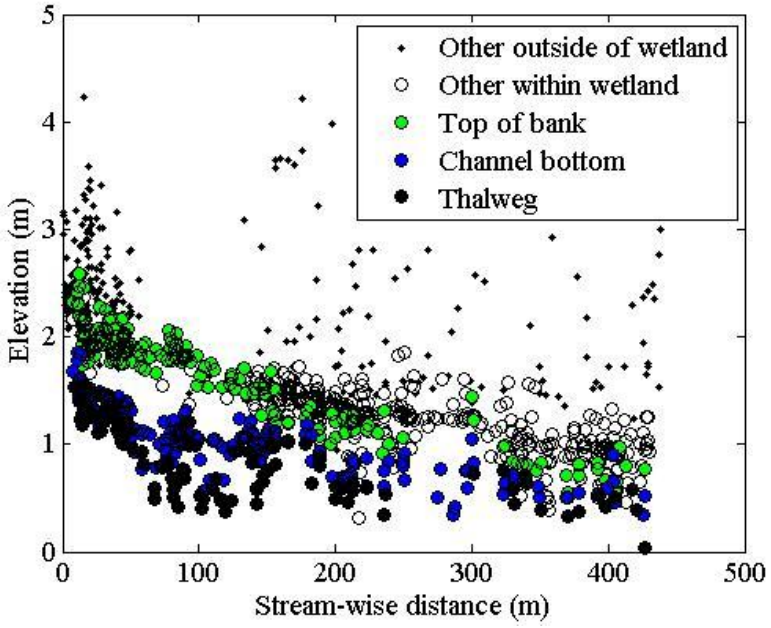

b)

Figure 18- (a) Interpolation of land/substrate surface elevations between surveyed points. The color scale shows the highest elevations in red, followed by lower elevations in orange, yellow, green, teal and the lowest elevation in blue. (b) The profile view of the site shows the vertical elevation changes through the wetland. The thalweg (large black dots) indicate the deepest part of the channel while channel bottom (blue dots) are other measurements take along the bottom of the channel.

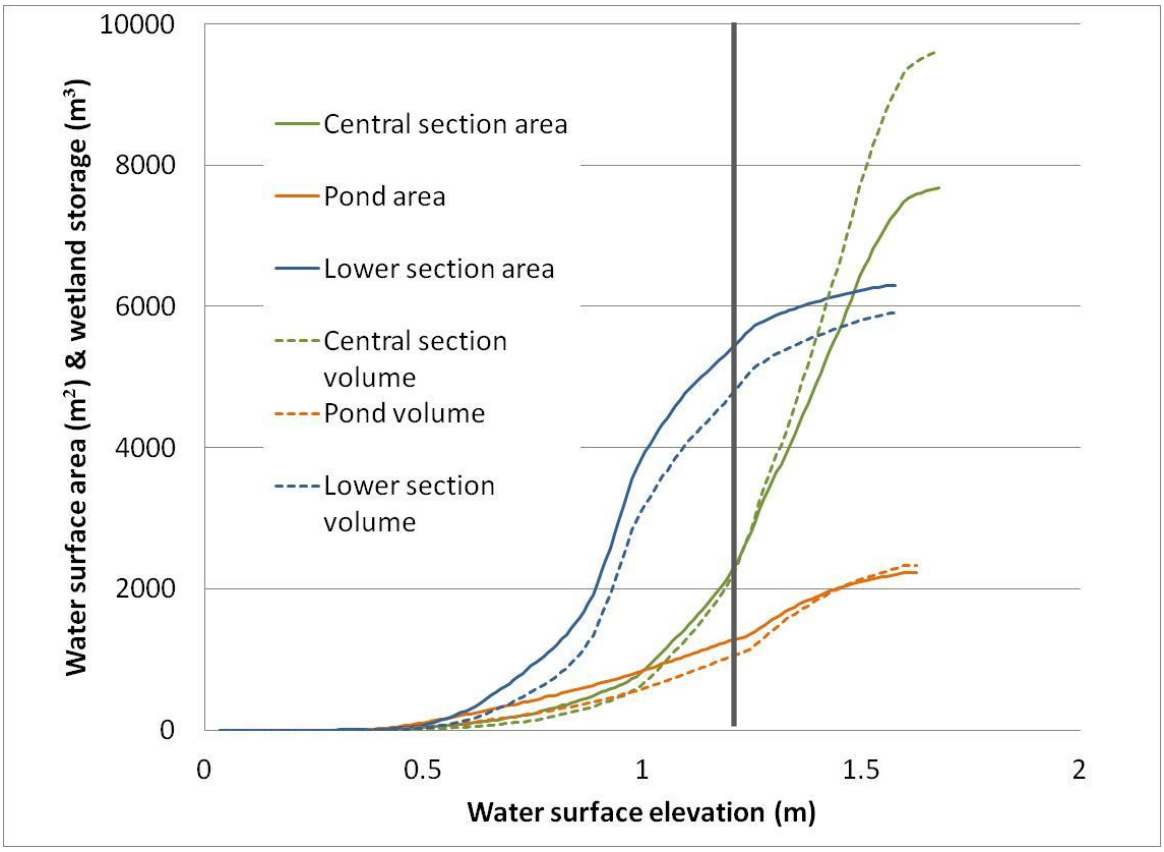

Figure 19– Wetland volume and water surface area as function of water surface elevation (based on recorded stage data) in central section, pond and downstream section as determined from survey data. The black vertical line indicates the approximate bankfull elevation based on topographic survey data in the central section

PRECIPITATION

Precipitation during 2011 occurred throughout the entire study period in distinct rain events of between 1 and 120 mm each with no seasonal trend (Figure 20). The average between May and November was 300 mm/month, which was much higher than the regional precipitation average of 80 mm/month (NCDC WBAN station #14739).

AIR & WATER TEMPERATURE

The air temperature and water surface temperature throughout the wetland are shown in Figure 20. Fluctuations in air temperature were greater than fluctuations in water surface temperature. The temperatures for both increased slowly through mid-summer and then decreased through late-summer and fall. Frequently, increases and decreases in water temperature lagged slightly behind changes in air temperature by 3 to 4 hours. The air temperature recorded at the upstream location was, on average, 1.5° (±4.1°C) lower than the air temperature recorded on the platform. This temperature difference was likely due to differences in vegetation cover: the relatively open platform allowed a greater amount of sunlight to reach the surface than was possible in the forested upper portion of the site. The potential for reduced air and heat flow within the PVC pipe may have also inflated the temperature measurements for the temperature recorder located on the platform.

The water temperature tended to be lower at the upstream end than the downstream end. Later in the fall the upstream and downstream water temperature dropped below those

recorded in the central section of the wetland. The water temperature recorded on the platform was generally higher than the upstream temperature and lower than the downstream temperature. The downstream water temperature often decreased at night so that it was colder than or more similar to the platform water temperature. The temperatures recorded in the central channel and the pond follow the same seasonal trend but lack the diurnal fluctuations seen in the rest of the measured temperatures. At the beginning of October through the rest of the fall, when the temperatures all decrease, the pond and central channel do not decrease as much as might be expected considering the temperature decrease measured at the upstream and downstream ends and on the platform.

Some of the warming that occurs between the upstream and downstream ends could be explained by the more direct sunlight allowed in the central section. However, the central channel water temperature is generally the lowest followed by the pond water temperature (this switches in early October). This could indicate another temperature input, such as cooler groundwater which might draw the water temperature in the channel and pond down. It could also indicate the occurrence of thermal stratification in the central channel and pond with the cooler, more dense water located at the bottom of the water column. At the beginning of October the central channel and pond are the two warmest locations. This is likely due to the relatively high heat capacity of water which causes it to take longer to cool down. It could also be explained by an inflow of groundwater which would be warmer than surface water during the colder months.

In Figure 21 all temperature data are shown at 15-minute intervals during a single event flow/base flow period from 7/9/2011 to 7/13/2011. This figure illustrates the diurnal temperature fluctuations with the highest water temperatures occurring between 2:00 p.m. and 4:00 p.m. and the lowest temperatures occurring at approximately 6:00 a.m. At the upstream end, the highest air temperatures occur at approximately 1:00 p.m. and the lowest occur at approximately 4:00 a.m. Air temperature recorded on the platform also has a low that occurs at approximately 4:00 a.m. However, there are generally two periods of high temperatures; the first occurs at 11:00 a.m. followed by a dip at 1:00 p.m. and another high that coincides with the timing of the high temperature recorded in the water. This drop in the air temperature during the middle of the day is possibly due to afternoon raincloud formation. Overall, the air temperature measured under the canopy at the upstream end does not get as hot during the day or as cold during the night as the air temperature measured on the platform. It is likely that the canopy acts as an insulator by reducing changes in air temperature.

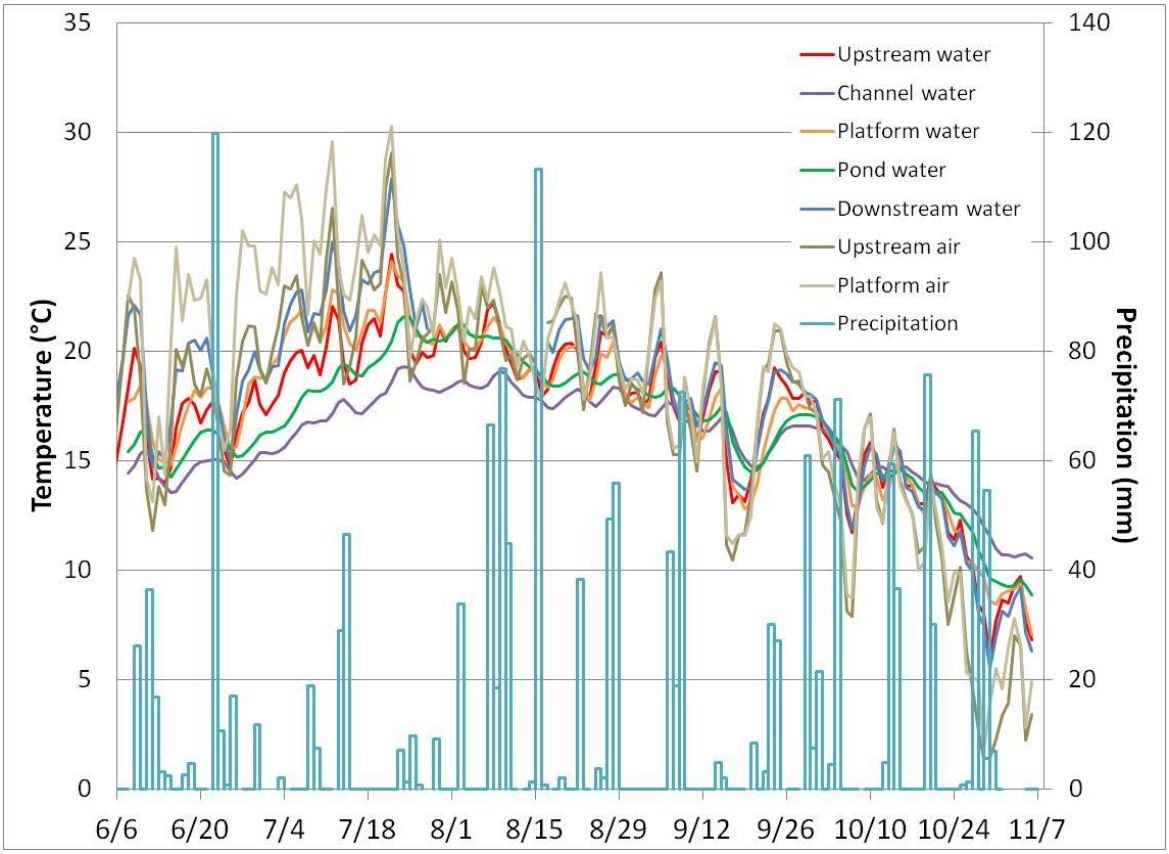

Figure 20– Water surface temperature and air temperatures recorded at 15-minute intervals and averaged over each day throughout the wetland. Precipitation events are shown on the left axis as dotted blue vertical lines.

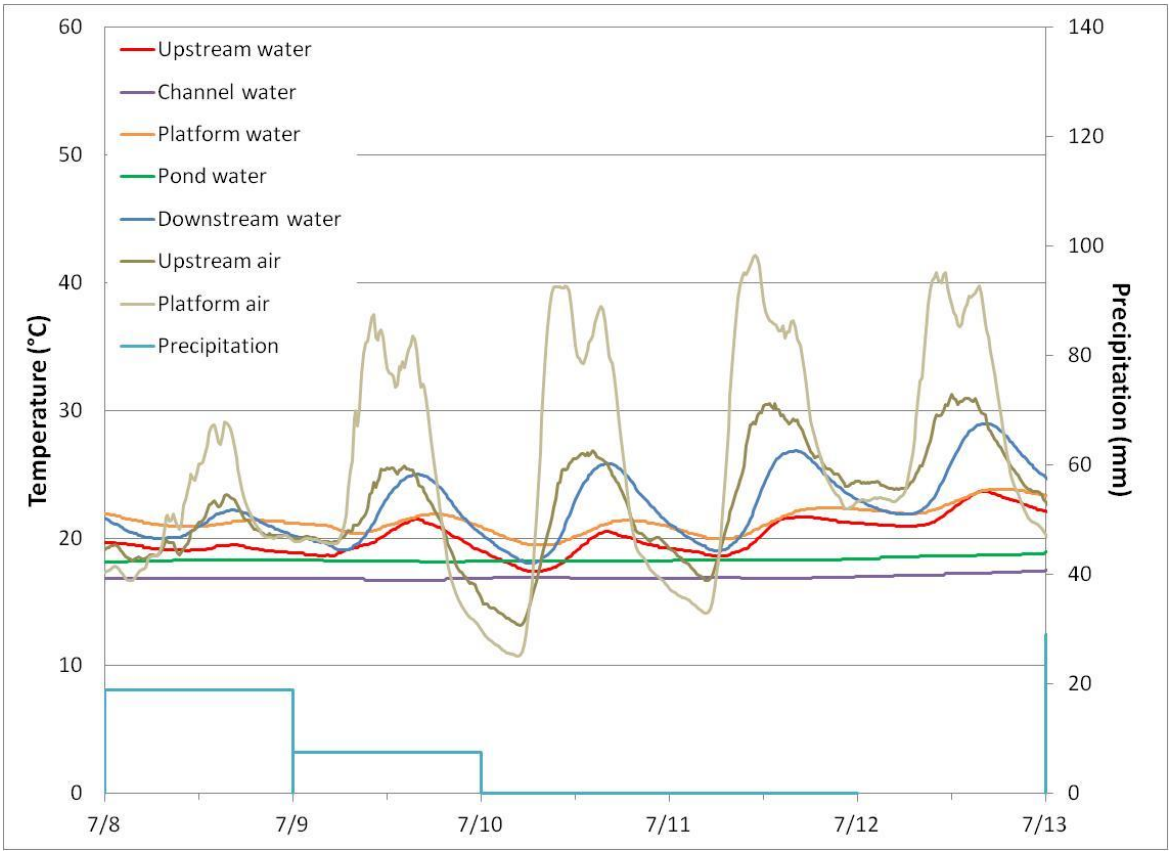

Figure 21 - Water and air temperatures recorded at 15-minute intervals between 7/8/2011 and 7/13/2011. Precipitation is shown as vertical dotted blue lines and is on the right-hand axis.

AIR PRESSURE

Barometric pressure recorded at the site fluctuated throughout the summer and fall with the magnitude of the changes greater in the fall than in the summer, reflecting the passage of several frontal systems in the fall (Figure 22).

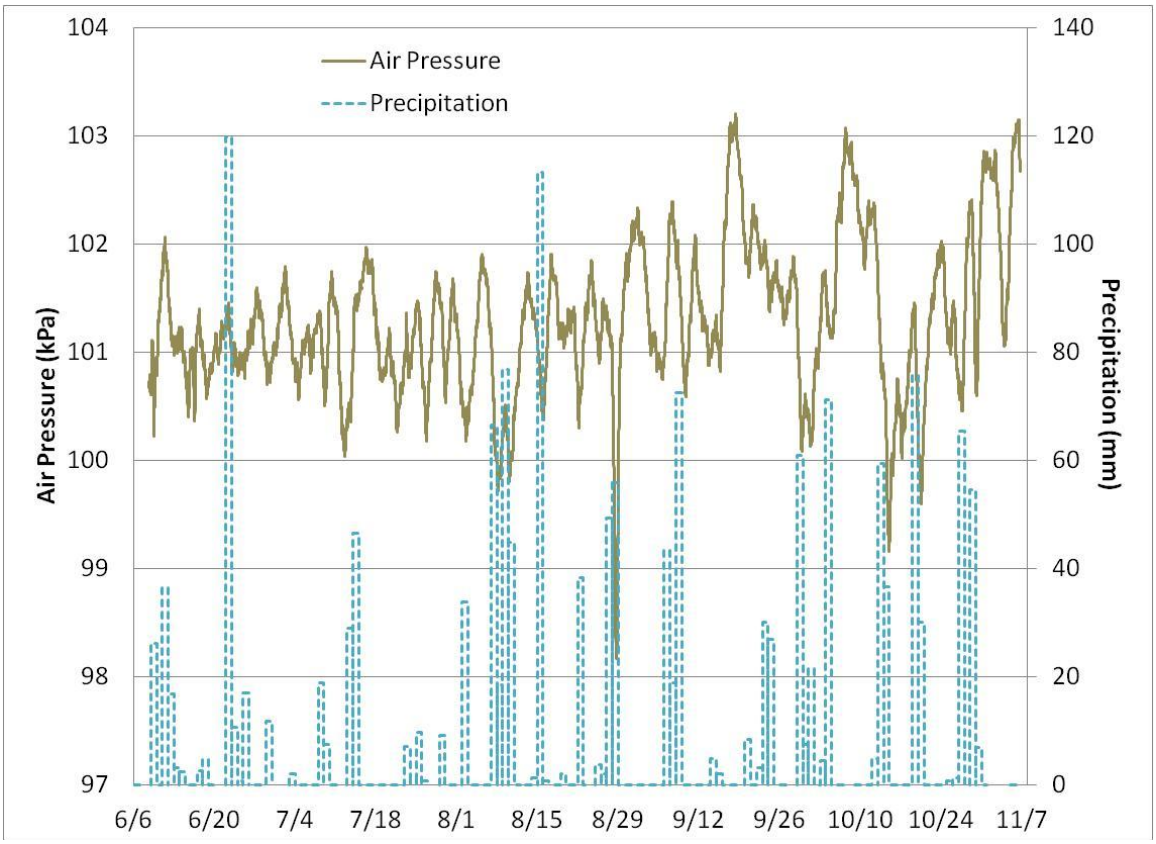

Figure 22– Barometric pressure measured at the upstream end of the site (solid brown, left axis) and precipitation events (dashed blue, right axis).

WIND SPEED

Daily average wind speed, measured at a height of 10 meters, shown in Figure 23, fluctuates day-to-day during the study period. For the most part it is between 2 m/s and 5 m/s with a few days having speeds above 6 m/s. The highest average wind speed, approximately 8 m/s at Hanscom and 12 m/s at Boston, was measured on August 28.

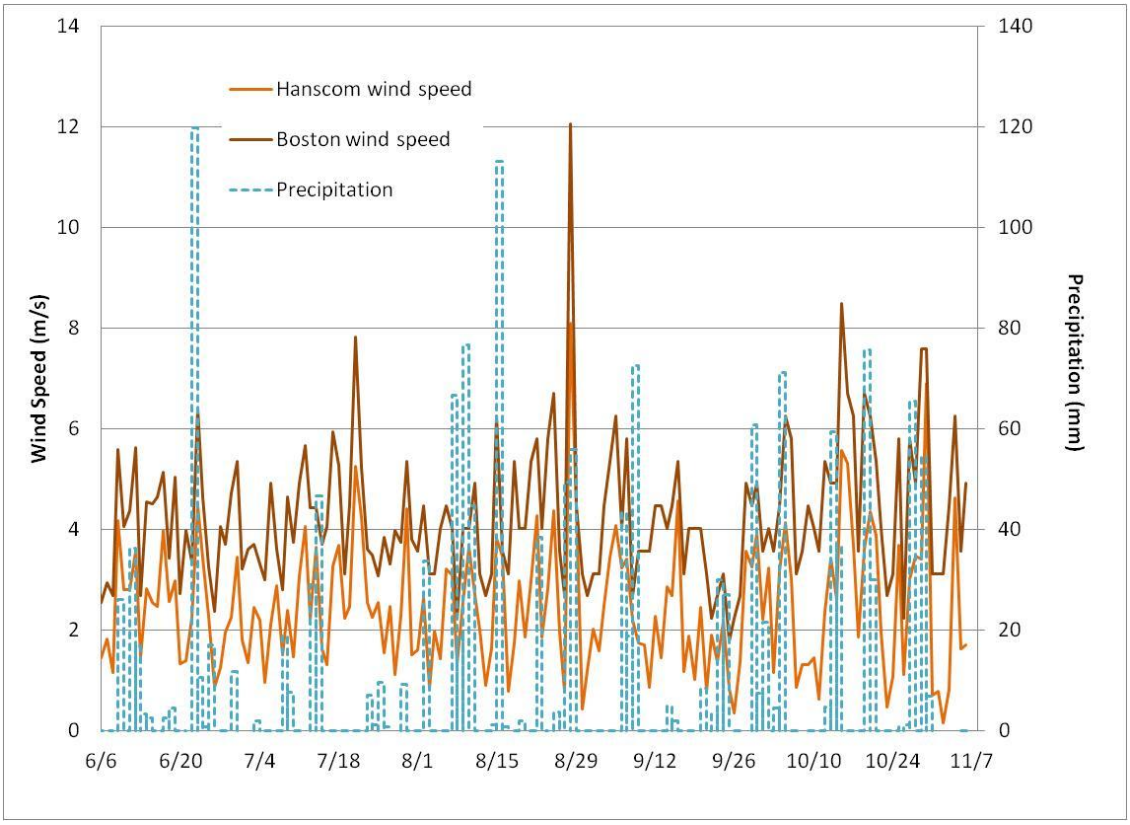

Figure 23– Average daily wind speed measured at Boston-Logan Airport (dark orange) and Hanscom Air Field (light orange) in Massachusetts. Precipitation events (right axis) are shown as vertical dotted blue lines.

NET SOLAR RADIATION

Incoming radiation (Figure 24) varies greatly from one day to the next, likely due to intermittent cloud cover. However, in general, it tends to decrease from 25 MJ/m^2/d in summer to 11 MJ/m^2/d in the fall. As expected, solar radiation is at its lowest on days during which there are precipitation events.

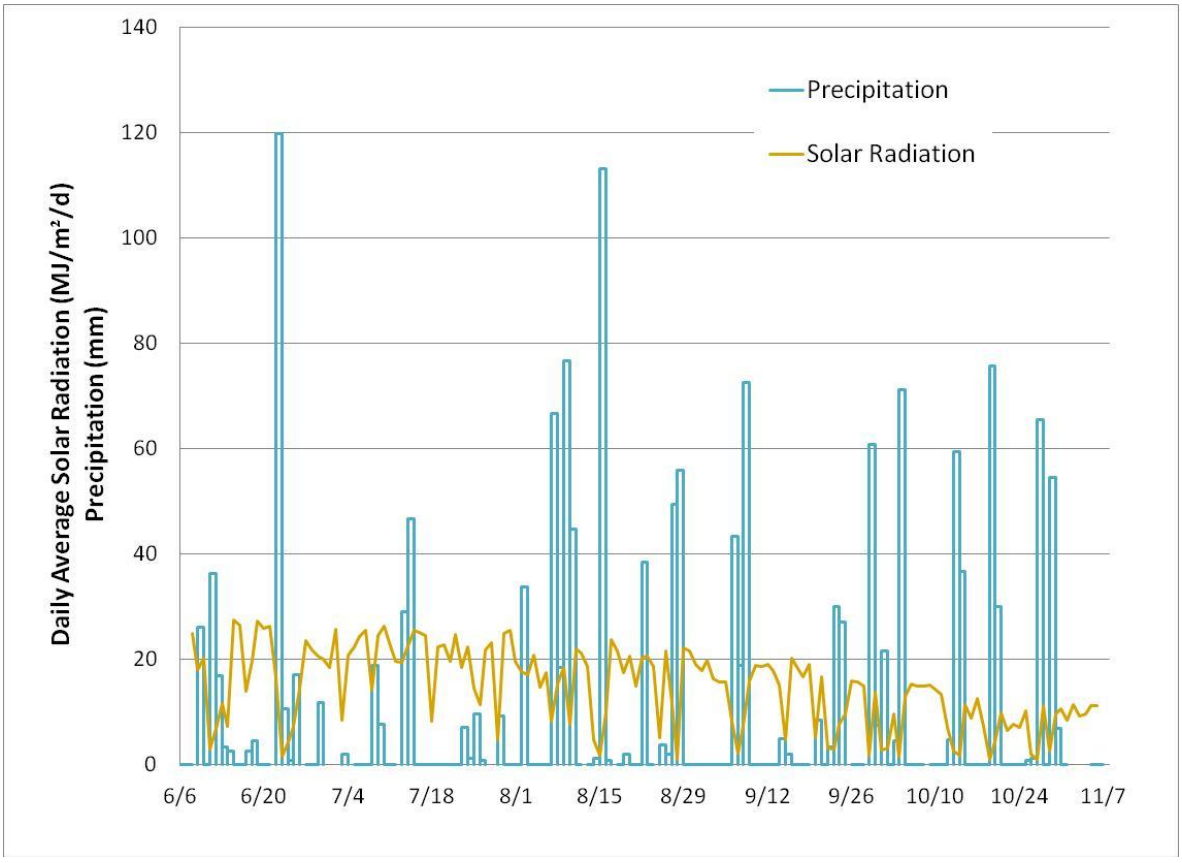

Figure 24– Daily average solar radiation measured in Durham, NH. Precipitation events are shown as vertical dotted blue lines.

EVAPOTRANSPIRATION

Potential open-water evaporation calculated using the Penman equation and evapotranspiration calculated using the Penman-Monteith equation (Figure 25) were within 10% of each other which was smaller than estimated uncertainty. Evapotranspiration increases from approximately 9 mm/d in spring to approximately 35 mm/d in mid-summer and then decreases through the late-summer and fall to less than 1 mm/d at the beginning of November. In general, evaporation and evapotranspiration are similar with evaporation having slightly higher peaks. Due to the small calculated difference, ET rates from the Penman-Monteith equation were assumed to represent both vegetated and unvegetated areas and were used in subsequent calculations.

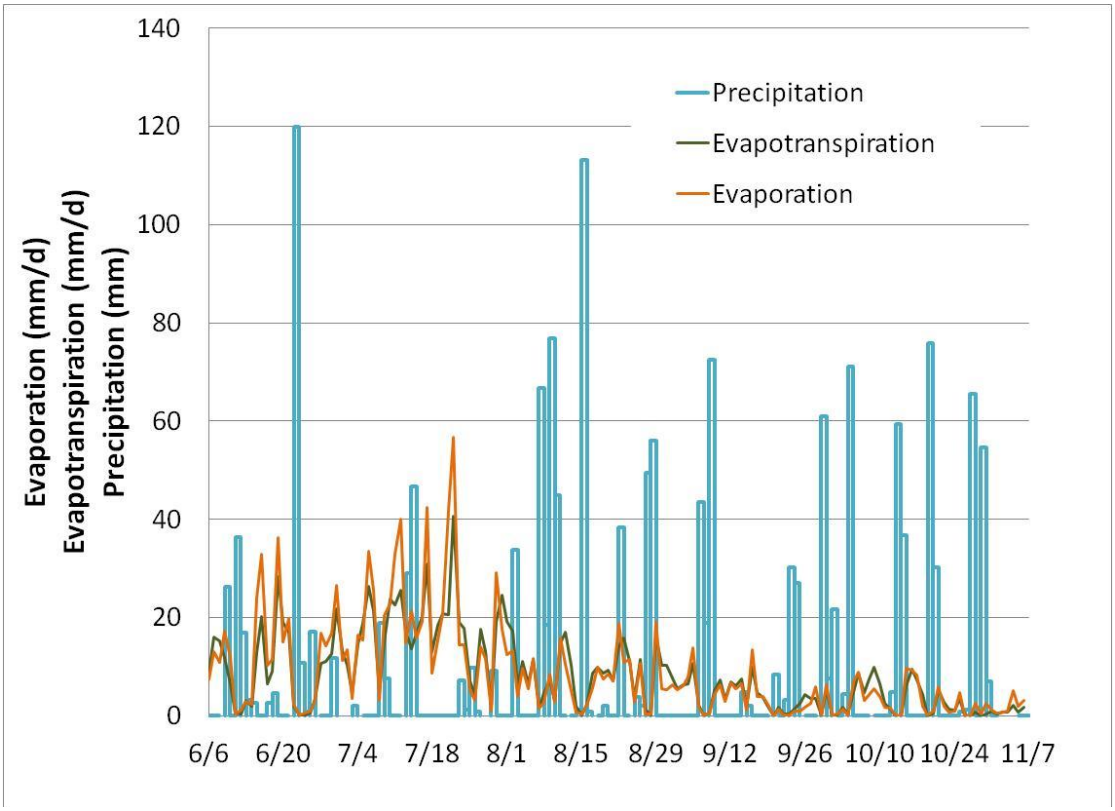

Figure 25 – Evaporation (orange) calculated from the Penman equation and evapotranspiration (green) calculated from the Penman-Monteith equation. Precipitation is shown as vertical dotted blue lines.

STAGE

Stage increased following precipitation. Within 24 hours of a rain event, wetland water surface elevations during 2011 rapidly rose generally between 5-10 cm (never more than 50 cm) over a period of approximately 6 hours, followed by a slow recession to base level (Figure 26). Increases in stage occur less than one day after a rain event.

Seasonally, there was a general decrease in stage through most of June, punctuated by several large precipitation events. Stage continued to gradually decrease through mid-summer. From mid-summer through the fall the stage increased to the level it was during the spring. These seasonal changes were greatest at the downstream end and central section, amounting to approximately 5-10 cm in seasonal change. In addition, there is a backwater that occurs only at the downstream end from September 9 to October 29, 2011. The backwater, possibly from beaver activity, results in the stage being kept higher than expected at the downstream end.

The relative elevation of the water surface between each location indicates the direction of flow between measured locations. In all cases, the water surface elevation was highest at the upstream end of the site, and then decreased as water flowed downstream through the wetland. The water surface elevations in the mid-wetland channel, pond, and on the platform were similar throughout the season. In general, the water surface elevation is greatest in the channel followed by the pond water surface elevation and the platform water surface elevation indicating that water flows from the channel onto the platform.

From 7/19/2011 to 8/7/2011 the stage recorded on the platform are considered unreliable The recorded platform water surface elevation during this period was relatively stable at approximately 1.19 m, and was usually higher than recorded channel water surface elevation, possibly reflecting peat moisture levels, or possibly a measurement artifact resulting from water trapped in the stilling well even as water levels throughout the rest of the platform decreased below the platform elevation.

Figure 27 shows the stage record during two event flow-base flow periods. The first occurs from 7/9/2011 to 7/13/2011 and occurs prior to the platform substrate drying out. The second occurs from 7/23/2011 to 7/25/2011, during the platforms dry period. During the first storm event (Figure 27 a), the stage at the upstream end and within the central section of the wetland rises and then drops back down relatively quickly while the stage at the downstream end takes much longer to decrease. Throughout the peak flow and base flow periods the platform stage is below the channel stage. This indicates that through the entire event, water is flowing from the channel onto the platform and either returning to the channel or the pond downstream.

Similarly, the second storm event (Figure 27 b), the upstream stage rises and falls much quicker than the stage at the downstream end. However, the platform stage doesn't start to rise until the channel stage reaches its highest point and the platform stage peaks shortly after that. As the channel stage drops, the platform stage very gradually decreases

and is eventually higher than the channel stage. This indicates that at the peak flow the platform is finally able to be accessed. As the water elevation in the channel drops below the platform substrate elevation, water on the platform gradually drains back into the channel.

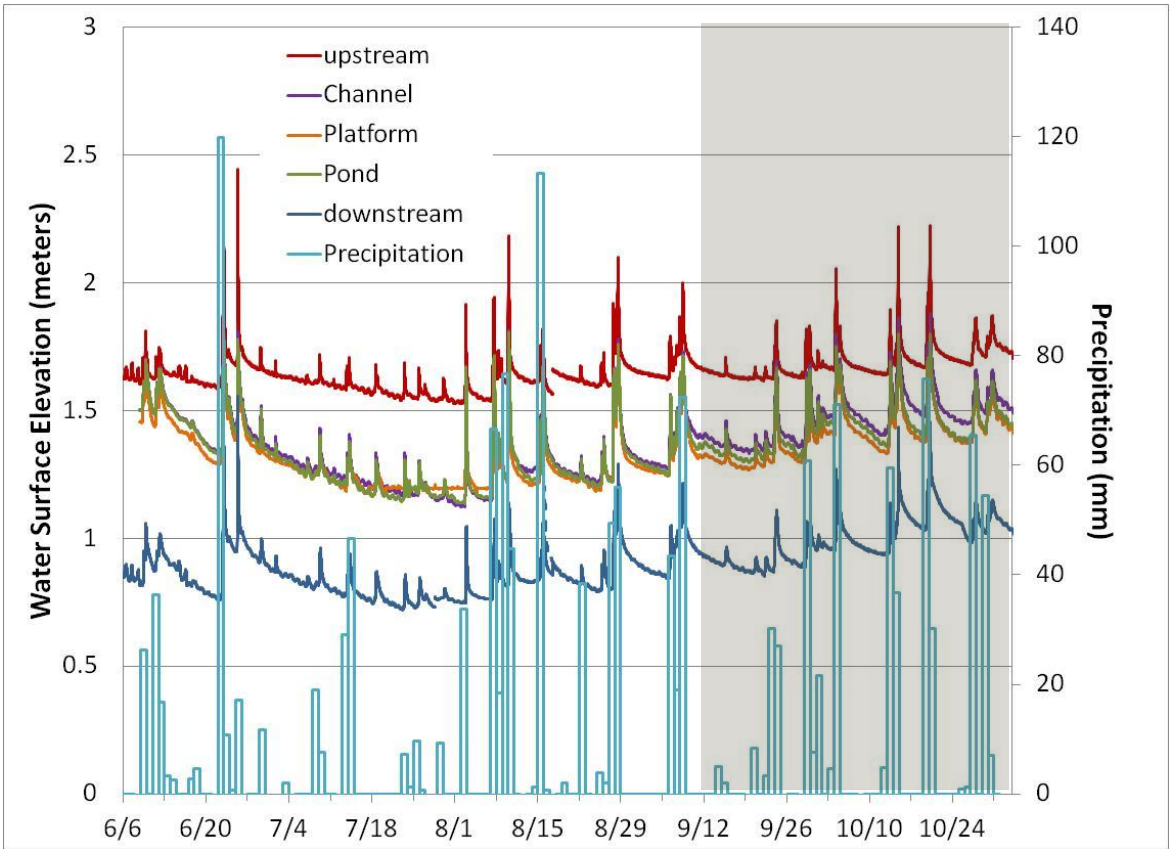

Figure 26 – A continuous record of stage (reported as water surface elevation) measured at different locations within the wetland at 15-minute intervals. The elevation of the peat platform is approximately 1.19 m, and recorded water surface elevations less than this are unreliable. The shaded rectangle shows the duration of the downstream backwater from September 9 to October 29. The dotted vertical lines are rain events with scale on the right axis.

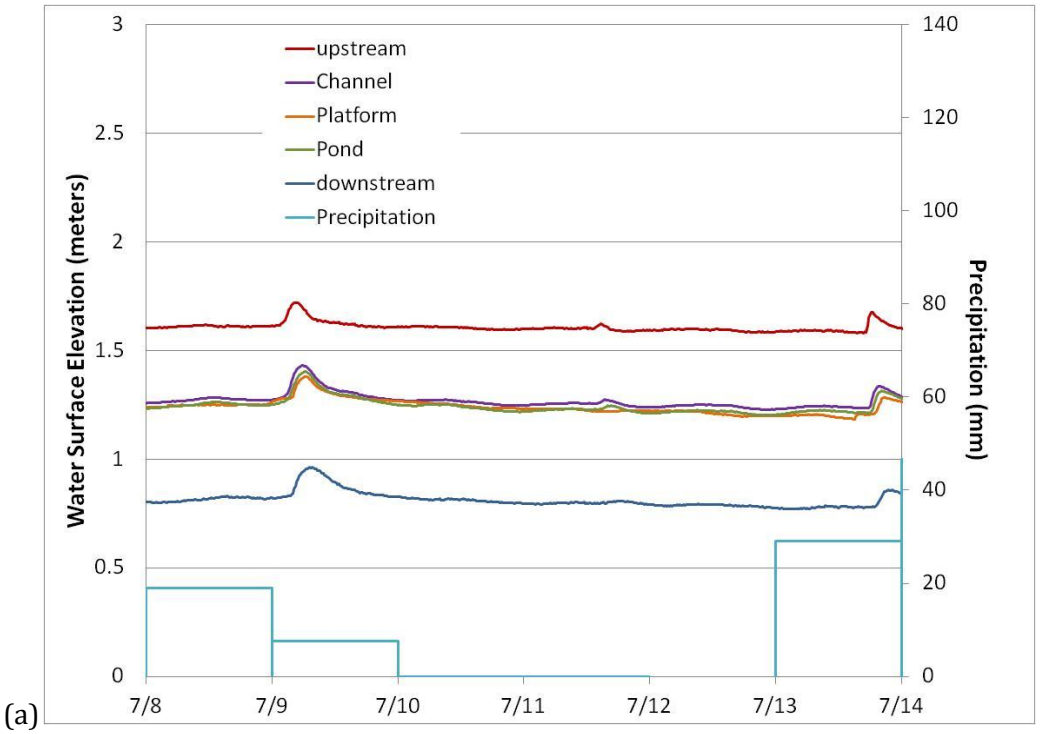

(a)

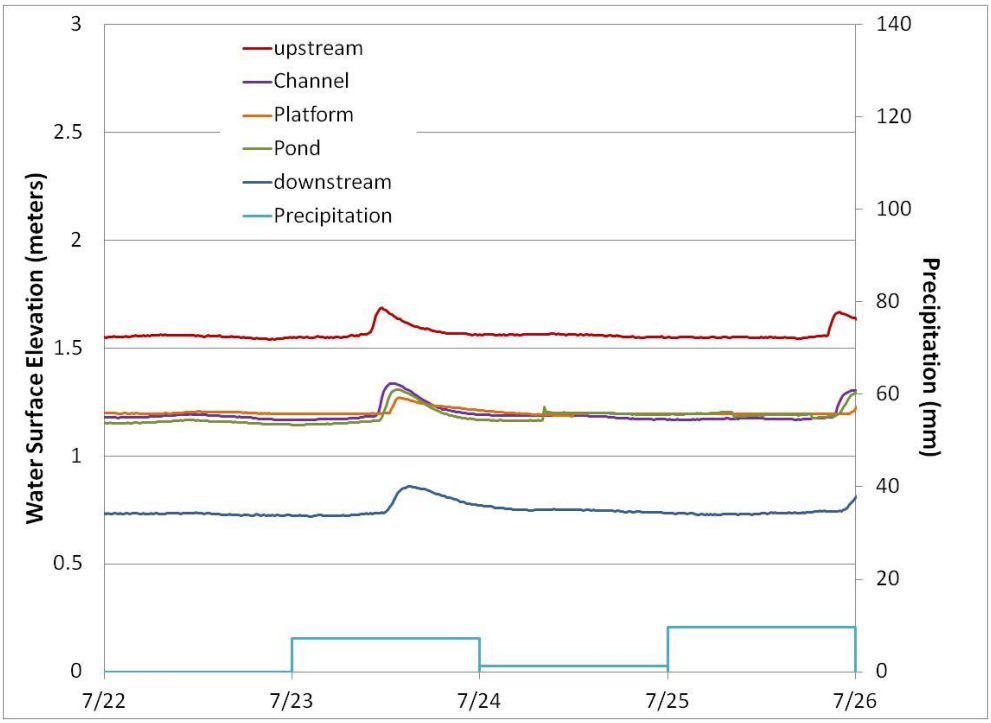

(b)

Figure 27- Stage record during a single event flow/base flow from (a) 7/9/2011 to 7/13/2011 and (b) 7/23/2011 to 7/25/2011. Precipitation events are on the right-hand axis.

SLOPE

The water surface elevations recorded in the central channel and the pond shown in Figure 26 were used to determine the longitudinal water surface slope in the central and lower sections of the wetland and the lateral water surface slope from the channel to the platform through the summer and fall (Figure 28). The longitudinal slope in the central section is between the pressure recorders in the central channel and the pond. The longitudinal slope in the lower section is between the pond and downstream pressure recorders. The lateral slope is between the pressure recorders in the central channel and platform. The longitudinal slope in both the central reach channel and lower study reach exhibit sudden periodic steepening immediately following rain events, superimposed on top of longer-term seasonal changes; with an increase in the central section slope through the summer and slight decrease in the downstream section slope through the summer. The decrease in the water surface slope in the lower section was most likely caused by a backwater that occurred there at the end of the summer and into the fall. In the central section of the wetland the longitudinal slope started around zero, then increased to 0.0025 m/m during the early summer, decreased and remained somewhat steady around 0.001 in the mid- to late-summer and then rose again to more than 0.005 in the fall. The longitudinal slope in the lower channel was steadier. It started around 0.005 in the early summer, decreased into the mid-summer to a value of 0.003, where it remained until the fall when it decreased slightly to 0.0025. For a short time at the end of July and several times during August the calculated longitudinal slope in the central section were estimated to be negative, likely due to measurement error.

The lateral water surface slope, defined by the change in water surface elevation between the central channel and platform, exhibited similar changes as the longitudinal slopes with the lateral slope becoming more negative following rain events and then a more gradual increase as the channel returned to base flow. The more negative lateral slope indicates that there was increased flow from the channel to the platform. Between the end of July and the beginning of August the lateral slope was often positive. This indicates that there was flow from the platform back into the channel. This could also be an artifact of the platform drying out during this period, stranding water in the stilling wells.

Figure 29 shows the longitudinal and lateral water surface slopes during two individual flow periods. The first, 7/9/2011 to 7/13/2011, occurs before the platform dries out and the second, 7/23/2011 to 7/25/2011, occurs after the platform dries out. During the first storm the lower section longitudinal slope increased approximately 0.001 following the rain event and a subsequent decrease. The central channel had a longitudinal slope increase and immediate decrease of approximately 0.0025 at the same time. The lateral slope decreases rapidly by over 0.005 before gradually increasing to almost 0. A very similar pattern is seen during the later storm event when the platform has dried out. The change in slope in the downstream channel is very small; again, approximately 0.001. The increase in central channel longitudinal slope is much larger at approximately 0.005

followed by a decrease of approximately 0.005. The bigger difference during this storm event is in the lateral slope which starts out positive (flow from platform to the channel) and decreases to approximately -0.01 (flow from channel to platform) followed by a more gradual increase to approximately 0.002 (flow from platform to channel). This indicates that during the storm water flows from the channel to platform and afterwards the platform flows back into the channel.

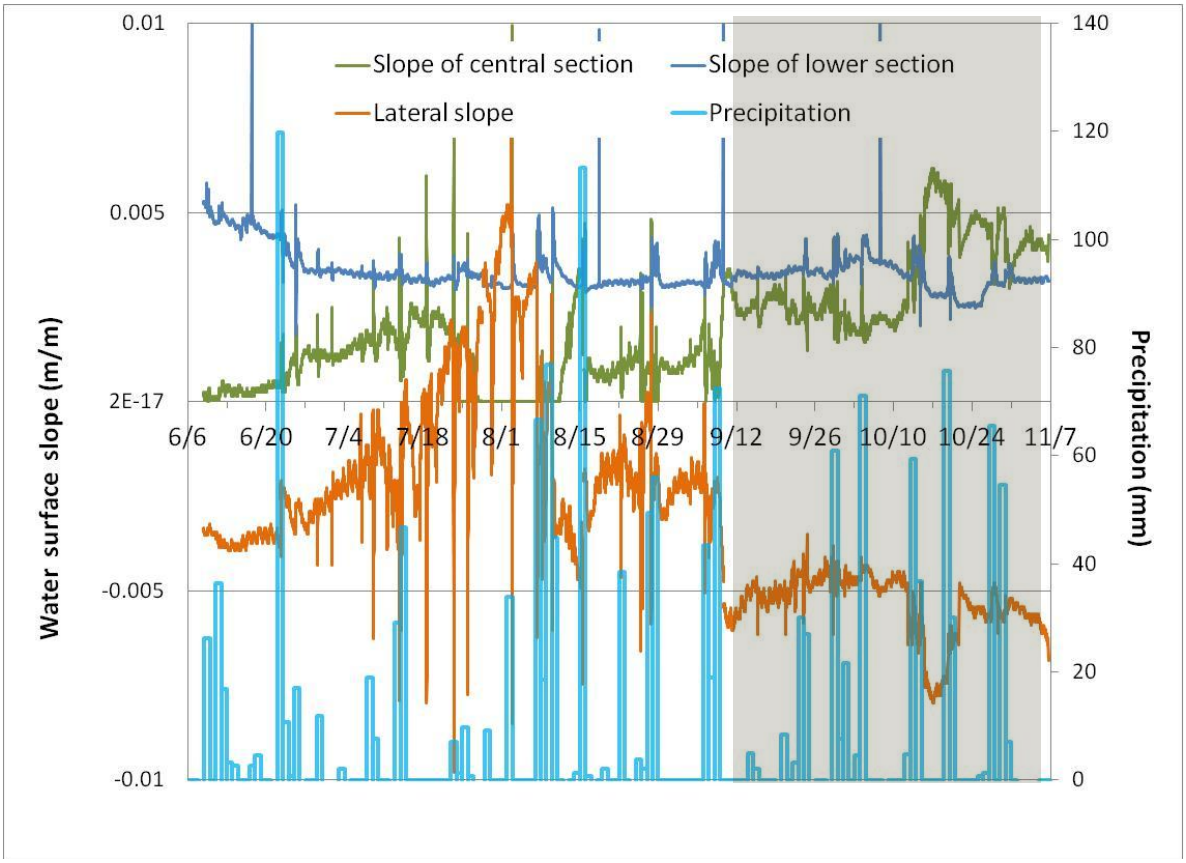

Figure 28– The water surface slope through the central and lower sections of the study wetland at 15-minute intervals. The lateral slope is between the central channel and the floodplain with a negative slope indicating flow from the channel to the floodplain. The shaded rectangle shows the duration of the downstream backwater from September 9 to October 29. Precipitation is shown on the right-hand axis as vertical blue dashed lines.

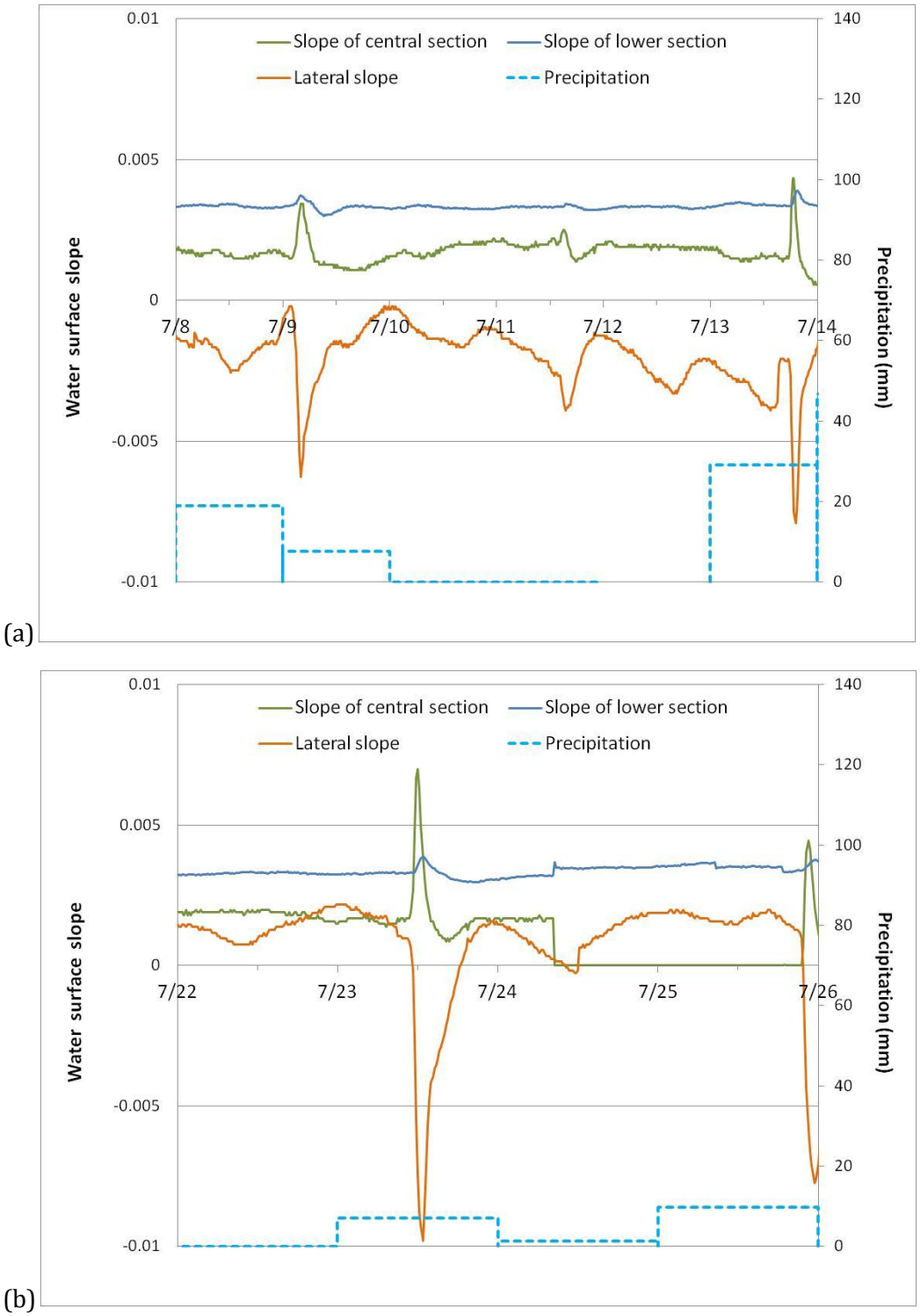

Figure 29 - Water surface slope during individual storm events from (a) 7/9/2011 to 7/13/2011 and (b) 7/23/2011 to 7/25/2011. Precipitation events are shown on the right-hand axis as vertical dashed lines.

STORAGE

The volume of water stored in the wetland was relatively high during the early summer at over 10,000 m^3 and decreases from June to early August to a low of 4000 m^3 (Figure 30). Storage then increases to over 12,000 m^3 through the fall.

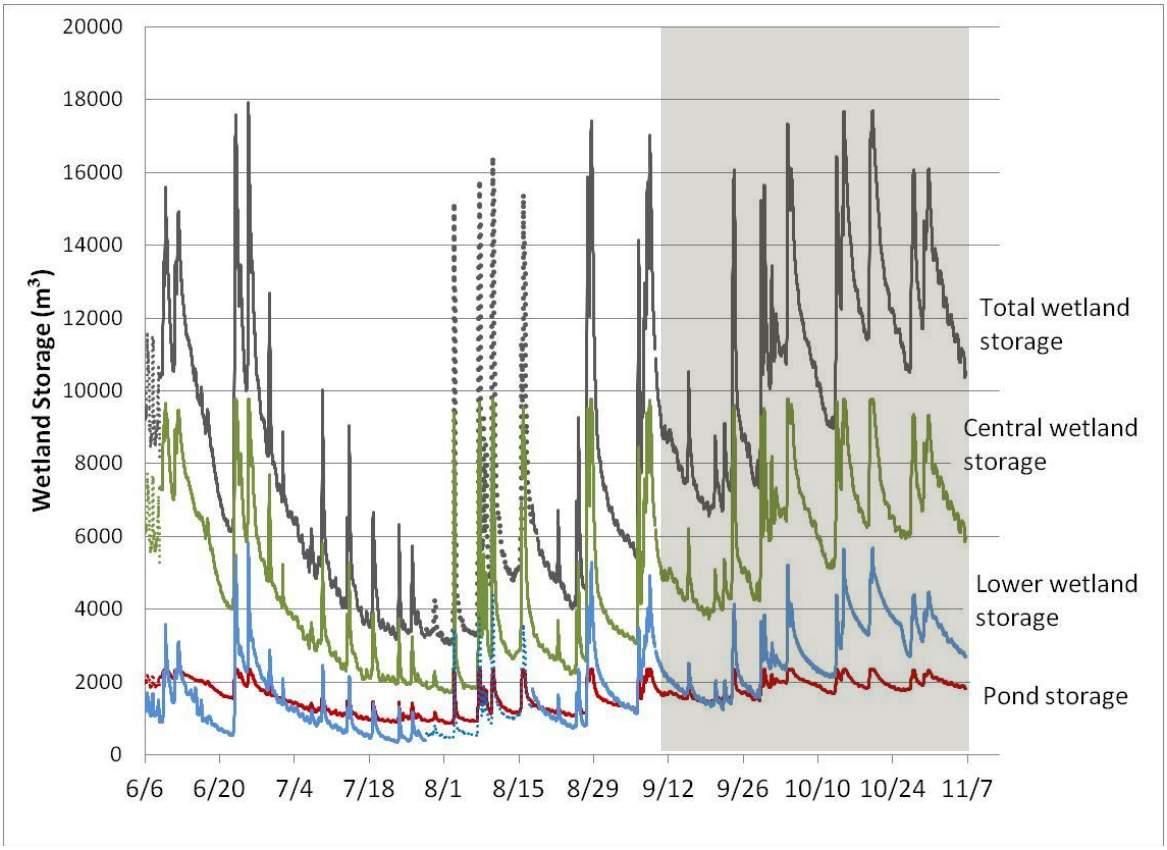

Figure 30 – Volume of water stored in the wetland. The purple line indicates the total wetland storage as the sum of the central wetland storage (green), pond storage (red), and lower wetland storage (blue). The dotted line sections indicate estimated storage when there was incomplete water elevation data at the downstream end. The shaded rectangle shows the duration of the downstream backwater from September 9 to October 29.

DISCHARGE

Discharge into and out of the wetland was relatively high during the early part of the summer at approximately 35 L/s and gradually decreases through the summer to a low of approximately 3 L/s (Figure 31). In August the discharge began to increase and continued to increase through the fall to nearly 127 L/s by the beginning of November. Periodic peaks in discharge, followed by a recession before the next peak, are associated with rain events throughout the summer and fall. In most storm events, the upstream discharge peaks at a higher discharge than the downstream discharge, but during base flow the discharge out of the wetland is typically slightly higher than discharge into the wetland.

Figure 32 shows close-up views of individual event flow-base flow periods. The first, occurs from 7/9/2011 to 7/13/2011, prior to the platform substrate drying. The second occurs from 7/23/2011 to 7/25/2011 during the platform dry period. In both events, the upstream discharge peak is narrower than the downstream discharge peak. This suggests that at the upstream end, the stream returns to base flow more quickly than the downstream end. During the 7/9/2011 to 7/13/2011event flow-base flow period, the upstream and downstream return to base flow levels that are roughly equal. However, during the 7/23/2011 to 7/25/2011 period the downstream base flow level is slightly higher than the upstream base flow.

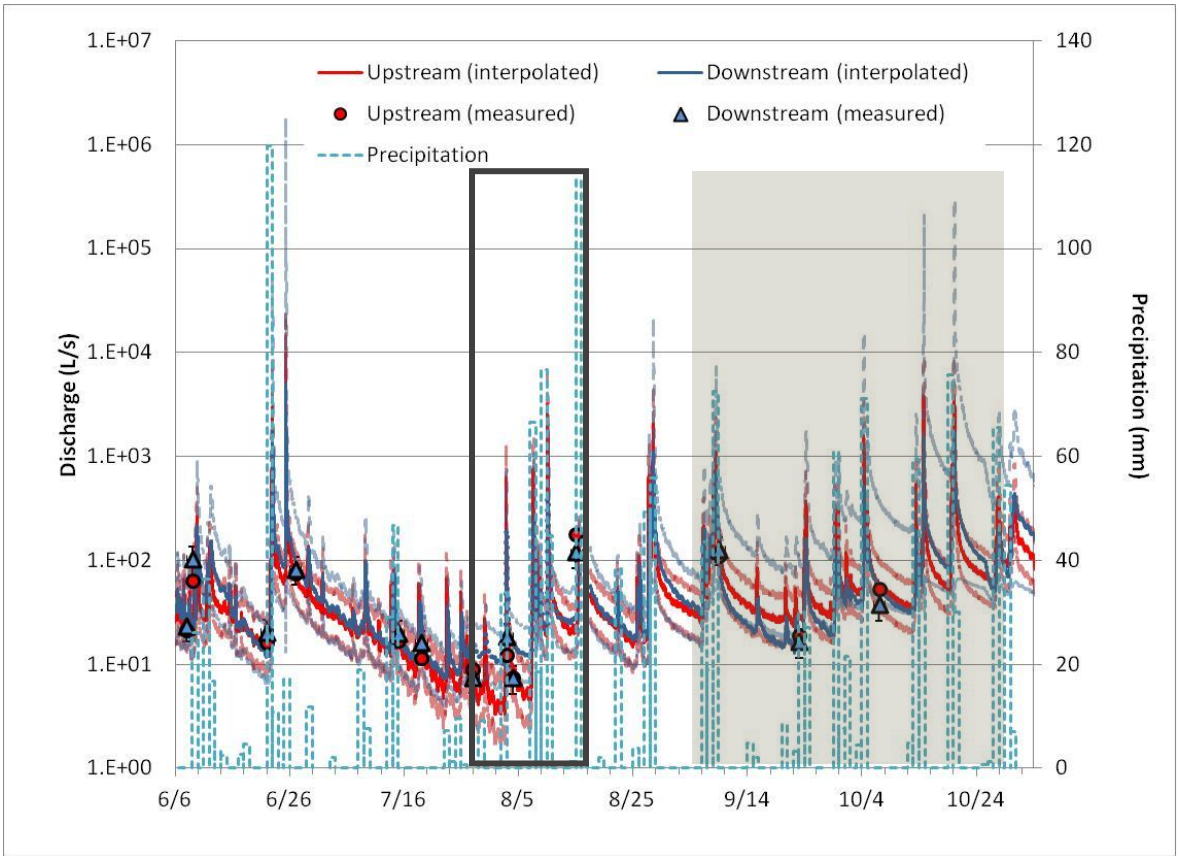

Figure 31– Discharge entering and exiting from the wetland interpolated from stage data at 15-minute intervals shown on a logarithmic scale. Points are measured values with vertical lines showing measurement uncertainty. Bright solid lines show values interpolated using the stage-discharge curve including the backwater correction between September 9 & October 29 (grey shaded box). Faded, dashed lines indicate the uncertainty from the interpolation. Dotted vertical lines show rain events and are on the right axis. Downstream discharge between July 28 & August 18 was estimated using a regression equation for the relationship between the water surface elevations at the downstream end and the mid-section channel (open black box).

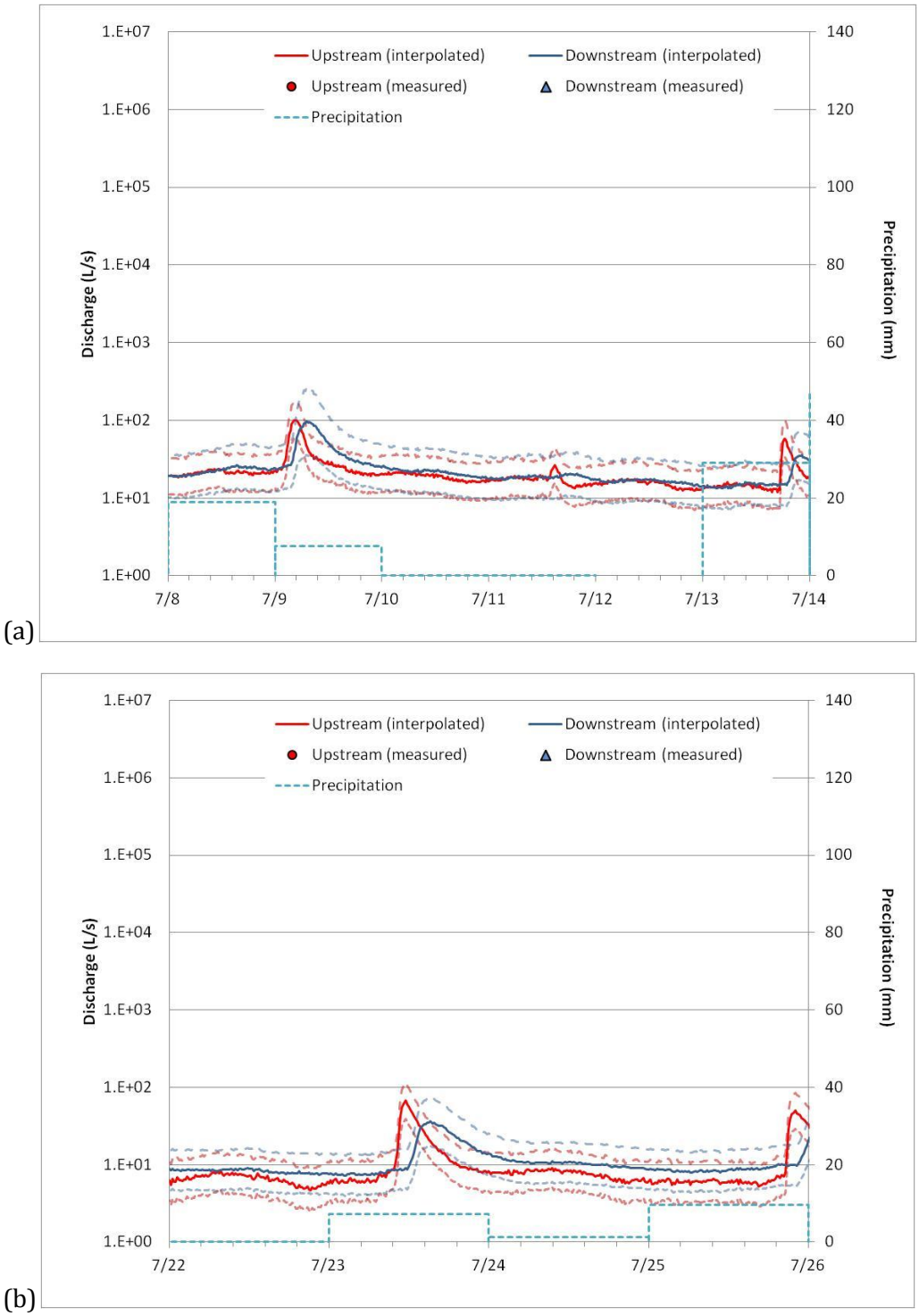

Figure 32 - Discharge during a single event flow-base flow period from (a) 7/9/2011 to 7/13/2011 and (b) 7/23/2011 to 7/25/2011. Precipitation events are on the right-hand axis. Dashed lines indicate the uncertainty in discharge from interpolation.

CONDUCTIVITY

Conductivity measurements taken on two separate days are shown in Figure 33. Between the two days the measurements taken on the marsh platform are similar and approximately 230 µS/cm. However, measurements taken in the channel are noticeably higher on August 5 at 675 µS/cm than on August 15 at 240 µS/cm. This indicates that connectivity between the channel and the marsh platform is somewhat limited. This suggests that once water enters the platform lateral flow is more restricted than longitudinal flow, perhaps by areas of denser vegetation.

In addition to differences in conductivity between the channel and the platform, conductivity was also different at different discharges. Discharge into the wetland on August 5 was approximately 506 m^3/d and was during a period of base flow. In contrast, August 15 occurs during a flow event with an incoming discharge of approximately 5573 m^3/d. The lower conductivity measurement on August 15 could be a result of dilution from the higher discharge. The similarity between the channel and platform measurements on this day could point to increased connectivity and mixing during higher flow. However, more data points would be needed to support the above speculations regarding the relationship between conductivity and discharge or location.

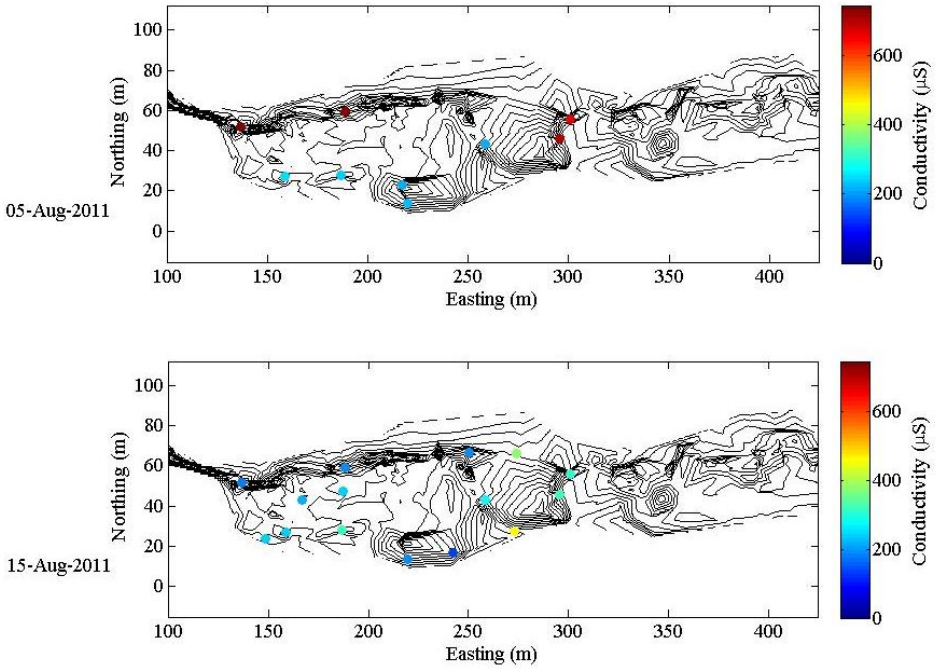

Figure 33– Measured conductivity is shown as colored dots. Blues indicate lower conductivity and reds indicate higher conductivity measurements.

ISOTOPES

Oxygen-18 isotope composition data (Figure 34a) and deuterium isotope composition data (Figure 34b) for the upstream and downstream ends and groundwater are shown with downstream discharge. Both isotopes show a great deal of variability from day to day. A large part of this variability is likely a result of isotopic composition variations in individual precipitation events. Typically, isotope values between groundwater samples are very similar and equal to the annual average precipitation signal (Frades 2007). However, the isotope ratios in the groundwater samples collected at the Chestnut wetland site are more varied and less negative than expected which is likely a reflection of variability in precipitation signatures of rain events that occurred shortly before samples were collected. Given that the groundwater wells were shallow it is possible that rain water infiltrating the surrounding soil was able to flow into the groundwater well. The average of these groundwater samples (Figure 35) falls on the LMWL. This supports the use of the Lamprey Meteoric Water Line developed by Frades (2007) as the Local Meteoric Water Line for the Chestnut wetland.

a)

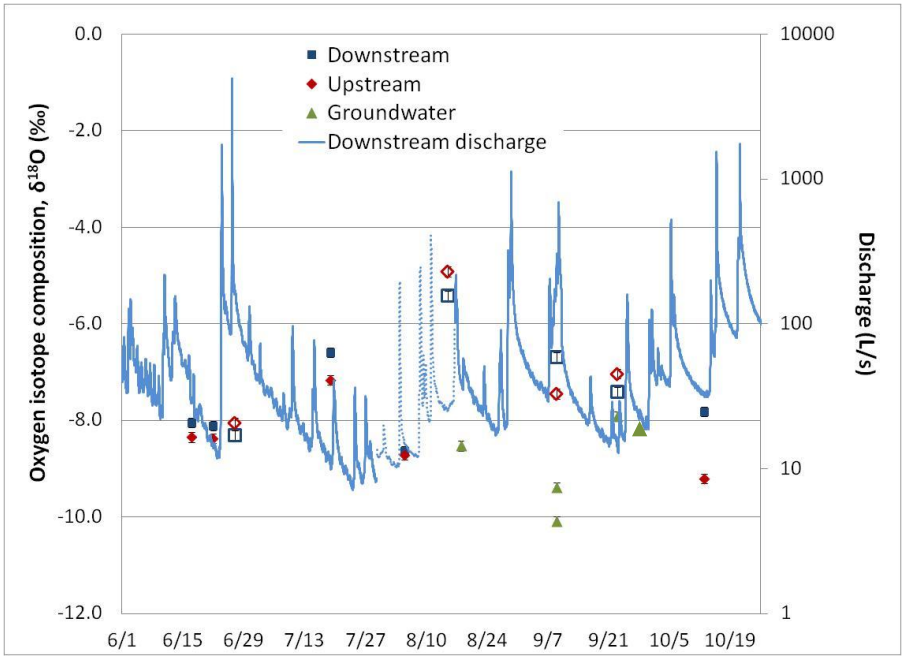

b)

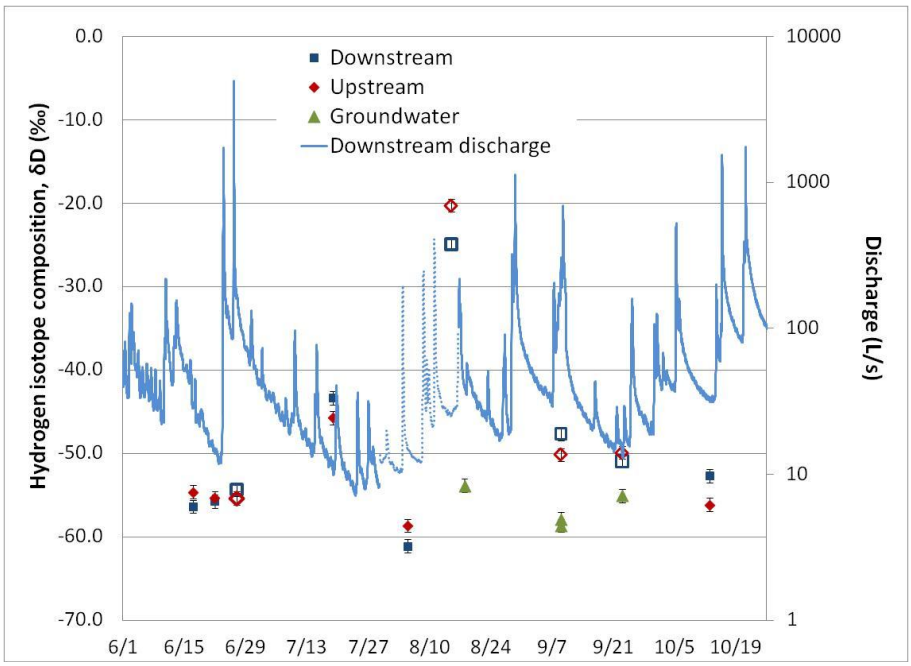

Figure 34– (a) Oxygen isotope composition and (b) deuterium composition within the wetland. The blue line represents the daily discharge at the downstream end with the peaks coinciding with precipitation events. Solid symbols were taken at base flow and open symbols at flood flow. Repeat groundwater samples were collected on September 9, 2011. Vertical error bars represent instrument error and, in most cases, are smaller than symbols.

The deuterium and ^{18}O values are plotted against each other in Figure 35. The distribution of data points along the LMWL (black line) likely indicates that they are influence by the isotope composition of individual precipitation events. The Local Evaporative Line (LEL) is shown by the dashed black line. The point at which the LEL intersects the LMWL (i.e. zero deviation from the LMWL) indicates no net evaporation. Greater deviation from the LMWL along the LEL indicates greater net evaporation. The samples collected at quasi-steady base flow (solid symbols) allow us to estimate evaporative enrichment of a single parcel of water traveling through the wetland. The solid grey lines in Figure 35 connect upstream and downstream samples collected on the same day at base flow. In two of the sample sets, the downstream sample shows increased deviation (with both deuterium and ^{18}O increasing in value) from the LMWL along the LEL, suggesting that there was some net evaporation during these times. During the remaining three samples sets the downstream samples indicate there was a very slight increase in the ^{18}O isotopic composition and a slight decrease in the deuterium isotopic composition. This could indicate that there was groundwater input. However, given that the changes for those three sets are very small this could also be a result of experimental or instrument error.

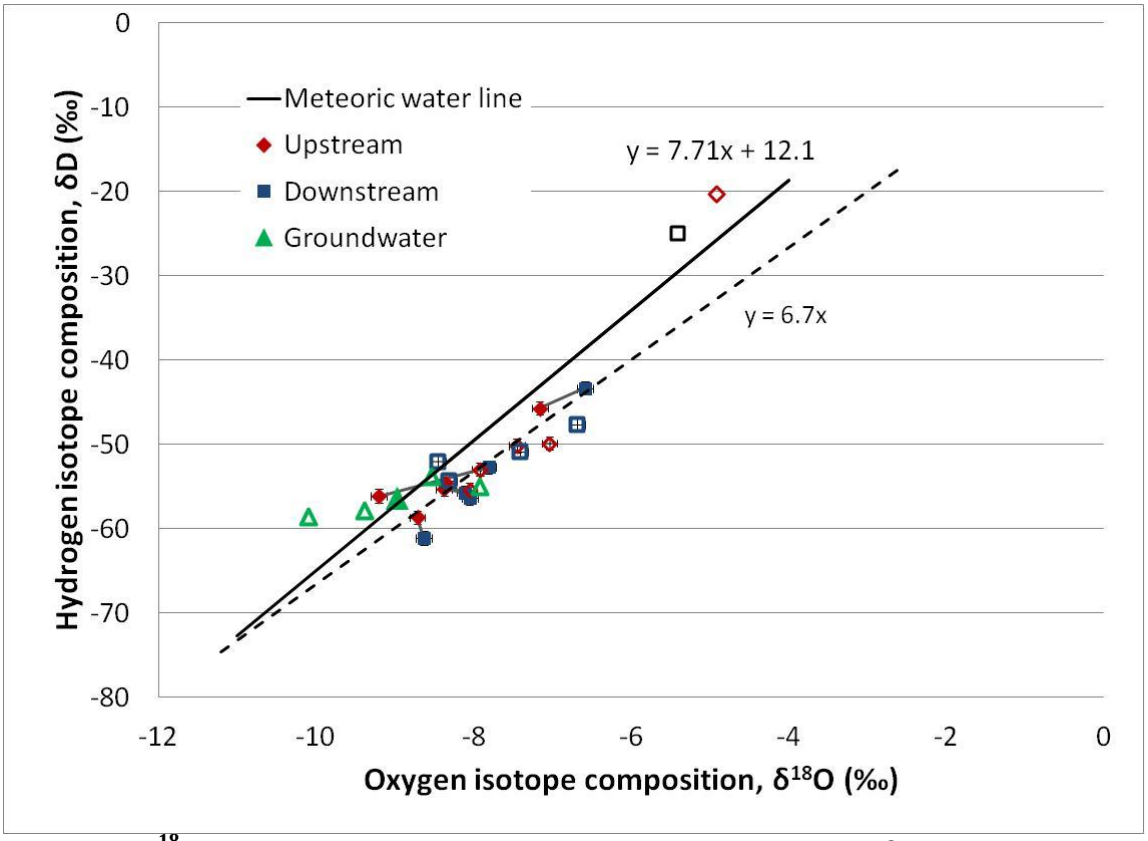

Figure 35– ^{18}O and deuterium isotope compositions (per mille) for upstream (red), downstream (blue) and average groundwater (green) are plotted against the Local Meteoric Water Line for the headwaters of the Lamprey River Watershed. The dashed line indicates the Evaporative Water Line. Open triangle (green) symbols indicate the individual groundwater samples used in determining the average groundwater isotopic composition. Solid symbols indicate samples collected during base flow with same-day samples connected by a solid line. Open square and diamond symbols indicate samples collected during flow events. The green triangle represents the average of four groundwater samples collected. The vertical and horizontal error bars represent instrument error and, in most cases, are smaller than symbols.

WATER BUDGET

The water budget for the wetland (Figure 36) was calculated using Equation 3 and stream discharge data (Figure 31), evapotranspiration (Figure 25), storage (Figure 30) and precipitation (Figure 26). The magnitudes of discharge into and out of the wetland and storage within the wetland were much larger than precipitation and evapotranspiration. This results in the water budget being dominated by surface water flow and storage. Dramatic increases in incoming fluxes following rain events through the summer and fall were not immediately balanced by an increase in outgoing fluxes resulting in positive changes in storage (increased storage). This allowed the wetland to serve as a reservoir that buffered peak flows during downstream transport.

Because precipitation and evapotranspiration were such a small fraction of the total water budget a simplified version of the budget considering only storage and stream discharge (Equation 12) was used in further analysis. The residual shown here was calculated using stream discharges determined from the best-fit rating curves and their uncertainties described above. The residual calculated from the simplified water budget has the largest magnitude in late June and October (Figure 37). Periods of positive residual tend to be focused during precipitation events. Otherwise, the residual tends to be slightly negative. Given the relatively high uncertainty in the residual, which is greatest during the flow events, it is difficult to determine whether the residual is positive or negative at any time.

a)

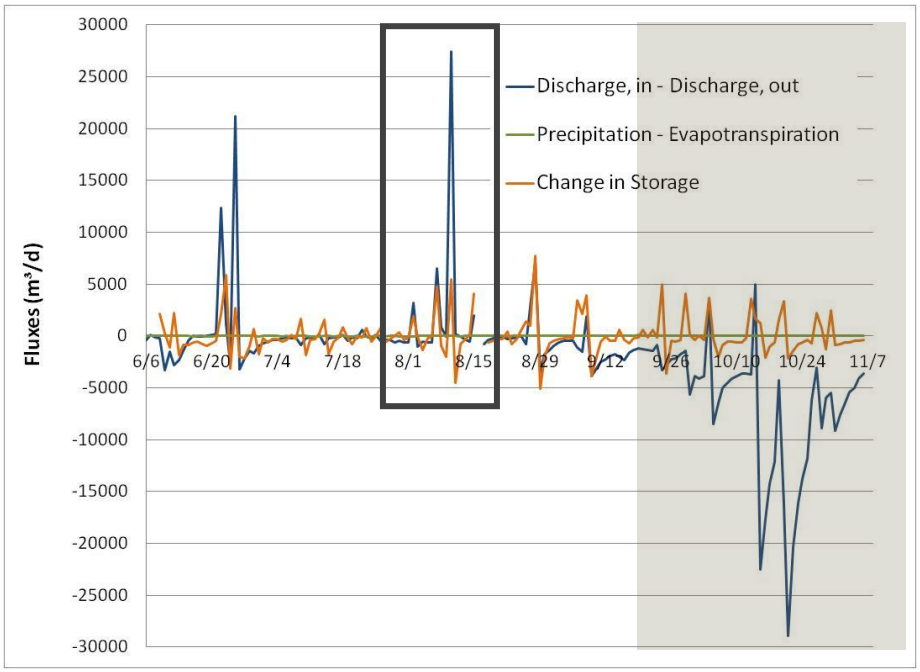

b)

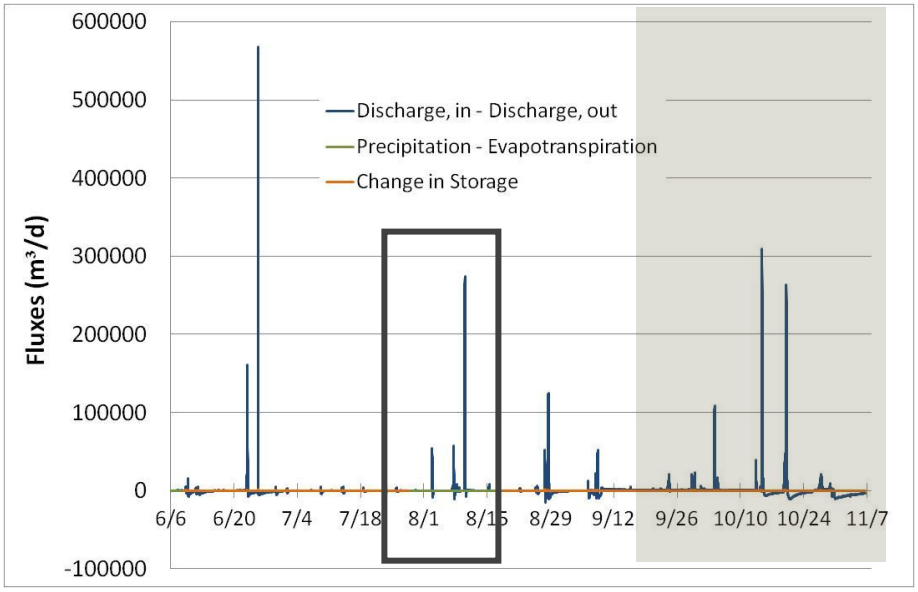

Figure 36– Fluxes used in the water budget equation with the change in discharge through the wetland (blue), difference between precipitation and evapotranspiration (green), and change in storage (orange) shown over time with (a) daily averaged data and (b) 15-minute discharge and storage data. Magnitude of discharge peaks are too brief to be captured in daily averaged data. The grey box indicates a period of backwater between September 9 and October 29, during which there was increased uncertainty in the discharge calculations. The black box indicates the period between July 28 and August 17, 2001 when downstream discharge and storage were estimated using data from water pressure recorders in the central channel of the wetland.

a)

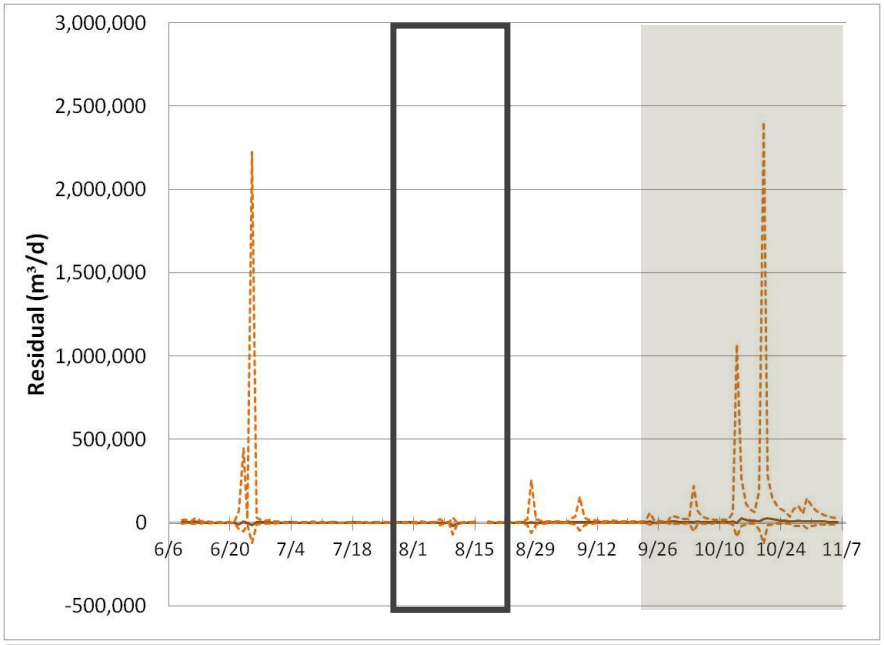

b)

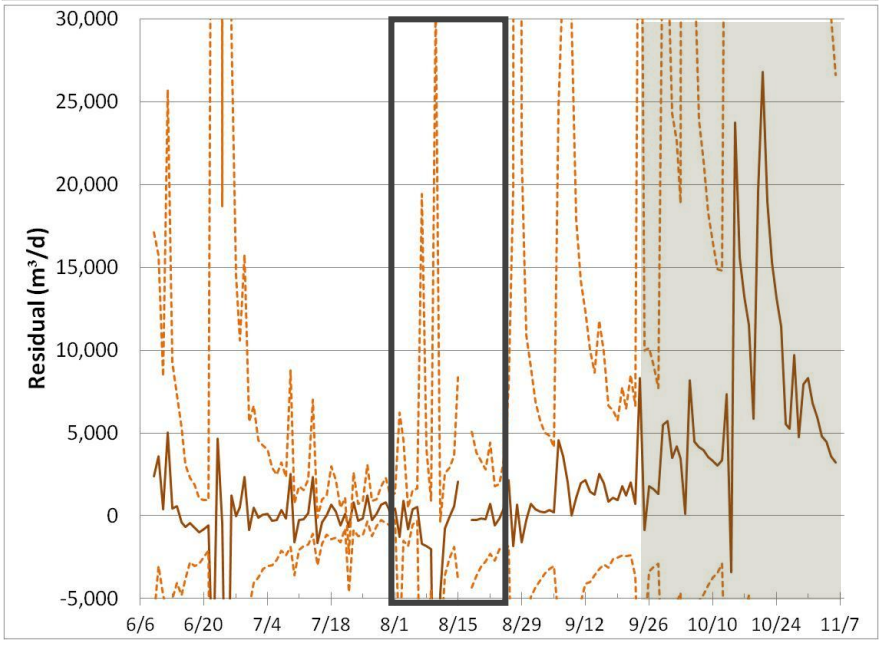

Figure 37– a) The solid line shows the water budget residual calculated using the best fit discharges. The dotted lines indicate the uncertainty resulting from high and low estimates in the incoming and outgoing discharges and storage. b) A close-up to show details of residuals close to zero. The grey box indicates a period of backwater between September 9 and October 29, during which there in increased uncertainty in the discharge calculations. The black box indicates the period from July 28 to August 17 when the downstream data was estimated using data from water pressure recorders in the central channel of the wetland.

If all important fluxes are included in the water balance (Equation 9) and properly estimated, then the sum of the change in storage, incoming discharge, outgoing discharge, precipitation, and evapotranspiration should be equal to zero with no residual. If the residual is not zero then either an important flux was not considered or there was large uncertainty in one or more of the estimated fluxes. Table 4 shows the net fluxes during the period from 6/9/2011 to 7/28/2011 which is the longest period (50 days) of reliable data. Over this period there is a large net negative residual of approximately 135 m^3/d that is dominated by a much larger volume of water entering the wetland than exiting (approximately 85 m^3/d). Simultaneously, there was a large decrease of approximately 50 m^3/d in wetland storage. This large negative residual suggests that there may have been a large outgoing flux that was not accounted for.

The water budgets for individual flow events and the following base flow period may show something very different than the much longer seasonal water budget. Table 5 shows the water balance during event flows and base flows during the summer and fall calculated by integrating the 15-minute discharge and wetland storage curves shown in Figure 36 (excluding precipitation and evapotranspiration). Three residuals (equations 12, 13 and 14) were calculated for each peak and recession using changes in discharge calculated from the best-fit rating curves, the smallest changes and largest changes in discharge calculated from the uncertainty associated with the rating curves, the best-fit estimate of rate of change in storage, and the high and low estimates of the rate of change

in storage. The residuals during the individual events tended to be positive and relatively small. Residuals calculated for event flows tended to be larger than the residuals calculated for base flow periods. This could, in part, be due to increased uncertainty at high discharges. However, two periods (6/22/2011 and 8/7/2011) had a very large negative residual. Both occured when there was a second peak flow that occurs before discharge is able to reach base flow.

Table 4 – Net fluxes calculated using 15-minute data for outgoing discharge – incoming discharge (Qout-Qin) and change in storage and average daily data for precipitation – evapotranspiration (P-ET) during the time period from 6/9/2011 to 7/28/2011. U_{GW} is the velocity of groundwater flowing into the wetland (positive values) or out of the wetland (negative values).

Qout-Qin m^3	P-ET m^3	Change in storage m^3	Residual m^3	U_{GW} m/d
-4231 (-364,441 to 3,012,937)	-199 (-216 to -182)	-2454 (-2494 to -2412)	-6685 (-366,695 to 3,010,682)	-1 (-72 to 639)

Table 5– Stream discharge, rate of change in storage, residual and groundwater flow rate were calculated using data collected at 15-minute intervals. Event flow and base flow were determined using hydrograph separation.

	Qout-Qin m^3/d	Rate of change in storage m^3/d	Residual m^3/d	U_{GW} m/d
6/9-6/11 (event)	1997 (-6224 to 16713)	249 (-38 to 536)	2246 (-6262 to 17,249)	0 (-1 to 4)
6/11 (base flow)	1331 (-2383 to 6574)	-1023 (331 to -2375)	308 (-2052 to 4199)	0 (0 to 1)
6/11-6/13 (event)	2424 (-5658 to 16730)	370 (151 to 588)	2794 (-5507 to 17,318)	1 (-1 to 4)
6/13-6/22 (base flow)	188 (-2495 to 3469)	-576 (-516 to -635)	-388 (-3011 to 2834)	0 (-1 to 1)
6/22-6/25 (event)	-4388 (-44,187 to 221,127)	1475 (1237 to 1710)	-2913 (-42,950 to 222,937)	-1 (-8 to 47)
6/25-6/30 (event)	-2226 (-28,264 to 419,237)	-406 (-297 to -514)	-2632 (-28,561 to 418,723)	-1 (-6 to 89)
6/30-7/9 (base flow)	357 (-2767 to 4248)	-286 (-221 to -350)	71 (-2988 to 3898)	0 (-1 to 1)
7/9 (event)	947 (-4408 to 8854)	1259 (469 to 2047)	2206 (-3939 to 10,901)	0 (-1 to 2)
7/9-7/13 (base flow)	169 (-1659 to 2235)	-496 (-378 to -614)	-327 (-2037 to 1621)	0 (0 to 0)
7/13-7/14 (event)	500 (-3070 to 5212)	699 (298 to 1099)	1199 (-2772 to 6311)	0 (-1 to 1)
7/14-7/18 (base flow)	170 (-1126 to 1600)	-421 (-295 to -547)	-251 (-1421 to 1053)	0 (0 to 0)
7/18-7/19 (event)	140 (-1902 to 2498)	287 (38 to 536)	427 (-1864 to 3034)	0 (0 to 1)
7/19-7/23 (base flow)	171 (-750 to 1169)	-187 (-87 to -287)	-16 (-837 to 882)	0 (0 to 0)
7/23 (event)	-53 (-2278 to 2433)	993 (369 to 1617)	940 (-1909 to 4050)	0 (0 to 1)
7/23-7/25 (base flow)	246 (-623 to 1212)	-220 (-24 to -417)	26 (-647 to 795)	0 (0 to 0)
7/25-7/26 (event)	98 (-1853 to 2296)	521 (23 to 1018)	619 (-1830 to 3314)	0 (0 to 1)
7/26-8/2 (base flow)	490 (-403 to 1567)	-105 (-57 to -154)	385 (-460 to 1413)	0 (0 to 0)

8/20-8/25 (base flow)	168 (-2235 to 2969)	-186 (-102 to -271)	-18 (-2337 to 2698)	0 (0 to 1)
8/25-8/26 (event)	549 (-3763 to 6420)	554 (155 to 953)	1103 (-3608 to 7373)	0 (-1 to 2)
8/26-8/27 (base flow)	247 (-1737 to 2529)	-448 (78 to -974)	-201 (-1659 to 1555)	0 (0 to 0)
8/27-9/3 (event)	-239 (-16,253 to 48,020)	215 (144 to 285)	-24 (-16,109 to 48,305)	0 (-3 to 10)
9/3-9/6 (base flow)	460 (-2958 to 4741)	-138 (60 to -335)	322 (-2898 to 4406)	0 (-1 to 1)

Below are the water budgets for two different storm events (Figure 38), the first prior to the period during which the water surface elevation dropped below the platform substrate elevation and the second during the period when the water surface elevation dropped below the platform substrate elevation. The first consists of a flow event on 7/9/2011 followed by a base flow period from 7/9/2011 to 7/13/2011. During this period there is generally more discharge flowing out of the wetland than flowing into it (Figure 38a), though the difference is much greater during the earlier peak flow on 7/9/2011, and an increase in storage during the initial event flow on 7/9/2011 followed by a decrease in storage during the subsequent base flow period. The transition from event flow to base flow can be seen when the incoming discharge shifts from being much higher than outgoing discharge (positive peak) to being much lower than outgoing discharge (negative peak) and can be interpreted as the flood pulse caused by the precipitation event traveling through the wetland. As shown in Table 5, these discharge and storage values result in a very large positive residual during the event flow followed by a much smaller negative residual during the base flow.

The second single storm event (Figure 38b) occurs from 7/23/2011 to 7/25/2011 during the period of time when the water surface elevation drops below the elevation of the platform substrate. Like the storm event described above, there was a large increase in storage during the event flow followed by a decrease in storage during base flow. Additionally, the transition of higher inflow to higher outflow can be seen in the sudden switch from a large positive peak to negative peak. Unlike the storm event water budget above, there was greater stream flow into the wetland during the peak flow on 7/23/2011 than there was flowing out when it returns to base flow. The slight increase in wetland storage during this time may account for the low outgoing discharge. The combination of discharge and storage patterns indicate a large positive residual during the initial peak flow event and a much smaller positive residual during the base flow that follows it (Table 5). These residuals, converted to groundwater velocity, indicate that any flux in or out associated with groundwater is minimal.

(a)

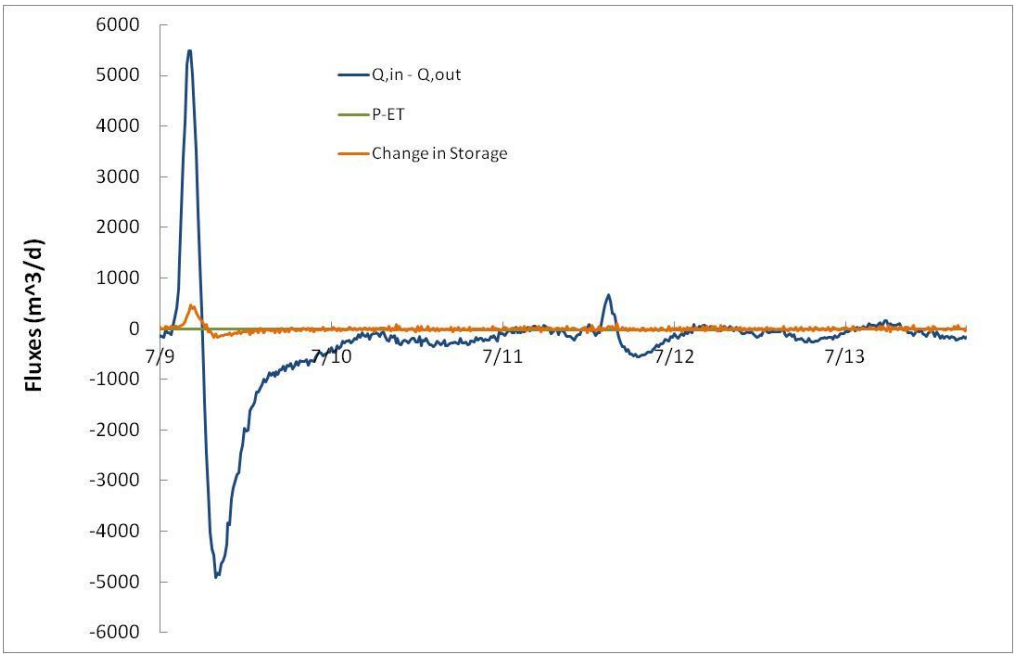

(b)

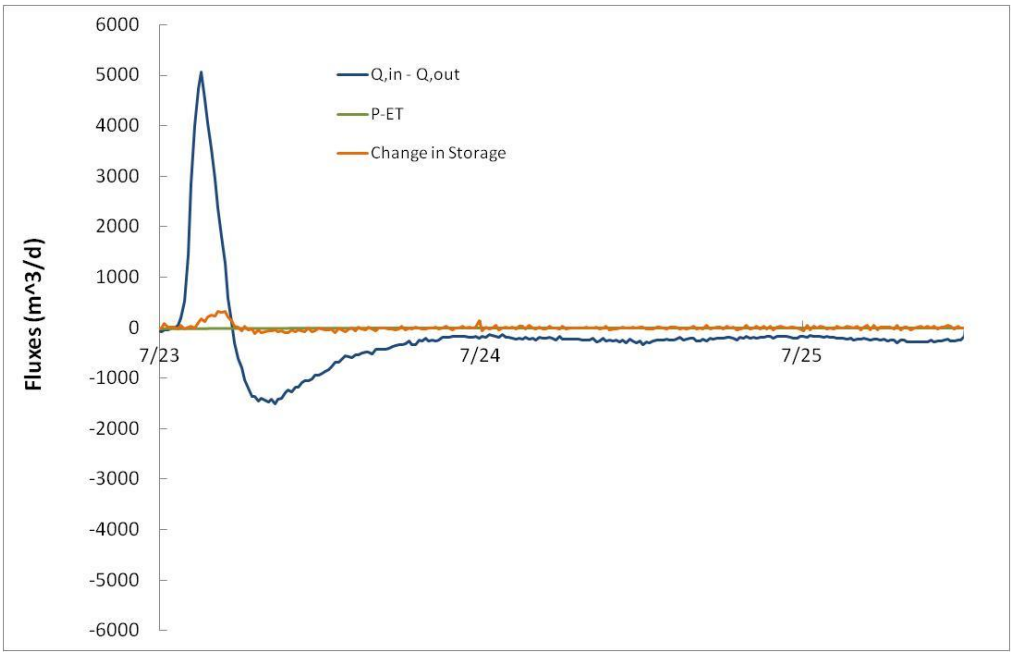

Figure 38 - Fluxes used in the water budget equation with the change in discharge through the wetland (blue), difference between precipitation and evapotranspiration (green), and change in storage (orange) shown during (a) a single flow event (7/9 12:15 am to 7/9 4:00 pm) and the following base flow period (7/9 4:15 pm to 7/13 5:00 pm) and (b) a single flow event (7/23 8:30 am to 7/23 10:30 pm) and the following base flow period (7/23 10:45 pm to 7/25 8:00 pm).

GROUNDWATER VELOCITY

Calculations of net groundwater velocity assumed that groundwater flow was the primary contribution to the residual, though it is important to note that large uncertainties in discharge and storage calculations were also likely to contribute to residual. Large positive residuals could indicate that there is groundwater flowing into the wetland (positive flow velocity). A large negative residual could indicate losses to groundwater outflow (negative flow velocity). Groundwater flowing into the wetland was assumed to enter over an area of approximately 4710 m^2 and out-flowing groundwater was assumed to flow through an area of approximately 5120 m^2 each including a section along the wetland perimeter and a section over the bed of the wetland. These areas are rough estimates based on the approximate length of the wetland edge with an assumed depth of 1 m and the area of the bed that groundwater is likely to flow through.

In most cases, there was a positive residual that was low enough to suggest no net groundwater flow, with a range of -1 m/d out of the wetland to 1 m/d into the wetland. Thus, the estimated best-fit groundwater velocities make it difficult to determine if the wetland is gaining, losing, or neither at any one time period. The high and low estimates (based on uncertainties) range from groundwater flowing into the wetland at the velocity of approximately 89 m/d to groundwater flowing out of the wetland and a velocity of approximately 8 m/d during a single flow event. All of the best-fit calculations for groundwater velocity are within the range of hydraulic conductivity that is considered

typical for glacial till, approximately 10^{-7} m/d to 1 m/d (Heath 1983). The larger estimates of groundwater velocity, up to 89 m/d, are within the range considered typical for sand, approximately 10^{-2} m/d to 10^{2} m/d, and gravel, approximately 10^{2} m/d to 10^{4} m/d (Heath 1983). This is consistent with observed sediment compositions at the Chestnut wetland and with the Stone & Stone surficial geology map of Massachusetts 2007 (Figure 3).

TRACER STUDIES

A continuous discharge record for each of the four tracer studies is shown in Figure 39. The outlet discharge was used for all analysis and the inlet discharge is shown here for comparison only. The outlet discharge during tracer study 1 varies throughout the study but always remains between approximately 100 L/s and 150 L/s with the inlet discharge roughly 50 L/s lower. The outlet discharge during tracer study 2 has similar small peaks of much smaller magnitude. Until approximately 1.75 days after release of the tracer the discharge (both inlet and outlet) remain between approximately 25 L/s and 50 L/s. After which the outlet increases to approximately 220 L/s and the inlet to approximately 265 L/s. Discharge during tracer study 3 was fairly constant with the outlet and inlet being approximately 15 L/s and 8 L/s, respectively. Outlet discharge during tracer study 4 started out high at 150 L/s and drops to 75 L/s at 0.5 days after the tracer entered the wetland. Throughout the remainder of the study it continued to gradually decrease to 35 L/s at 2.5 days after the tracer enters the wetland. The inlet discharge during tracer

study 4 was much steadier and decreased from approximately 50 L/s at the start to just over 30 L/s at the end. During each tracer study there was more discharge out of the wetland than into it which would result in greater dilution of the tracer at the downstream end of the wetland. This was accounted for by using concurrant outgoing discharge and fluorescence measurements to calculate the volume of RWT exiting the wetland.

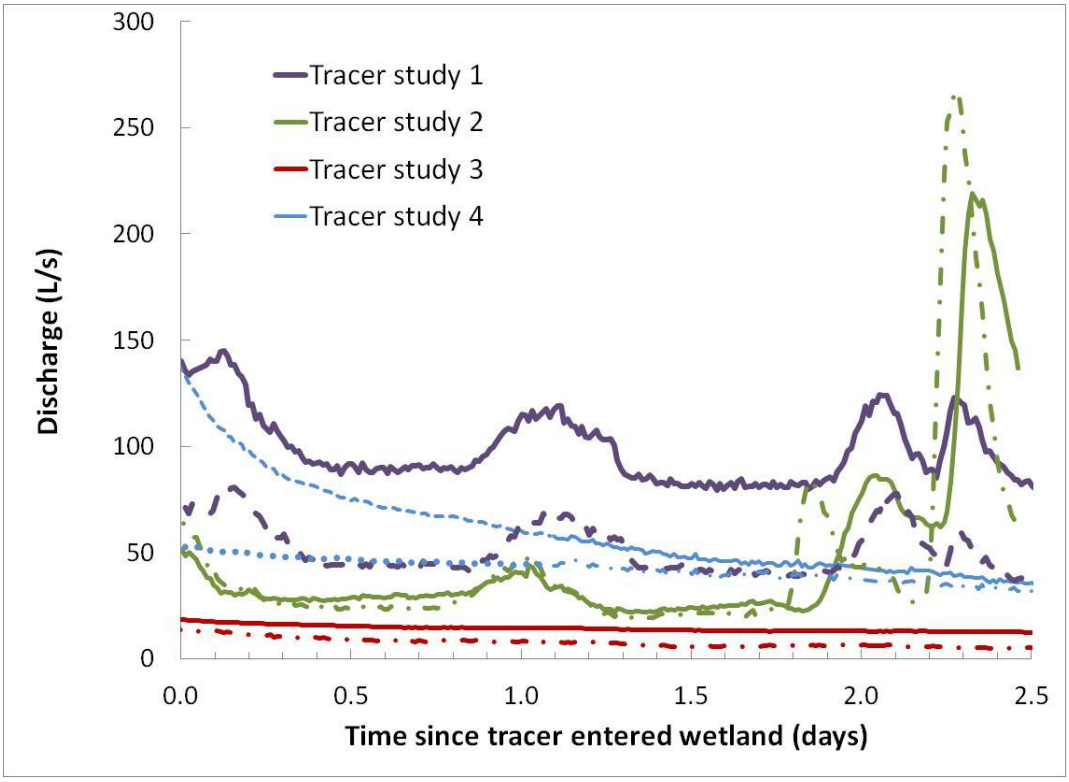

Figure 39 - Outgoing discharge (solid lines) and incoming discharge (dash/dot lines) for each of the four tracer studies with time normalized to "Time since tracer entered wetland". Outlet dscharge during the first half of tracer study 4 was estimated using the relationship between the water surfaces elevations at the downstream end and the mid-channel. The inlet discharge during this same period was recorded using a different stage recorder which is indicated by the dotted portion of the line.

Tracer measurements collected at the outlet of the wetland during each of the tracer studies show an initial, high concentration pulse exiting the wetland relatively early in the study (Figure 40). Figure 40 shows the excess rhodamine concentration with background concentration subtracted from raw concentration values.Figure 40 – Excess RWT concentrations as parts per million by volume during each of the four studies as measured at the outlet of the wetland. After the initial pulse, the RWT exits the wetland in decreasing concentrations over the remainder of the study period. Given the distance that the pulse of RWT traveled through the wetland it is likely that the data spikes that occur close together are a result of scatter in data rather than real sudden increases and decreases in fluorescence. Table 6 summarizes the results of the tracer studies. In all cases, the volume of tracer recovered at the outlet is greater than the volume of tracer released at the inlet. This is likely due to relatively sparse measurements taken during the peak which would cause the width of the peak and the volume of tracer to be overestimated. Additionally, errors in discharge would cause increased error in calculating the recovery of the tracer.

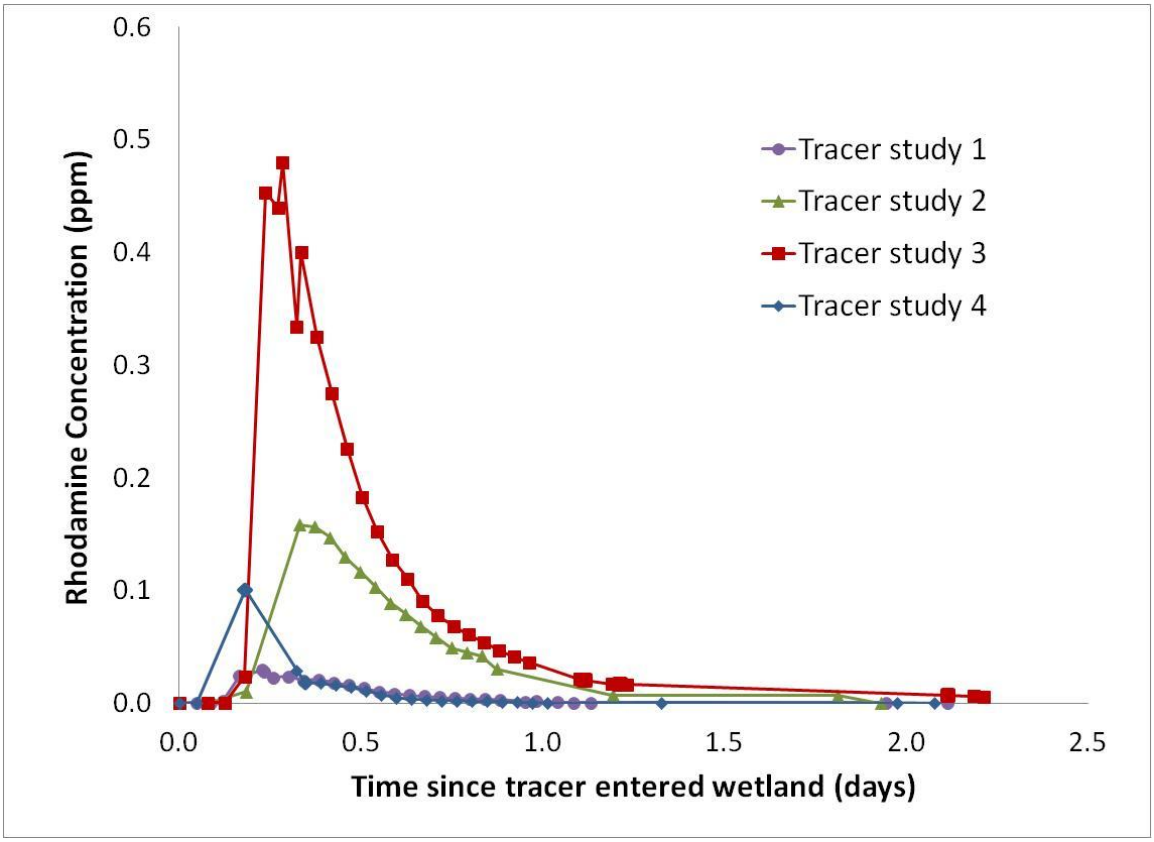

Figure 40 – Excess RWT concentrations as parts per million by volume during each of the four studies as measured at the outlet of the wetland.

Table 6 - Summary of results for tracer studies. Values marked with an * are estimates.

	Tracer Study 1	Tracer Study 2	Tracer Study 3	Tracer Study 4
Date	5/25-27/2011	6/7-9/2011	8/3-5/2011	8/16-18/2011
Average Q (L/s)	103	32	16	82*
Tracer volume released (mL)	20	60	60	100
Tracer volume recovered (mL)	93	191	190	82
Average wetland volume (m^3)	14115*	9193*	3876*	7109*
Detention time (days)	0.3951	0.5920	0.5078	0.2789

Additional data from throughout the wetland show that early in each study (data collected during Study 1 were not included in this analysis) the RWT concentrations are higher in the stream channel than on the platform (Figure 41). Later in the study, after the high concentration pulse has been flushed quickly through the stream channel and out of the wetland, some of the RWT has remained on the platform, giving it a higher RWT concentration than the stream channel at the end of the study. Figure 42 shows the RWT concentrations (normalized by the volume of RWT released during each study) in the upper channel, upper platform, and the pond during tracer studies 2, 3, and 4. While the concentration on the upper platform is much lower than the concentration in the upper channel for each study, the platform concentration is sustained over a much longer period of time. The tracer also remains in the pond long after it has been flushed from the upper channel.

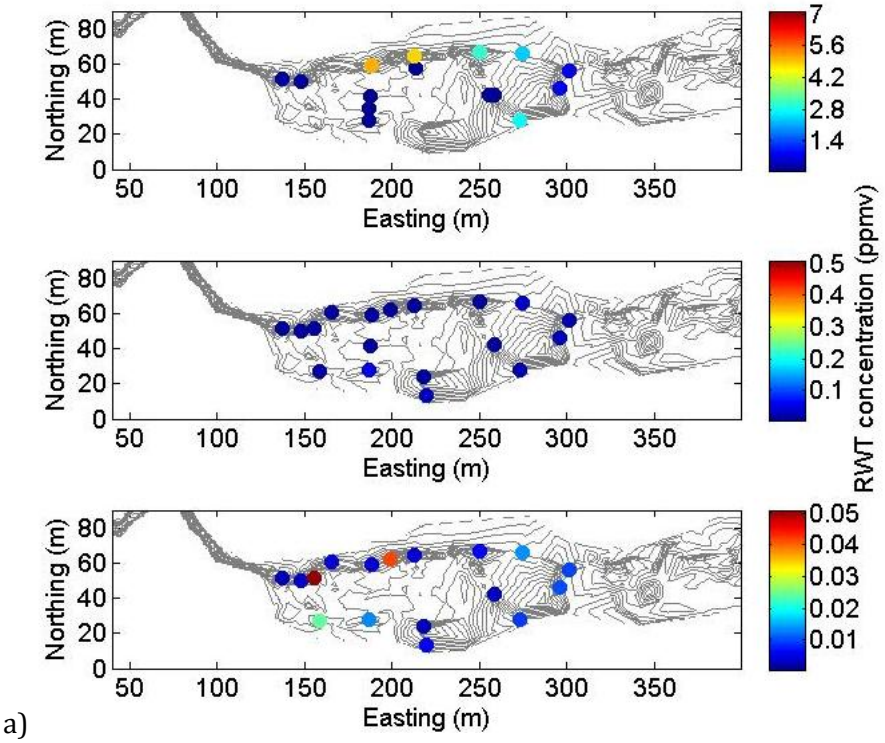

a)

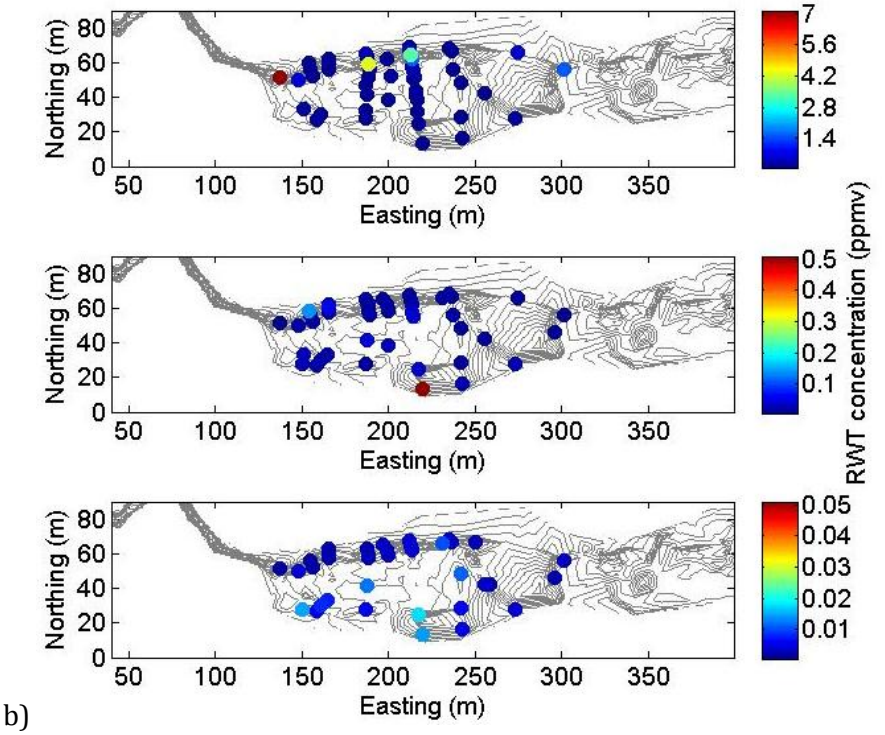

b)

Figure 41– Changes in RWT concentration throughout the wetland over the duration of the (a) tracer study 3 and (b) tracer study 4. The magnitude of the color scale to the right of each map changes for each day.

a)

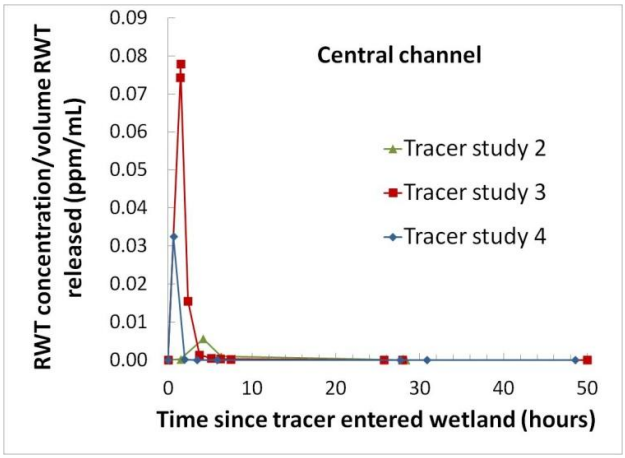

b)

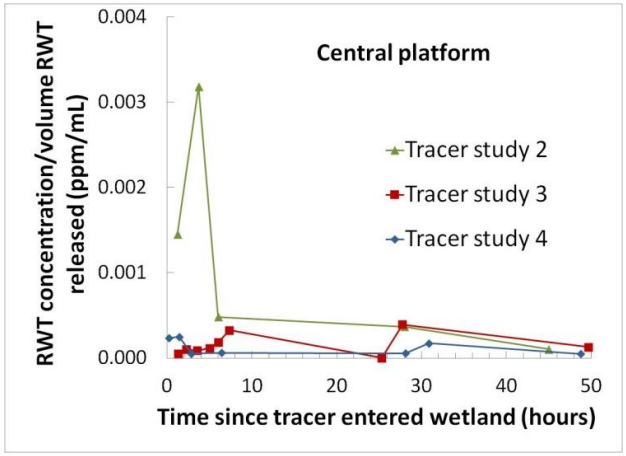

c)

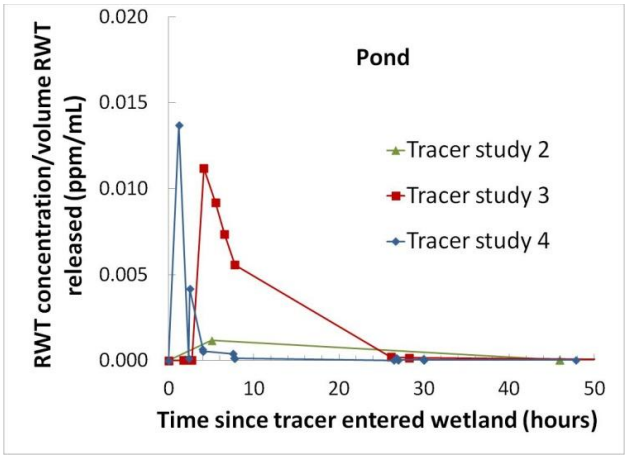

Figure 42 - Tracer concentrations measured in the (a) upper channel, (b) upper platform at a transect approximately through the middle of the central section, and (c) pond outlet during tracer studies 2, 3, and 4. Note that the y-axis is different on each of the plots.

RESIDENCE TIME DISTRIBUTIONS

Each RTD has a similar shape with a peak early on and a gradually decreasing tail over the remainder of the study which indicates a pulse of water moving through the wetland relatively quickly followed by the rest of the water exiting over a longer period of time (Figure 43). Different discharges during the tracer studies result in different arrival times for the peaks at the wetland outlet. The largest discharges are associated with pulses that arrive earlier than pulses during lesser discharges. Measurements taken early during tracer study 2 appear to have missed the initial peak pulse at the downstream end of the wetland. This is indicated by the first observed peak being measured after the first peak during tracer study 4, which has a similar discharge. The four tracer studies, each conducted at a different discharge, each produced a different RTD with a similar shape; the largest peak occurring relatively early, followed by one to two peaks decreasing in size, and a tail tapering off over a longer period of time. The only exception is tracer study 1which has only one peak and a long gradual tail. This may be a result of the much higher discharge during this study which may indicate a slight change in flow patterns at very high discharges. Error in downstream discharge and its impact on percent recovery of RWT may change the size of peaks in the RTDs but should not change the overall shape (large peak and long tail) of the RTDs.

A single flow path model attempted to model the wetland as a simple channelized system. The resulting outputs of the model for each study are shown in

Table 7. The single flow path model approach could not produce RTDs that matched the peak and the tail of RTDs calculated from data collected during the tracer studies (Figure 43).

Table 7 - Optimized parameter (number of tanks in series) and the output values for each tracer study. Measured detention times are repeated here for comparison.

	Tracer study 1	**Tracer study 2**	**Tracer study 3**	**Tracer study 4**
Number of tanks, N	4	7	6	4
Sum squared error	0.005	0.04	0.05	0.04
Simulated detention time, T_d (days)	0.43	0.47	0.43	0.26

a)

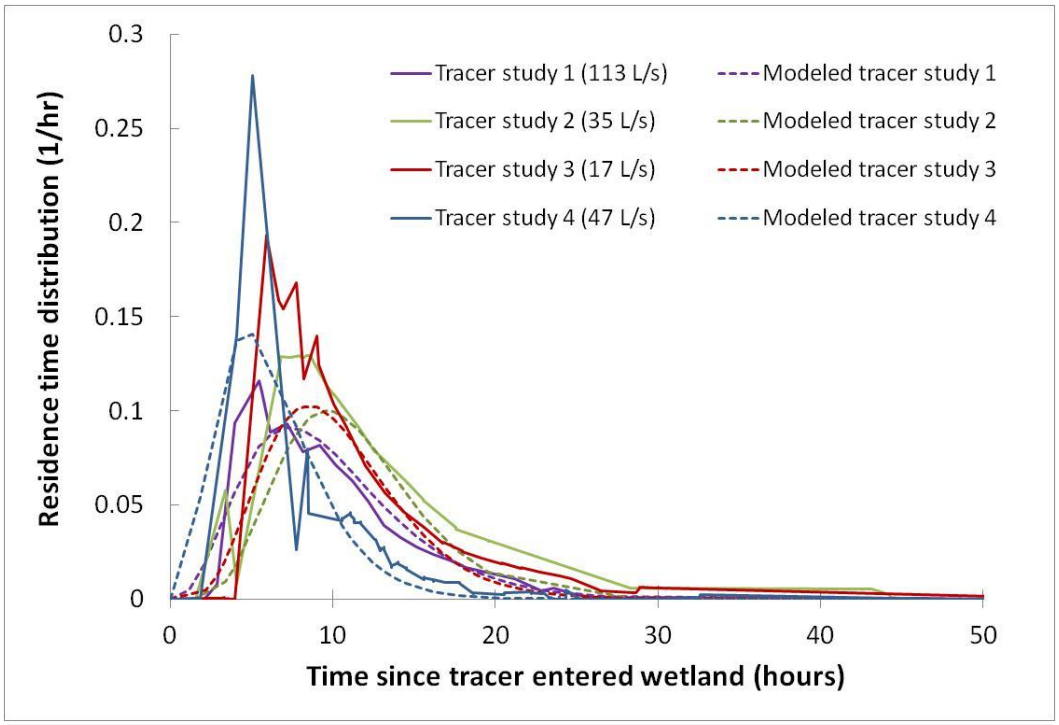

b)

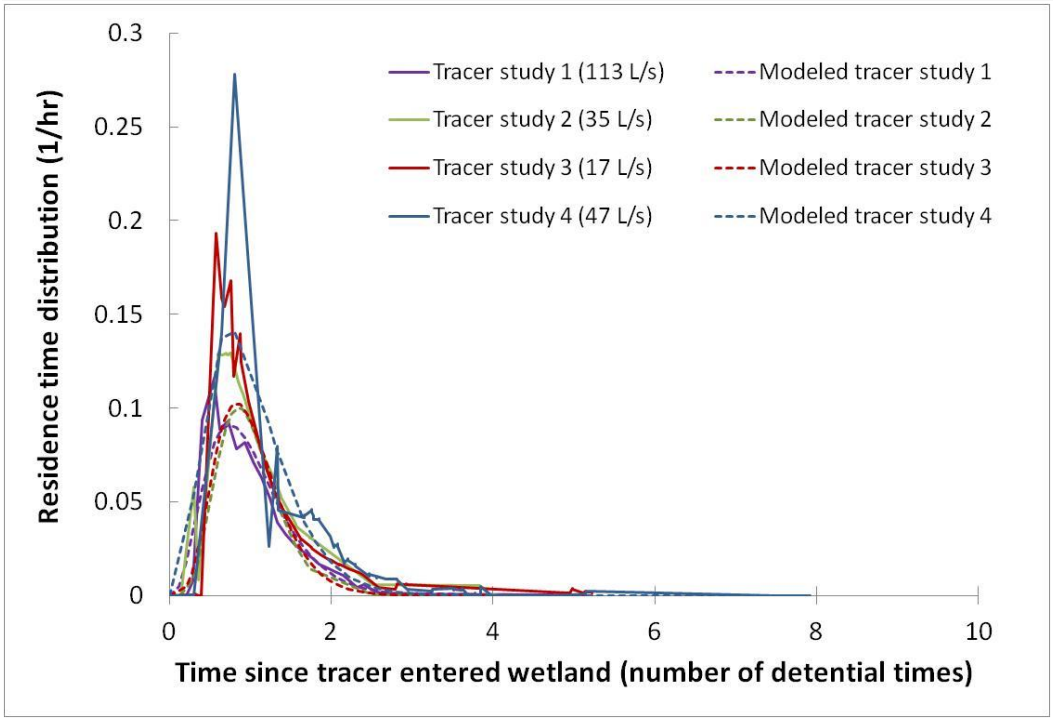

Figure 43 - Residence time distributions of the four tracer studies (a) against time since the tracer entered the wetland and (b) time normalized by the detention time for each tracer study. Solid lines indicate RTDs from measured values. Dashed lines indicate RTDs modeled from the single flow path model described below. Outgoing discharges for each tracer study are shown in the legend.

INTERNAL RESIDENCE TIME DISTRIBUTION

The internal RTDs shown in Figure 44 were estimated using the Monte Carlo method (see methods section). The internal RTDs for each study are separated into the central section, pond, and lower section. The $RTD_{central}$ for tracer studies 3 and 4 are relatively short (<2 hours) and increase and decrease rapidly. This indicates that relatively little longitudinal dispersion occurred. The $RTD_{central}$ for tracer study 2 is much wider around the peak and peaks later (4 hours) than the other two tracer studies. This indicates that there is much more longitudinal dispersion occurring during tracer study 2.

The RTD_{pond} for all the tracer studies show a quicker rise followed by a tail that is more gradual. For tracer study 4 the tail is only slightly more gradual than the rise and the peak is somewhat narrow which indicates that at that discharge (82 L/s) flow in the pond was greatly dominated by advection. The more gradual rise and very long tail in the RTD_{pond} for tracer study 3 indicates that at the lower discharge (16 L/s) dispersion played a much larger role. During tracer study 2 the pond appears to behave more like a contiuously stirred tank reactor (CSTR) with the tail displaying approximate exponential decay.

The RTD_{lower} for tracer study 2 rises quickly and plateaus for several hours before gradually decreasing. The RTD_{lower} for tracer study 3 also rises quickly but does not plateau before the long gradual decrease. The RTD_{lower} for tracer study 4 is unique because it increases gradually over a period of approximately 3 hours and then quickly decreases in about half that time. This indicates that longitudinal dispersion is very important. Since tracer study 4 occurred at a relatively high discharge (82 L/s) it is likely that it accessed portions of the lower wetland that were not available at lower discharges. This would have changed the shape of the RTD.

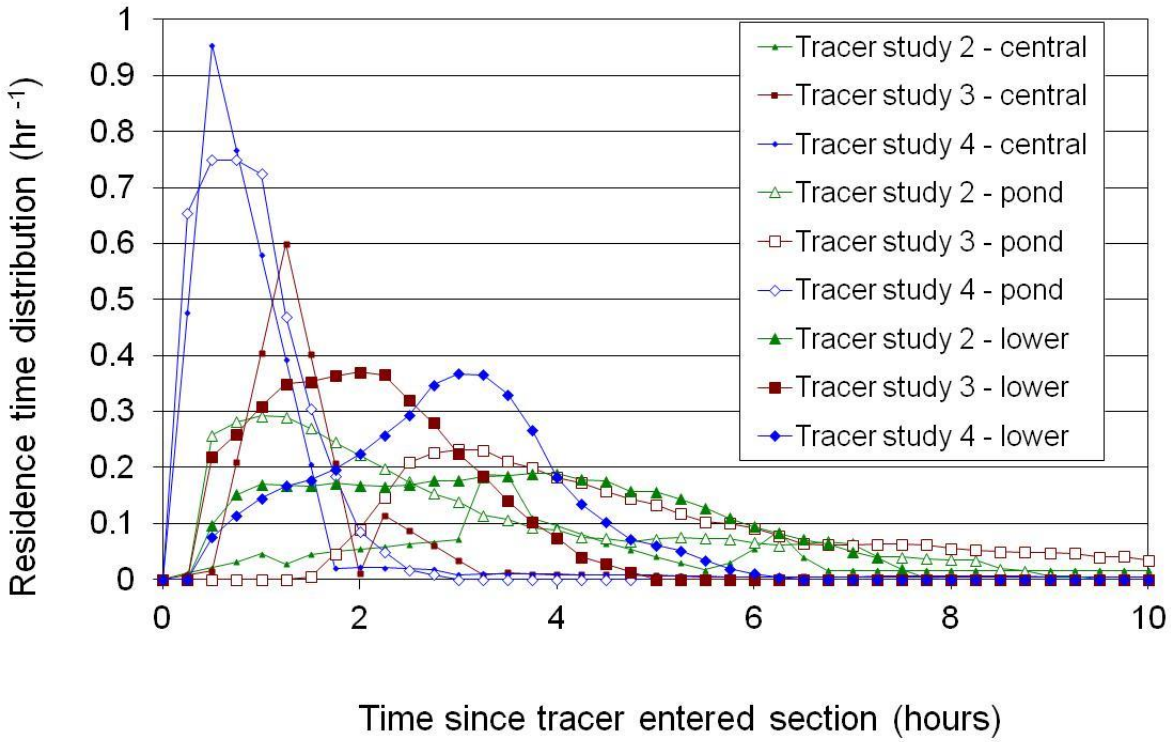

Figure 44 - Internal RTD for the central section (channel and platform), pond, and lower section for tracer studies 2, 3, and 4.

Figure 45 shows the detention times for each of the individual sections separately and the wetland as a whole. The detention time in the central section behaves similarly to the wetland as a whole with the detention time increasing between 16 L/s to 32 L/s and then dropping at 82 L/s. The detention time in the pond appears to decrease steadily as discharge increases. This indicates that the volume of the pond does not increase significantly when discharge increases. The opposite occurs in the lower reach with the detention time increasing steadily with discharge. This indicates that additional areas of the lower platform are accessed regularly as discharge increases causing the detention time to be longer at higher discharges.

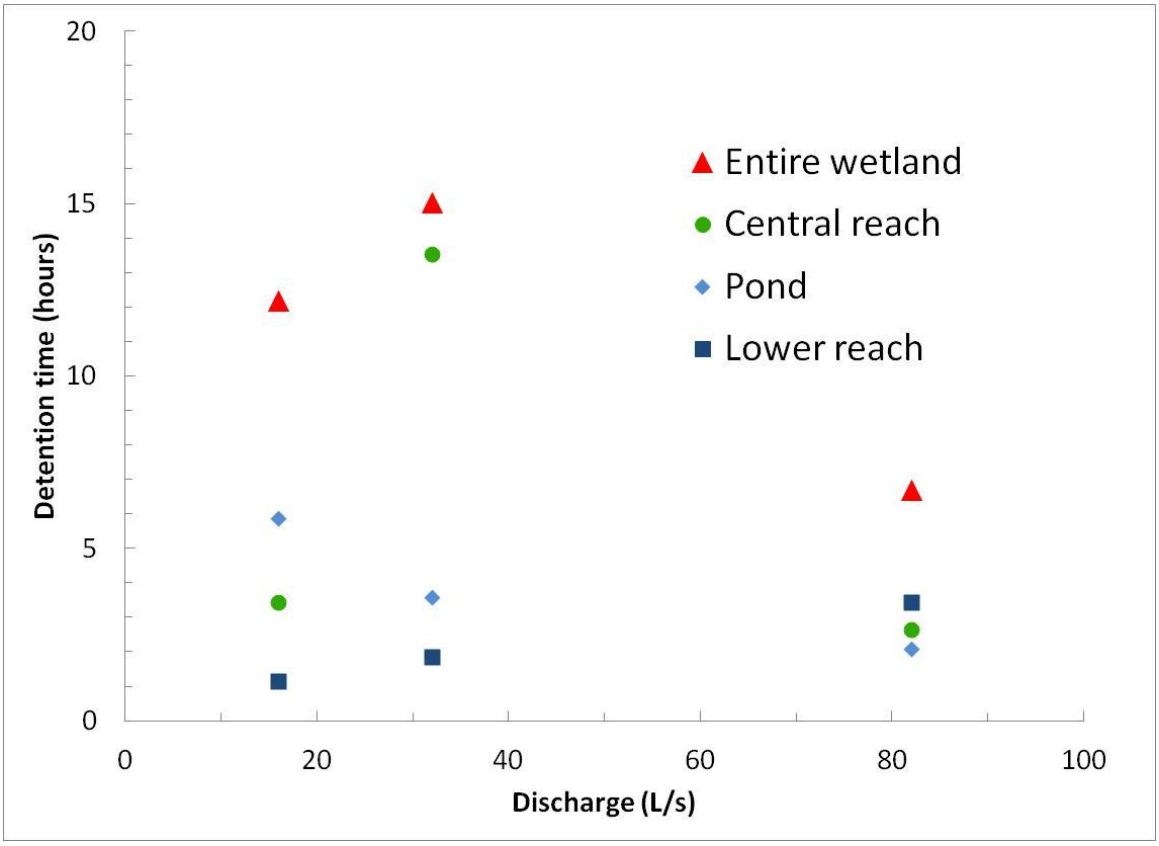

Figure 45 - Detention times for the central reach (green circle), pond (light blue diamond) and lower reach (dark blue square) seperately and the entire wetland (red triangle) as a whole.

PREDICTING REMOVAL

The relationship between the discharge and the expected removal for each study can be used as a quick way to estimate the removal of a non-conservative substance at some other discharge (Figure 46). The data suggest that lower percentages of removal can be expected at higher discharges. However, the Tracer Study 1 data, with the highest discharge, suggest that there may be some threshold discharge, between 32 L/s (tracer study 2 discharge) and 103 L/s (tracer study 1 discharge), at which the expected fraction of removal may begin to increase, perhaps due to increased access to the floodplain.

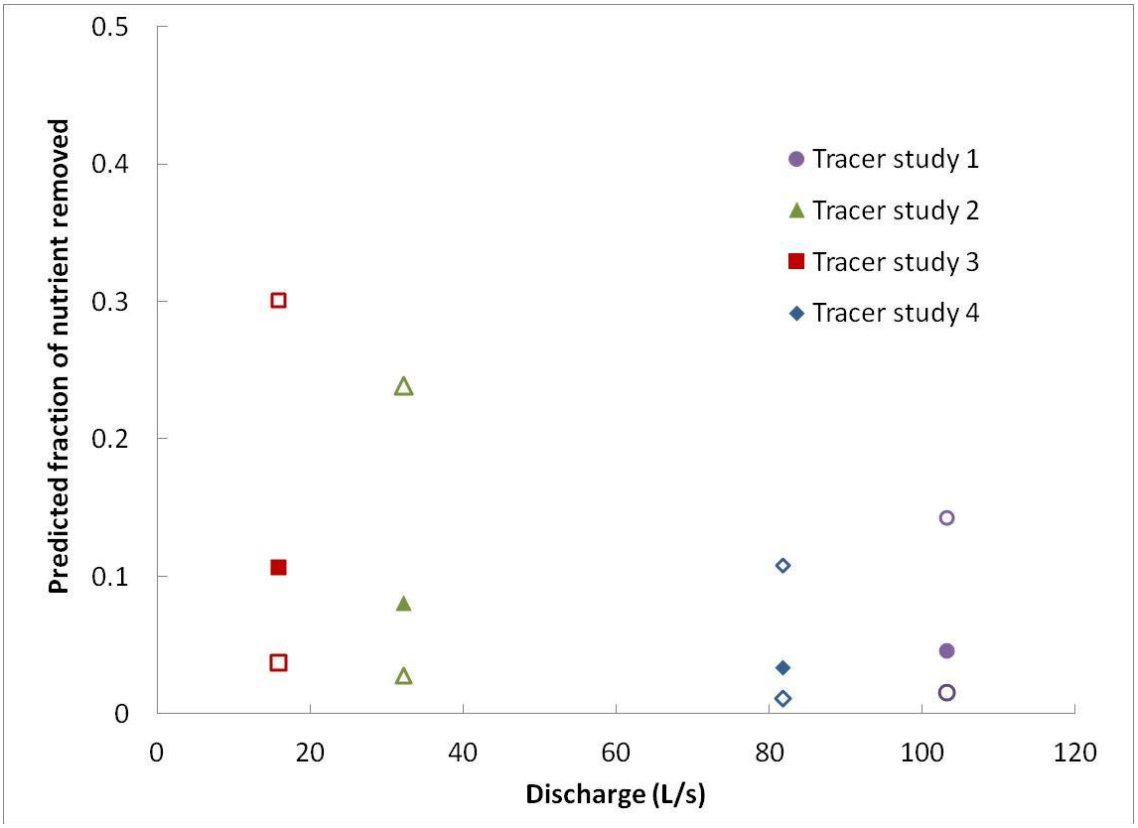

Figure 46 – The expected amounts of removal for each of the tracer studies changes with the discharges during each study. The solid symbols indicate moderate removal with an volumetric removal rate of 3 d^{-1}. The open symbols indicate high and low amounts of removal with volumetric removal rates of 10 d^{-1} and 1 d^{-1}, respectively.

Cumulative removal in the upper section, pond, and lower section (Figure 47) indicate removal occurs, in varying degrees, throughout the wetland. Tracer study 2 has high removal in the upper section and much lower removal in the pond and lower section. Tracer study 3 has high removal in the upper section and pond. The lower section has the least amount of removal. Tracer studies 2 and 3 both have high overall removal at 84% and 76%, respectively. Tracer study 4, has the lowest removals in the upper section and pond and higher removal at the lower end. Overall, tracer study 4 has the least amount of removal at 46%.

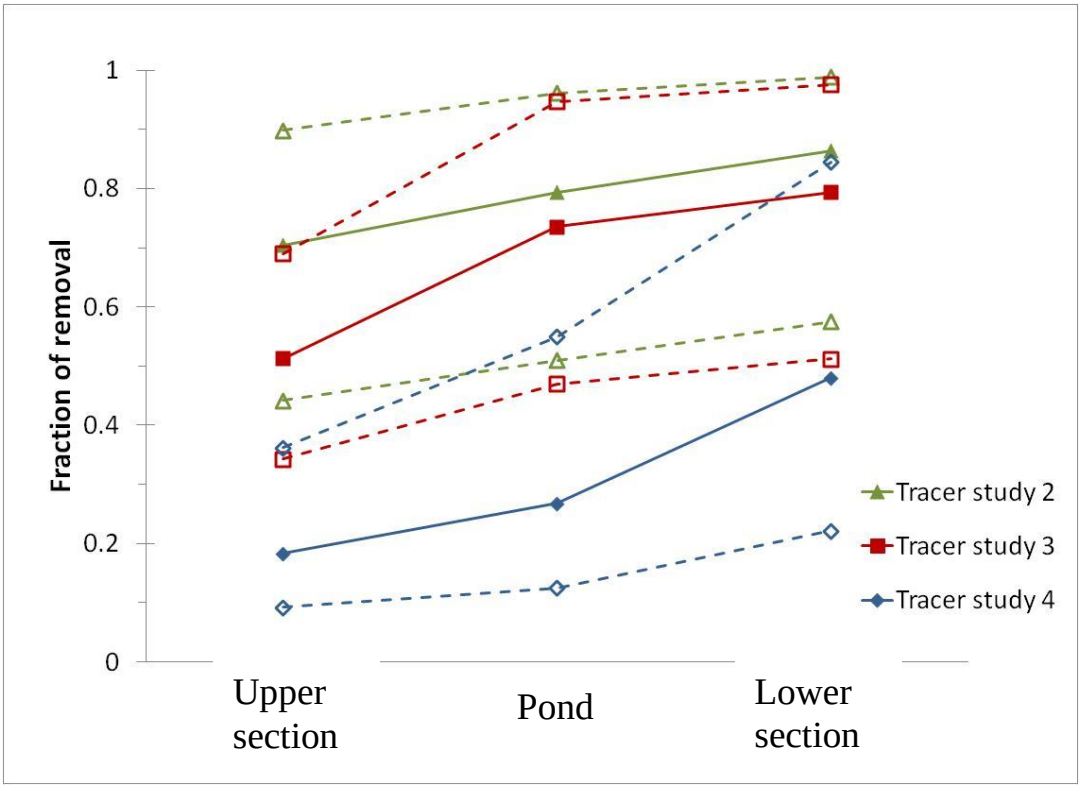

Figure 47 – Cumulative removal in the upper section, pond, and lower section during each tracer study. All three sections have the same volumetric removal rate constant. The dashed lines indicate high and low estimates of fraction of removal.

It is very likely, given the differences between the sections, that the wetland does not have a consistent removal rate constant throughout. The first scenario analyzed here assumes the upper section has a much higher removal rate of 10 d^{-1} while the pond and lower section remain the same with a removal rate constant of 3 d^{-1} (Figure 48a). Even though there is high removal in the upper section alone, overall removal experiences only slight increases from the sceneraio in Figure 47. In tracer study 2 the overall removal remains at 85%. In tracer study 3 the overall removal increases from 76% to 79%. In

tracer study 4 the removal increases from 46% to 48%. Increases the volumetric removal rate constant in the pond appears to have a bigger impact on the overall removal (Figure 48b). Again, the overall removal in tracer study 2 remains at 85%. However, during tracer study 3 the overall removal increases to 92% and in tracer study 4 it increases to 57%. This brief analysis suggests that, not only is it important to increase accuracy in estimating the volumetric removal rate constant, but it is also important which areas of the wetland have higher or lower removal rate constants.

a)

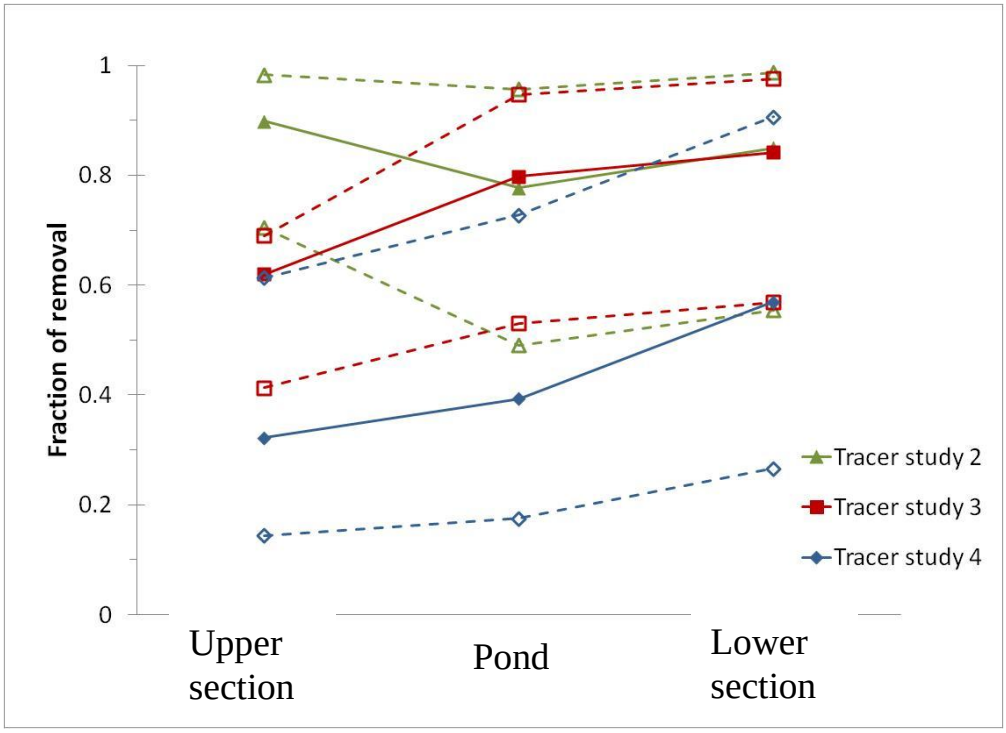

b)

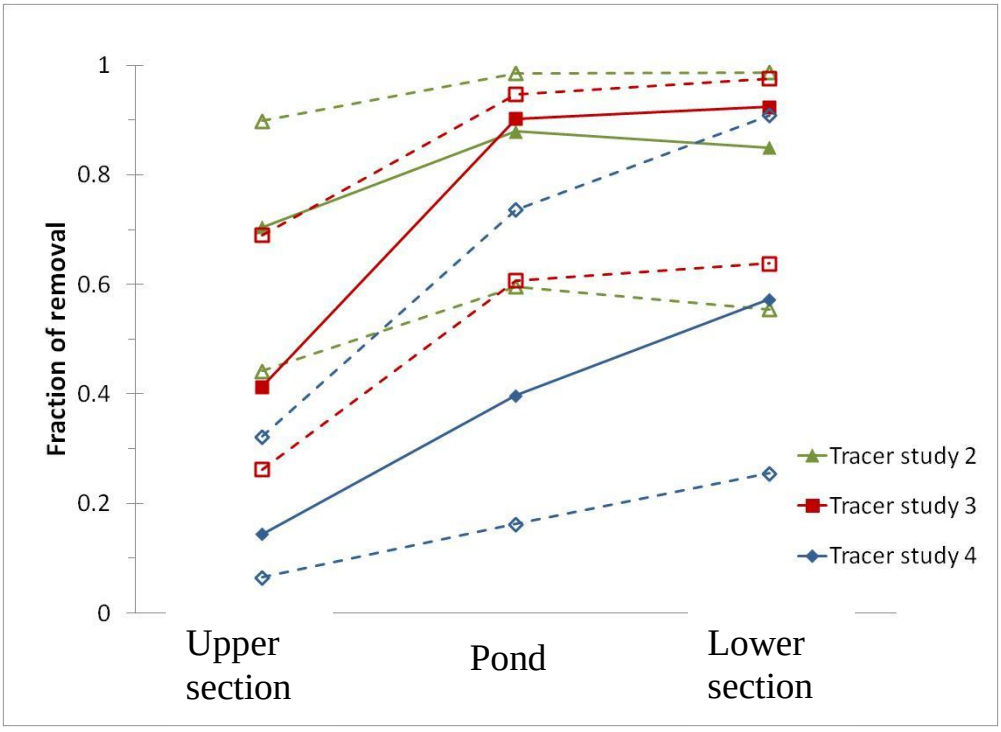

Figure 48 – Cumulative internal predicted removal with variable removal rate constants with (a) the upper section having a higher volumetric removal rate and (b) the pond having a higher volumetric removal rate.

CHAPTER 5

DISCUSSION

WATER BUDGET – IS THE WETLAND GAINING OR LOSING?

Integrating the incoming and outgoing discharge curves over the duration of the study suggests that on average slightly more water is entering rather than exiting the wetland. The upstream discharge averages 56±221 L/s and the average downstream discharge is 54±111 L/s. Even though the downstream average is slightly less than the upstream average, the downstream discharge was observed to be greater the majority of the time. Out of 18,957 measurements, the downstream discharge was higher than the upstream discharge during 13,314 of them. Peak discharges at the upstream end were much higher than the corresponding peak discharges at the downstream end which may account for the similarity in the average discharges at the two locations. However, because the uncertainty in the rating curve, particularly at larger discharges, is relatively high, it cannot confidently be concluded that the average discharge entering the wetland is greater.

When looking at the whole water budget over a shorter period, 6/9/2011 to 7/28/2011, there is a large negative residual that suggests a groundwater velocity of approximately 1 m/d (equivalent to 5120 m^3/d) out of the wetland. However, in separating the water budget into a series of discharge peaks and recessions it becomes apparent that the

incoming discharge is less than outgoing discharge during the majority of events with a few exceptions where incoming discharge is greater than outgoing discharge, exclusively during rain events. Similarly, with a few exceptions, storage tends to increase during the peaks and then decrease during the recessions. The exceptions to this occur from 8/13/2011 to 8/15/2011 when the downstream stage is estimated. The estimated residuals throughout the base flow and event periods were used to calculate the groundwater inflow and outflow. For the most part, the residuals tend to indicate that at base flow the wetland is neither gaining nor losing. There are seven base flow periods with no apparent groundwater flow, two that suggest groundwater inflow, and four that indicate losses to groundwater. Event flows are weighted heavily toward suggesting there is groundwater inflow during these periods (eight events), only one event with no apparent groundwater flow, and four that indicate losses to groundwater. Because of the large uncertainty associated with the stream discharges the estimated ranges of groundwater velocities for each time period make it very difficult to decisively conclude that the system is gaining or losing. Additionally, the data described and analyzed here are most reliable for the early summer months. Seasonal trends during the winter or at other times of the year could be quite different from those suggested by the data presented above.

Paired sets of isotope data from concurring upstream and downstream samples can also be used to determine whether there is any groundwater entering the wetland. Of the five sets of isotope data points, two (7/19/2011 and 10/13/2011) show the downstream becoming less negative, heavier, indicating that there is net evaporation occurring. The

other three (6/17/2011, 6/22/2011, and 8/5/2011) show the downstream is slightly lighter than the upstream. This could indicate some groundwater input. However, the isotopic composition change in these three pairs is so small that it could be attributed to instrumental error or sample collection error. The estimated residuals on two of those days (6/17/2011 and 6/22/2011) suggest that there is a net loss to groundwater. However, on 8/5/2011 both the water budget and the isotopic compositions suggest groundwater inflow. Limited isotope data during the study period make it difficult to draw any conclusions regarding the groundwater flow into or out of the wetland.

FLOW PATTERNS & PREDICTING REMOVAL

The RTDs for the wetland generally have very similar shapes with one peak early in the study followed by a long tail. Attempts to model the RTD for each of the studies using a simple single flow-path tanks-in-series model were unsuccessful. This suggests that flow patterns through the wetland are much more complicated than can be predicted by such a simple model.

Additionally, plots of the average discharge vs. detention time, T_d, for each of the four studies indicates that the relationship cannot clearly be classified as directly or indirectly related. However, the two studies with the lowest discharges (16 L/s and 32 L/s) have the two longest detention times at 0.51 days and 0.63 days, respectively. The two studies

with the highest discharges (82 L/s and 103 L/s) have the shortest detention times at 0.28 days and 0.43 days, respectively. Interestingly, the lowest discharge study and the highest discharge study have the detention times that are closest to each other at 0.51 days and 0.43 days, respectively. In a very simple system it would be expected that as discharge increased the detention time would decrease; a parcel of water would flow more quickly out of the system. However, in this wetland, as the discharge increases from 16 L/s to 32 L/s and again from 82 L/s to 103 L/s the detention time also increases. This indicates that more of the wetland, presumably additional areas of the platform, is accessed by these increases in discharge. The relationship behaves as expected, with a decrease in detention time when the discharge increases from 32 L/s to 82 L/s.

When considering the RTDs and T_d for the tracer studies, it is important to understand the impact of the percent of tracer recovered; the amount of tracer measured exiting the wetland vs. the amount injected into the wetland. Realistically, this value should be less than 100% for RWT because it experiences some degree of photolysis and sorption as it flows through the wetland, though these are generally negligible in studies lasting only a few days (Dieberg & DeBusk 2005). In all four of the tracer studies the tracer recovery was greater than 100% with recovery ranging from approximately 165% to 464% of tracer released at the upstream end. There are two plausible explanations for the significant overestimation of tracer leaving the wetland. Firstly, uncertainty in the downstream rating curve is relatively high. If the actual discharge is less than the

calculated discharge, any conversions of RWT concentration to RWT mass would artificially inflate the RWT mass passing out of the wetland. Secondly, as Dierberg and DeBusk (2005) found, collecting too few tracer measurements in the descending tail of the concentration curve can result in recovery rates greater than 100%. It is likely that the combination of these two that contributed to the very high apparent tracer recovery at Chesnut Wetland. While it is unlikely that increased sampling in the tail would significantly change that general shape of the RTD, it may result in a steeper descending arm from the peak which could result in a shorter T_d.

Tracer study data collected throughout the wetland were used to produce RTDs of the different sections of the wetland; central section, pond, and lower section. A Monte Carlo method was used to deconvolute the pond data and estimate RTDs for the pond and for the lower reach. The RTDs for the central section are relatively peaky with the peaks being high and narrow at the lowest and highest discharges (16 L/s and 82 L/s). At the lower discharge, a larger portion of the flow is confined to the channel which allows it to exit the section with limited dispersion. Similarly, at the higher discharge, flow on top of the platform may be deep enough that apparent roughness at the substrate is reduced. The central section peak at a discharge of 32 L/s is spread out and delayed. This suggests that a large portion of the flow is not confined to the channel. Also, flow on the platform is shallow enough, relative to the vegetation and substrate roughness, for there to be significant dispersion.

The RTDs from the pond shows that most of the water exits relatively quickly with varying degrees of dispersion. During the higher discharges, there is less dispersion and the detention times are lower. At the lowest discharge there is much more dispersion and a longer detention time. At all discharges, the lower section displays much more dispersion than the upper section. This could be caused by the channel, which would inhibit dispersion, being less defined in the lower section. While the RTDs at 16 L/s and 32 L/s behave as expected with the majority of water exiting early, followed by a long tail, at 82 L/s the opposite occurs. There is a slow lead in to the peak followed by a quick decline. This could indicate that a large area of the lower platform is accessed at this point and that there is a large amount of dispersion as a result.

The detention times for each of the three sections increase or decrease with discharge depending on the geometry of the reach. The initial, significant increase in detention time in the central reach followed by the much shorter detention time at higher discharges indicates the at some point (approximately 17-25 L/s) the platform is accessed resulting in an increasing proportion of the total volume of water located on the platform where it has a lower velocity. The decrease in detention time between 32 L/s and 82 L/s indicates that additional areas of the wetland are no longer being accessed. At that point the impact of the increased discharge is much larger than the impact of any changes in volume when determining the detention time. The steady decrease in detention time of

the pond as discharge increases suggests that the volume of the pond does not change significantly with discharge. The opposite appears to be true of the lower reach. The increasing detention time with discharge suggests that the volume of that reach increases enough compared to the discharge to cause the detention time to become longer. Understanding the behavior of water flowing through each of these sections shows how complicated flow through the wetland is.

A 2011 study in the Atchafalaya River Basin (BryantMason et al. 2013) looked at the potential for nutrient removal in adjacent wetlands and floodplains during the 2011 Mississippi River flood. BryantMason et al. (2013) hypothesized that the increased access to the wetlands and floodplains, known to be areas of larger potential for nutrient retention, during such a large flood would result in significant decreases in the mass of nitrate exiting the Atchafalaya River into the Gulf of Mexico. However, their results suggested the opposite; that at such high discharges, removal in the wetlands and floodplains was insignificant due to shorter residence times (BryantMason et al. 2013).

Clearly, Chestnut Wetland differs from the Atchafalaya River and its wetlands/floodplains in many ways, including size (approximately 4 km^2 vs. approximately 5700 km^2). The Mississippi River, which feeds the Atchafalaya River, is heavily developed and confined by levees; as is the Atchafalaya River to a lesser degree. This results in limited access to the wetlands/floodplains at low and moderate flows

(BryantMason et al. 2013). Though, several orders of magnitude smaller, similar observations were made at Chestnut Wetland with reduced residence times at peak flows limiting potential nutrient retention on the floodplain. However, because access to the floodplain at Chestnut Wetland is not restricted at moderate flows there may be times when access to the floodplain and its greater potential for removal are more effectively utilized due to somewhat longer detention times.

Looking at the detention times of each of the individual sections of Chestnut Wetland, as described above, can help indicate which areas are most effective at potentially removing nutrients at different discharges. The central section has the longest detention time, by far, at a discharge of 32 L/s. It is significantly lower at 16 L/s and 82 L/s. Therefore, potential for removal is highest at 32 L/s. The pond, on the other hand, has the best potential for removal (longest detention time) at the lowest discharge, 16 L/s. Conversely, the lower reach has the highest removal potential at the largest discharge, 82 L/s.

In the 2011 study of the Atchafalaya River, NO_3 levels were lower during the flood peak and increased during the flood recession due to transport from subsurface soils into the upper Mississippi River (BryantMason et al. 2013), suggesting that lateral flow between the wetlands/floodplains and the main channel may play a vital role in nutrient transport and retention. BryantMason et al. (2013) suggest that the low NO_3 levels during the peak

may be a result of flushing of stored water that has already undergone nutrient removal and the following high NO_3 levels during the recession are a result of water that has not had a chance to experience nutrient removal due to short residence times. Though there is no corresponding nutrient data from Chestnut Wetland, similar lateral flow was observed during peak flows and the subsequent recession flows. Calculations of lateral water surface slope between the channel and platform indicate that the flow pattern in the central section is not only dependant on discharge but also on whether the discharge is increasing or decreasing. This could be important when considering where water is flowing and where removal might be maximized. During event flows, when discharge increases in response to precipitation events, water flows laterally from the channel to the platform. If the platform has higher potential for removal the direction of flow from the channel to the platform could allow for more of that potential to be utilized. Conversely, following the event flow, the platform drains with water flowing from the platform into the channel. This could result in less removal as nutrient-bearing water moves into the channel where is it transported more quickly from the wetland.

The potential for nutrient removal was estimated by assuming a constant removal rate (provided by Wollheim et al. In Review) and applying it to the measured RWT concentration values, which were used as a proxy for NO_3 concenrations, exiting the wetland. The outcome of this analysis indicates that the potential for removal is higher at lower discharges and lower at higher discharges, though the actual range of predicted

removal is small; between approximately 3% and 10%. However, the potential for removal seems to be slightly higher at 103 L/s (5% removal) than it is at 82 L/s (3% removal). This, like the RTD and detention time data discussed above, indicate that at some threshold discharge additional areas of the wetland may be utilized and aid in removal. Even though Chestnut Wetland is relatively small, the evidence for an ideal discharge, or range of discharges, for nutrient retention could help to inform projects utilizing the nutrient retention of wetlands and floodplains. In the instance of the Mississippi River, levees greatly inhibit access to the floodplain and development has diminished areas of natural wetlands which have reduced the potential for NO_3 retention (BrayantMason et al. 2013). Had the rivers access to these areas during moderate and high flows been maintained the amount of NO_3 entering the Gulf of Mexico may have been much lower. While the Ipswich River is not constricted by levees like the Mississippi River, it is heavily developed in areas, which creates the two-fold problem of reducing wetland and floodplain area, which could act as a NO_3 sink, as well as increasing runoff, which becomes a NO_3 source and may result in shorter residence times due to increased discharge (Wollheim er al. 2005).

The above statements assume uniform and constant uptake time constants throughout the wetland. Given the variations in substrate, vegetation, and bathymetry it is likely that this is not true. Further investigations would need to be conducted to determine the actual removal rates for each section of Chesetnut Wetland. While there seems to be an ideal

discharge at which the floodplain is accessed, if the uptake velocities are significantly different for each section, there might be a different ideal discharge at which the overall removal potential is maximized. Further investigations would be needed to determine how the uptake velocities may vary spatially and temporally.

CONCLUSION

When considering the potential for removal in the Chestnut wetland, discharge may not be a reliable indicator for how much removal to expect. Rather than using discharge to predict removal, it may be more important to determine a more accurate removal rate for the wetland. At the Chestnut wetland the fraction of removal changed by less than 8 percentage points over all the discharges studied (a range of nearly 100 L/s). However, by increasing or decreasing the removal rate by a factor of roughly 3, the range of the fraction of removal is much greater; 1% removal at the lowest to 30% removal at the highest. Additionally, estimating individual removal rates in each unique section of the wetland (i.e. – channel, platform, pond) can result in more accurate predictions of removal. The extensive analysis described above also makes it clear that while Chestnut wetland is relatively small, like many headwaters wetlands, its capacity for nutrient removal is potentially large.

Much of the analysis conducted in this study assumes that the wetland experiences steady flow rates. While there are times when changes in discharge are small, there are many times when discharge increased or decreased drastically over a period of only a few hours due to precipitation events. The changes in discharge associated with small storms can be important in flushing the wetland. This was seen in the lateral water surface slope which showed that at the beginning of the flow event water moves from the channel onto the platform and near the end of the event it moves back into the channel. This can also effect removal of nutrients by introducing new nutrient-rich water early in the storm event or flushing it out at the end of a flow event.

In much of the analysis dealing with potential removal, it is assumed that the removal rate is constant. However, variations in the removal rate from one location in the wetland to another can have important impacts on overall removal. Additionally, this analysis did not address nutrient supply limitations. If the wetland, or parts of the wetland, is not receiving as much nutrients as it is capable of processing, then its full potential is not being realized.

LIST OF REFERENCES

Boyer EW, Goodale CL, Jaworski NA, & Howarth RW. 2002. Anthropogenic Nitrogen Sources and Relationships to Riverine Nitrogen Export in the Northeastern USA. Biochemistry Volume 57/58: 137-169.

BryantMason A, Xu YJ, & Altabet MA. 2013. Limited Capacity of River Corridor Wetlands to Remove Nitrate: A Case Study on the Atchafalaya River Basin During the 2011 Mississippi River Flooding. Water Resources Research Volume 49: 283-290.

Buda AR & DeWalle DR. 2009. Dynamics of stream nitrate sources and flow pathways during stormflows on urban, forest and agricultural watersheds in central Pennsylvania, USA. Hydrological Processes Volume 23: 3292-3305.

Cirpka OA, Fienen MN, Hofer M, Hoehn E, Tessarini A, Kipfer R, & Kitanidis PK. 2007. Analyzing bank filtration by deconvoluting time series of electric conductivity. Groundwater Volume 45 (Issue 3): 318-328.

Clarke RT. 1999. Uncertainty in the estimation of mean annual flood due to rating-curve indefinition. Journal of Hydrology Volume 222 (Issue 1): 185-190.

Dierberg FE & DeBusk TA. 2005. An Evaluation of Two Tracers in Surface-Flow Wetlands: Rhodamine-WT and Lithium. Wetlands Volume 25 (Issue 1): 8-25.

Dingman SL. Physical Hydrology. 2nd Edition. Illinois: Waveland Press, Inc; 2002.

Frades MC. (2005). Hydrologic analysis of the headwaters Lamprey River watershed using water isotopes (Master Thesis). Retrieved from Thesis/Dissertation database (Nt.F79925).

Hagy JD, Boynton WR, Keefe CW, & Wood KV. 2004. Hypoxia in Chesapeake Bay, 1950-2001: Long-term change in relation to nutrient loading and river flow. Estuaries Volume 27 (Issue 4): 634-658.

Harmon C. 1961. Isotopic variations in meteoric waters. Science Volume 133 (Issue 3465): 1702-1703.

Holland JF, Martin JF, Granata T, Bouchard V, Quigley M, & Brown L. 2004. Effects of wetland depth and flow rate on residence time distribution characteristics. Ecological Engineering Volume 23 (Issue 1): 189-203.

Jacobs JM & Sumner DM. Utility of Penman-Monteith, Priestley-Taylor, reference evapotranspiration, and pan evaporation methods to estimate pasture evapotranspiration. Journal of Hydrology Volume 308 (Issue 1): 81-104.

Kadlec RH. 2010. Nitrate dynamics in event-driven wetlands. Ecological Engineering Volume 36 (Issue 4): 503-516.

Kadlec RH & Knight RL. Treatment Wetlands. Boca Raton, FL: Lewis Publishers; 1996.

Keefe SH, Barber LB, Runkel RL, Ryan JN, McKnight DM, & Wass RD. 2004. Conservative and reactive solute transport in constructed wetlands. Water Resources Research Volume 40 (Issue 1).

Lightbody AF, Avener ME, & Nepf HM. 2008. Observations of short-circuiting flow paths within a free-surface wetland in Augusta, Georgia, USA. Limnology and Oceanography Volume 53 (Issue 3): 1040-1053.

Mackin K & Wagner L. 2002. Ipswich River Basin conservation report card: Grading the communities of the Ipswich River Basin on water conservation and water use efficiency. Ipswich River Watershed Association. Available from: http://ipswich-river.org/wp-content/uploads/2010/03/ipswich_riv_rep.pdf

McConnell RL. 1995. The human population carrying capacity of the Chesapeake Bay Watershed: A Preliminary analysis. Population and Environment Volume 16 (Issue 4): 335-351.

NCDC. 2014. U.S. Surface Climate Observing Reference Networks. [Online]. Available from: ncdc.noaa.gov/crn/elements.html. Accessed 2014 March 9.

Pellerin BA. (2004). The influence of urbanization on runoff generation and stream chemistry in Massachusetts watersheds (Ph.D. Dissertation). Retrieved from Thesis/Dissertation database (NtP38745)

Scavia D & Bricker SB. (2006). Coastal eutrophication assessment in the United States. Biogeochemistry Volume 79 (Issue 1): 187-208.

Shabaga JA & Hill AR. (2010). Groundwater-fed surface flow path hydrodynamics and nitrate removal in three riparian zones in southern Ontario, Canada. Journal of Hydrology Volume 388 (Issue 1-2): 52-64.

Smil V. Cycles of Life: Civilization and the Biosphere. New York, NY: Scientific American Library; 2001.

Southeastern Natural Science Academy 2006

Valiela I & Bowen JL. (2001). Nitrogen sources to watersheds and estuaries: role of land cover mosaics and losses within watersheds. Environmental Pollution Volume 118 (Issue 2): 239-248.

Wollheim et al., In Review.

Wollheim WM, Pellerin BA, Vorosmarty CJ, & Hopkinson CS. (2005). N retention in urbanizing headwater catchments. Ecosystems Volume 8 (Issue 8): 871-884.

Wollheim WM, Peterson BJ, Thomas SM, Hopkinson CH, & Vorosmarty CJ. (2008). Dynamics of N removal over annual time periods in a suburban river network. Journal of Geophysical Research Volume 113 (Issue G3).